From the
Department of Veterinary Sciences
Faculty of Veterinary Medicine
Ludwig-Maximilians-Universität München
Chair for Molecular Animal Breeding and Biotechnology
Univ.-Prof. Dr. Eckhard Wolf

This work was conducted at
Helmholtz Zentrum München
Institute of Clinical Molecular Biology and Tumor Genetics
Head: Prof. Dr. Georg W. Bornkamm
Under the supervision of Dr. Marcus Conrad

Complex Redundancy between the Mammalian Thioredoxin and Glutathione Systems in Cell Proliferation and Tumorigenesis

Thesis for the attainment of the title Doctor in Veterinary Medicine
from the Faculty of Veterinary Medicine of the
Ludwig-Maximilians-Universität München

by
Pankaj Kumar Mandal
from
Jamalpur, India

Munich, April 2009

Aus dem
Department für Veterinärwissenschaften
Tierärztliche Fakultät
Ludwig-Maximilians-Universität München
Lehrstuhl für Molekulare Tierzucht und Biotechnologie
Univ.-Prof. Dr. Eckhard Wolf

Die Untersuchungen wurden durchgeführt am
Helmholtz Zentrum München
Institut für Klinische Molekularbiologie und Tumorgenetik
Direktor: Prof. Dr. Georg W. Bornkamm
Unter der Leitung von Dr. Marcus Conrad

Komplexe Redundanz zwischen dem Thioredoxin- und Glutathion-abhängigen System in der Zellproliferation und Tumorenstehung

Inaugural-Dissertation
zur Erlangung der tiermedizinischen Doktorwürde
der Tierärztlichen Fakultät
der Ludwig-Maximilians-Universität München

von
Pankaj Kumar Mandal
aus
Jamalpur, Indien

München, April 2009

Gedruckt mit Genehmigung der Tierärztlichen Fakultät
der Ludwig-Maximilians-Universität München

Dekan:	Univ.-Prof. Dr. Braun
Berichterstatter:	Univ.-Prof. Dr. Wolf
Korreferent/en:	Univ.-Prof. Dr. Hirschberger
Summa cum laude	
	Priv.-Doz. Dr. André
	Univ.-Prof. Dr. Wanke
	Univ.-Prof. Dr. Gabius

Tag der Promotion: 17th Juli 2009

Dedicated to

Dear Father and Uncle

Table of contents

List of abbreviations

2-ME	β-mercaptoethanol
Amp	Ampicillin
ASK-1	Apoptosis stimulating kinase 1
BSO	L-buthionine sulfoximine
CMV	Cytomegalovirus
Cre	Cre recombinase
Cys	Cysteine (reduced)
$(Cys)_2$	Cystine (oxidised Cys dimer)
DCF	Dichlorofluorescein (CM-H2DCFDA)
DMSO	Dimethylsulfoxide
EDTA	Ethylenediamine-N,N,N',N'-tetra-acetic acid
eGFP	Enhanced green fluorescence protein
FACS	Fluorescence activated cell sorting
FAD	Flavin adenine dinucleotide
FCS	Fetal calf serum
fl	LoxP flanked allele
γ-GCS	γ-glutamylcysteine synthetase
Gclc	Catalytic subunit of γ-GCS
Gclm	Modulator subunit of γ-GCS
Glrx	Glutaredoxin gene
GRx	Glutaredoxin
GSH	Glutathione (reduced)
GSS	Glutathione synthetase
GSSG	Glutathione (oxidized)
Gsr	Glutathione reductase gene
GR	Glutathione reductase
GRx	Glutaredoxin
H_2O_2	Hydrogen peroxide
HIF	Hypoxia-inducible factor
IRES	Internal ribosomal entry site
kDa	Kilodalton
LMP agarose	Low melting point agarose
LTR	Long terminal repeat
MAPK	Mitogen activated protein kinase

MEFs	Murine embryonic fibroblasts
MTT	Methylthiazolyldiphenyl-tetrazolium bromide
NAC	N-acetylcysteine
NADPH	Nicotinamide adenine dinucleotide phosphate
NFκB	Nuclear factor κB
nucmemb	Nuclear membrane anchor
pac/ Puro	Puromycin acetyltransferase
PAGE	Polyacrylamide gel electrophoresis
PBS	Phosphate buffered saline
PEITC	Phenyl ethyl isothiocyanate
Prx	Peroxiredoxin
PFA	Paraformaldehyde
PI	Propidium iodide
ROS	Reactive oxygen species
SAPK/JNK	Stress activated protein kinase /Jun-amino terminal kinase
Se	Selenium
SDB-F	7-fluoro-benzo-2-oxa-1,3-diazole-4-sulfonate
SDS	Sodium dodecyl sulfate
Sec (U)	Selenocysteine (21st amino acid)
SECIS	Selenocysteine insertion sequence
SFFV	Spleen focus forming virus
SF-tag	Strep-FLAG-tag
SF-Txnrd1	Strep-FLAG tagged mouse thioredoxin reductase 1
TEP Au	Triethylphosphine gold (I) chloride
TNF	Tumour necrosis factor
Trx	Thioredoxin
TrxR1	Human thioredoxin reductase 1
Txnrd1	Murine thioredoxin reductase 1 gene
Txnrd1	Murine thioredoxin reductase 1 protein
Txnrd2	Murine thioredoxin reductase 2 (mitochondrial isoform)
Wt	Wild-type

1. Introduction

Maintenance of a reduced intracellular environment is crucial for the survival of cells. This is underscored by the fact that life evolved in an anaerobic, non-oxidative environment, which not only prevented the destruction of nascent macromolecules from oxidation, but also provided the conditions in which fundamental enzymatic and biochemical reactions were invented and integrated in simple metabolic pathways. The products of anaerobic metabolisms like ethanol, sulfide and nitrite have antioxidant properties. So when aerobic life forms began to appear and oxygen was used for respiration, antioxidants were probably available to protect them against oxygen radicals produced during aerobic metabolism (Symons and Gutteridge, 1998). Subsequently, microorganisms acquired oxygen tolerance in a gradually oxidizing environment by inventing the antioxidant defense systems and abandoning the molecules which were highly prone to oxidation. Even today, oxidative microenvironments are compartmentalized within cells (mitochondria, endoplasmic reticulum, peroxisomes, and phagosomes), and the cytoplasm displays a network of enzymes and molecules exclusively dedicated to maintain the reduced intracytoplasmic condition (Lopez-Mirabal and Winther, 2008). Being known for their antimicrobial and apoptosis-inducing capabilities, reactive oxygen species (ROS) were initially considered to exert detrimental effects on cell survival. However, a clearer understanding of redox chemistry showed that mammalian cells produce H_2O_2 also to mediate various physiological responses (Rhee et al., 2000). Compelling evidence established that “redox” regulation of protein function is an additional regulatory mechanism of normal cell physiology, and perturbation of which may lead to oxidative stress-mediated patho-physiological processes like Alzheimer and cancer (Rhee, 2006). The present study aims to dissect the role of one component of the antioxidant defense system, the **cytosolic thioredoxin reductase,** in physiology and disease.

2. Review of Literature

2.1 Reactive oxygen species in physiology and disease development

2.1.1 Reactive oxygen species- sources and effects

With the emergence of free oxygen in the environment, the metabolic processes ultimately shifted from fermentation to oxidative respiration; the latter being considerably more efficient in energy generation. The leakage of electrons from the electron transport chain during a stepwise single electron reduction of molecular oxygen to water (Figure 1) generates partially reduced oxygen-derived intermediates, so-called ROS, as inevitable by-products of the aerobic metabolism. Although ROS include superoxide anion (O_2^-), hydrogen peroxide (H_2O_2), the highly reactive hydroxyl radical ($HO^\bullet$), singlet oxygen ($^1O_2$), peroxyl radical ($RO_2^\bullet$), alkoxyl radical ($RO^\bullet$) and hydroperoxyl radical ($HO_2^\bullet$), H_2O_2 is the most extensively studied. H_2O_2 is very stable *per se*, but in presence of transition metal like iron and copper, its reduction generates highly reactive species. Being more reactive than molecular oxygen itself, ROS are primarily responsible for oxygen-mediated toxicity (Imlay, 2008).

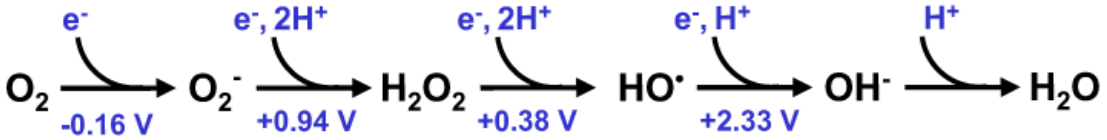

Figure 1. ROS are by-products of aerobic metabolism. Reactive oxygen species are generated during single electron reduction of oxygen. The redox state and standard reduction potential of each intermediate are depicted (**O_2** molecular oxygen, **O_2^-** superoxide anion, **H_2O_2** hydrogen peroxide, **$HO^\bullet$** hydroxyl radical, **OH^-** hydroxide) (Imlay, J.A.; 2008).

ROS can be generated by both exogenous and endogenous sources. Within the cell, ROS are mainly produced by the mitochondrial respiratory chain. 2% of the oxygen consumed by an organism is believed to be converted to O_2^- and H_2O_2 during normal respiratory processes in mitochondria due to single electron transfer through the respiratory chain to molecular oxygen. The concentration of ROS within normal cells has been estimated to be around 10^{-11} M for superoxide, 10^{-9} M for hydrogen peroxide, and 10^{-15} M for hydroxyl radicals. Additionally, xanthine oxidase, cytochrome P450, NADPH oxidase, peroxisomes and microsomes, arachidonic acid

metabolites, growth factor stimulation, and inflammatory responses against invading microorganisms contribute substantially to the overall ROS burden. Exogenous sources of ROS include environmental factors like radiation, non-genotoxic carcinogens, and xenobiotics that directly or indirectly inflict their deleterious effects by increasing ROS production (Valko et al., 2006). During evolution, biological systems have developed elaborate antioxidant defense systems and ROS-scavenging enzymes in order to adapt to the aerobic habitats and to harness the potential of ROS for purposeful chemistry in a highly controlled manner. Therefore, modern life forms maintain high titers of antioxidant systems.

2.1.2 ROS as signaling molecules

Over the last two decades, an extensive amount of research has revealed that ROS have dual functions in both physiology and diseases. Meanwhile, the implications of ROS as second messenger molecules in cellular signaling has been comprehensively elucidated and incorporated into the existing signaling pathways (Veal et al., 2007). A growing body of evidence indicates that redox signaling by ROS is an integral part of the normal metabolism in non-stressed cells, which is dramatically amplified or modulated under oxidative stress.

Unlike ligand-receptor interactions, which occur at macromolecular levels, ROS-mediated signaling involves chemical reactions at the atomic level, resulting in reversible covalent protein modifications (Nathan, 2003). Because of that, ROS have the ability to react indiscriminately with biological macromolecules. For example, a transient burst of oxidants generated in the vicinity of a receptor upon engagement provides specificity to the otherwise fleeting and short-lived ROS molecules. Thus, they act as second messengers for numerous receptor-agonists such as growth factors and hormones. Transient production of H_2O_2 has been shown as an important signaling event (Rhee, 2006; Valko et al., 2007) for many cell surface receptors like platelet derived growth factor (PDGF) (Sundaresan et al., 1995), epidermal growth factor (EGF) (Bae et al., 1997), basic fibroblast growth factor (bFGF) (Lo and Cruz, 1995), insulin (May and de Haen, 1979), granulocyte-macrophage colony stimulating factor (GM-CSF) (Sattler et al., 1999), cytokines like interleukin-1 (IL-1) (Krieger-Brauer and Kather, 1995), IL-3 (Sattler et al., 1999), interferon-γ (IFN-γ) (Lo and Cruz, 1995), tumor necrosis factor-α (TNF- α) (Krieger-Brauer and Kather, 1995; Lo

and Cruz, 1995), T cell receptor (Tatla et al., 1999) and GTP-binding protein (G-protein)-coupled receptors (GPCRs) like angiotensin II (Ushio-Fukai et al., 1999; Zafari et al., 1998). Results from PDGF or EGF receptor signaling studies showed that ligand-induced H_2O_2 production is required for the oxidation of the catalytically essential Cys residue and thus inactivation of protein tyrosine phosphatase (PTPs) to achieve a steady state level of protein tyrosine phosphorylation (Bae et al., 1997; Sundaresan et al., 1995). Subsequent reactivation of PTPs by electron donors (like thioredoxin in the case of PTP1B (Lee et al., 1998)) leads to the inactivation of the kinase and to an attenuation of the signal. The fact that receptor kinase-driven signaling can be inhibited by exogenous catalase (Sundaresan et al., 1995; Ushio-Fukai et al., 1999), the addition of the NADPH oxidase inhibitor diphenylene iodonium (Ushio-Fukai et al., 1999), or the administration of NAC (Cunnick et al., 1998; Greene et al., 2000) provides further evidence for a role of H_2O_2 in receptor signal transduction. The underlying molecular mechanism responsible for H_2O_2-mediated activation of several protein tyrosine kinases (PTKs) is the selective oxidation of redox-sensitive cysteine residues which are highly conserved in various non-receptor PTKs including Abl, Src, Lck and c-Ret and are crucial for their catalytic or transforming abilities (Rhee et al., 2000).

2.1.3 Thiol-based regulatory switches and principles of redox regulation

Reversible oxidation-reduction of the thiol group of cysteine residues in proteins is thought to be the major mechanism by which ROS modulate signal transduction pathways. Redox-sensitive cysteine residues in these proteins function as switches that exploit the unique chemistry of sulfur to flip from one oxidation state to the other on exposure to ROS (D'Autreaux and Toledano, 2007; Paget and Buttner, 2003). The mechanisms of redox signaling by selective thiol-disulfide exchange reactions and signal transmission can be explained by three models/pathways. The **thermodynamic model** implicates a change in cellular redox buffer (like oxidation of glutathione: GSH to GSSG) leading to the oxidation of the protein´s thiol groups, based on the redox potential of target cysteines. **The direct targeting model** takes the local environment of specific target cysteines into consideration for selectively enhanced reactivity towards the oxidants. In **the facilitated targeting model**, extremely reactive sensor proteins scavenge the signaling oxidant and facilitate the oxidation of target proteins through specific protein interactions and thiol exchange reactions (Figure 2) (Winterbourn and Hampton, 2008). The thiol-disulfide exchange

reaction is an evolutionary conserved mechanism of redox regulation for many transcription factors from prokaryotes (OxyR, OhrR, PpsR, SoxR) to eukaryotes (Yap1, Pap1, and Sty1 in yeast) and finally to mammalian cells (p53, AP1, NFκB, and NRF2 etc.) (D'Autreaux and Toledano, 2007; Paget and Buttner, 2003). Thus, redox regulation of cell signaling comprises the major regulatory networks of cells and has the capacity to modulate important aspects of cell physiology.

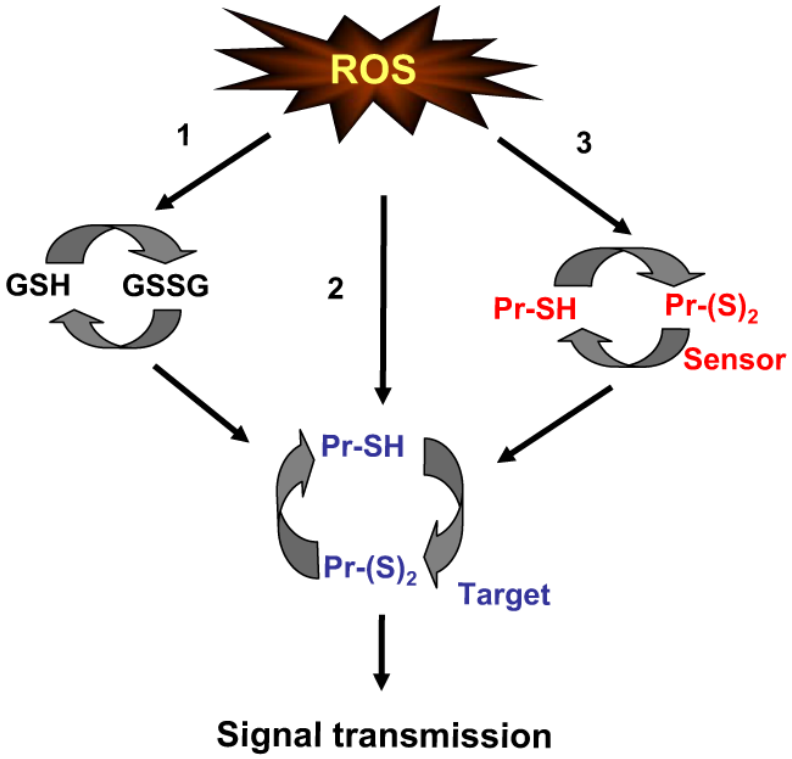

Figure 2. Generalized mechanisms of redox regulation of cell signaling. Exposure of cells to ROS causes selective oxidation of thiols of sensor/target proteins, change in redox balance and signal transmission. (1) Thermodynamic model (2) Direct targeting model (3) Facilitated targeting model. Pr: protein, sensor protein (in red) and target protein (blue) (modified from Winterbourn and Hampton; 2008)

2.1.4 Oxidative stress: The dark side of ROS

A state of oxidative stress ensues when the formation of ROS is greatly increased and/or protective mechanisms are compromised. If persistent, this can lead to oxidative damage of macromolecules (DNA, RNA, protein and lipid). ROS has been implicated in pro-inflammatory cytokine TNF-α, INF-γ and IL-1β-induced inflammatory responses (Yang et al., 2007), and in the induction of tissue injury as exemplified by oxidative damage in eye disorders like macular degeneration (Winkler et al., 1999) and cataracts (Truscott, 2000) and septic shock (Andresen et al., 2008; Victor et al.,

2004). While oxidative stress is one of the causes of aging, chronic oxidative stress has been implicated in conditions like diabetes mellitus, uremia, atherosclerosis, hyperlipidemia, rheumatoid arthritis, adult respiratory distress syndrome, ischemia/reperfusion injury, human immunodeficiency virus infection, cystic fibrosis, Friedreich's ataxia, neuro-degenerative disorders (Alzheimer, Parkinson), and cancer (Chinta and Andersen, 2008; Niwa, 2007; Ozben, 2007; Shi and Gibson, 2007; Valko et al., 2007). Since a major part of the present work is devoted to address the role of cytosolic thioredoxin reductase in tumor development, the role of oxidative stress in cancer shall be outlined in more detail in section 2.7.

2.2 Antioxidant defense systems

To antagonize the deleterious effects of ROS, numerous antioxidants have been invented during evolution. An antioxidant is defined as any substance that when present at a low concentration, compared to those of the oxidizable substrate, significantly delays, or inhibits, oxidation of that substrate (Halliwell, 1989). Antioxidants can act at many different stages in an oxidative sequence. For example, antioxidants can prevent radical formation by removing catalytic metal ions or by quenching oxygen, intercept formed radicals by scavenging key reactive oxygen species and initiating radicals, or by breaking the chain of an initiated sequence (Symons and Gutteridge, 1998). Many antioxidants have more than one mechanism of action. Based on their mode of action, they can be classified into enzymatic and non-enzymatic antioxidants.

2.2.1 Non-enzymatic antioxidants

Glutathione (GSH) is the major component of the non-enzymatic antioxidant pool which is present in millimolar concentration within cells. Vitamin E is an extremely efficient antioxidant when incorporated into the membrane bilayer. Together with β-carotene, vitamin E prevents lipid peroxidation. System $\mathbf{X_c^-}$ is a transmembrane anti-porter of cysteine. By regulating the extracellular and intracellular levels of cysteine, it contributes to the over-all antioxidant defense. Other non-enzymatic antioxidants include vitamin C, albumin, transferrin, metallothioneins, celuroplasmine, bilirubin, glucose, protein and non-protein thiols (β-mercaptoethanol, N-acetyl cysteine), free amino acids, metabolic intermediates, and small molecules.

2.2.2 Enzymatic antioxidants

The major enzymatic antioxidants are superoxide dismutases, catalases, cytochrome oxidase, glutathione peroxidases, glutaredoxins, glutathione reductase and thioredoxin/thioredoxin reductases. Their localization and function are summarized in Table1. Due to their relevance for the present study, system $\mathbf{X_c^-}$, the glutathione-dependent system, and the thioredoxin/thioredoxin reductase system, shall be described in detail in the following sections.

Table1: Enzymatic antioxidant defense systems within cells

Antioxidants	**Location**	**Functions**
Superoxide dismutases (Cu, Zn, Mn)	c, m	Conversion of superoxide to H_2O_2
Catalases	C	Removes H_2O_2 at high concentration
Glutathione peroxidases	c, n, m	Removes H_2O_2 (at low concentration) and organic hydroperoxides
Thioredoxins/thioredoxin reductases	**c, m**	**Thiol-disulfide oxidoreductase**
Peroxiredoxins	c, m	Reduction of H_2O_2 and organic hydroperoxides
Cytochrome oxidase (Cu)	M	Prevention of ROS formation during reduction of O_2 to H_2O
Glutaredoxin	c, m	Thiol-disulfide oxidoreductase
Glutathione reductase	C	Reduction of GSH and glutahionylated proteins

c= cytosol, n= nucleus, m= mitochondria

2.3 System X_c^- and the cystine/cysteine cycle

Cysteine (Cys) is a sulfur-containing amino acid in which the sulfur is contained in a sulfhydryl (-SH) group. By virtue of the ability of sulfur to exist in several oxidation states, thiols can exist in diverse forms like sulfhydryl (-SH), thiolate anion ($-S^-$), thilyl radical, disulfide (-S-S-), sulfenic (-SOH), sulfinic ($-SO_2H$), sulfonic ($-SO_3H$) and selenodisulfide (-Se-S-) groups depending on the oxidation status of the surrounding milieu. Thus, the oxidation of sulfhydryl groups serves as an important post-translational modification of redox-regulated proteins and makes them to work as molecular sensors or switches to perceive ROS burden and oxidative stress (Paget and Buttner, 2003). Cysteine residues not only determine the tertiary structure of proteins, but also regulate the functions by undergoing reversible oxidation-reduction.

Since the extracellular milieu is oxidizing, any free cysteine (Cys) is immediately

oxidized into cystine $(Cys)_2$. The extracellular cystine is imported across the membrane by system $\mathbf{X_c^-}$, a trans-membrane cystine/glutamate anti-porter that consists of xCT light chain which mediates cystine-transport specificity, and the 4F2 heavy chain (Sato et al., 1999). System $\mathbf{X_c^-}$ facilitates the uptake of cystine in exchange to glutamate at an equimolar ratio (Figure 3). Intracellularly, the imported cystine is reduced to cysteine. GSH has been considered as the major reducing power being present in millimolar concentration. Yet the mechanism of intracellular reduction of cystine is poorly understood as under GSH-depleted conditions the reduction of cystine is unperturbed (Banjac et al., 2008). The cysteine is then utilized for various processes. It mainly acts as precursor for GSH synthesis, it is used for protein biosynthesis or it remains as a source of free thiol. Although *xCT* knockout mice develop normally and are fully viable, *xCT*$^{-/-}$ mouse embryonic fibroblasts (MEFs) failed to survive in routine culture medium which can be rescued by supplementation with thiol-containing compounds like ß-mercaptoethanol and NAC (Sato et al., 2005). In fact, it has been shown that xCT overexpression sustains the proliferation of Burkitt´s lymphoma cells at low cell density (Banjac et al., 2008), and rescues GSH deficiency in *γ-GCS* knockout cells (Seiler, 2008). Thus, system $\mathbf{X_c^-}$ is the main driving force for the $(Cys)_2$/Cys cycle across the membrane and exerts its cyto-protective effect by facilitating cellular uptake of cystine, increasing intracellular cysteine concentration and strongly boosting the level of extracellular cysteine.

2.4 The glutathione-dependent system

2.4.1 Glutathione

Glutathione (L-gammaglutamyl-L-cysteinylglycine or GSH) is the predominant non-protein sulfhydryl compound in the cell (up to 10 mM) and serves as a ROS scavenger and co-factor of GSH utilizing enzymes. γ-glutamylcysteine synthetase (γ-GCS) is the rate limiting enzyme in glutathione synthesis. Deletion of *γ-GCS* in mice causes early embryonic lethality (E7.5) (Shi et al., 2000), which underscores the importance of GSH for viability. BSO was shown to be a selective inhibitor of γ-GCS (Spyrou and Holmgren, 1996) as the *γ-GCS*$^{-/-}$ ES-like cells were highly resistant to BSO treatment (Seiler, 2008). It is thus an important means to deplete GSH from the cells. γ-GCS along with glutathione synthetase (GSS) directs the synthesis of the tripeptide from cysteine (Cys), glutamate (Glu) and glycine (Gly). Glutathione has a multitude of functions. Being present in millimolar concentration, it serves as redox

buffer that maintains the redox state of the cell (Meister, 1994; Meister and Anderson, 1983). The cellular redox state, which largely depends on external stimuli, ROS burden, and antioxidant status, determines the cell fate. For example, proliferation occurs at a redox state of approximately -240 mV, differentiation at -200 mV and apoptosis at -170 mV (Watson et al., 2003). Within cells, GSH exists either in the reduced (GSH) form, the oxidized (GSSG) form or as mixed disulfide form with other proteins. Under normal conditions, about 1% of total cellular GSH is in the oxidized (GSSG) form.

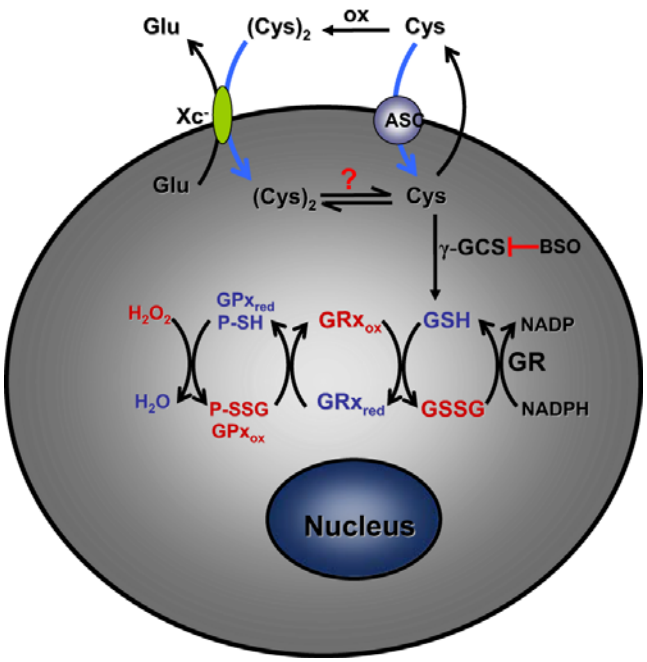

Figure 3. Schematic representation of the cysteine-glutathione-glutathione reductase axis. Cystine $(Cys)_2$ is imported into cells by system $\mathbf{X_c^-}$ in exchange for glutamate (Glu) and is then reduced intracellularly to cysteine (Cys). Cysteine is used for glutathione (GSH) and protein synthesis. A fraction of Cys is released into the extracellular space to maintain the redox balance of the surrounding environment. Protein-S-SG mixed disulfides are reduced by glutaredoxin (GRx). Oxidized GRx is recycled by GSH which is maintained in the reduced form at the expense of NADPH by glutathione reductase (GR). ASC: a shared amino acid transporter for Ala, Ser, and Cys, BSO: L-buthionine sulfoximine, a specific inhibitor of γ-GCS, GPx: glutathione peroxidase.

Although, the GSH/GSSG ratio may not have physiological significance *per se*, it is an important factor in determining the redox state of redox-sensitive cysteines in some proteins (e.g. glutaredoxins) involved in the redox regulation of cell signaling (Lillig et al., 2008). In conjunction with glutathione peroxidases, GSH is involved in the scavenging of ROS, in the inactivation of hydroperoxides, and in the detoxification of xenobiotics along with glutathione S-transferase. In addition, it also serves as a source of cysteine. Upon oxidative stress, GSH undergoes disulfide bond

formation either with itself (GSSG) or with other proteins (mixed disulfide: protein S-glutathionylation).

2.4.2 Glutaredoxin and glutathione reductase

Reversible protein S-glutathionylation is an important post-translational modification which not only provides protection to redox-active cysteines from irreversible oxidation, but also modulates the activities of diverse proteins. Thus, reversible S-glutathionylation of proteins has regulatory roles in cell signaling (Gallogly and Mieyal, 2007; Ghezzi, 2005) and has been reported for a number of key proteins like actin (Wang et al., 2001), glyceraldehyde 3-phosphate dehydrogenase (Mohr et al., 1999), protein tyrosine phosphatase 1B (Barrett et al., 1999; Kanda et al., 2006) , c-Jun (Klatt et al., 1999), the p50 subunit of NFκB (Pineda-Molina et al., 2001; Reynaert et al., 2006), caspase-3 (Sykes et al., 2007), and the Ras protein (Adachi et al., 2004).

The family of GSH-dependent oxidoreductases, the glutaredoxins (GRx), is responsible for the deglutathionylation of proteins. Glutaredoxins are small proteins of 9-15 kDa, which exist in all GSH-containing life forms in numerous isoforms. They are usually classified into two categories: the **dithiol GRxs,** which have two cysteines in their active site (-Cys-Pro-Tyr-Cys), and the **monothiol GRxs**, that are characterized by one redox-sensitive cysteine in their active sites (-Cys-Gly-Phe-Ser-). The cytosolic GRx (GRx1) and the mitochondrial GRx (GRx2) are two dithiol GRxs in yeast and mammals. Dithiol GRxs are general thiol-disulfide oxidoreductases with higher specificity towards protein-SSG mixed disulfide. Monothiol GRxs from *E. coli*, yeast and vertebrates including humans are crucially involved in iron-sulfur cluster biogenesis and the regulation of iron homeostasis (Fernandes and Holmgren, 2004; Lillig et al., 2008; Lillig et al., 2005).

Cytosolic glutaredoxin (GRx1) is the best characterized and probably the predominant deglutathionylating enzyme in mammalian cells as *Glrx1* knockout mice exhibited no deglutahionylating activity in tissues (Ho et al., 2007). Like GRx1, the mitochondrial isoform, GRx2, exhibits deglutathionylating activity, albeit 10-fold lower than GRx1. Human GRx2 was identified as the first glutaredoxin that contains a

redox-sensitive iron-sulfur cluster $[2Fe\text{-}2S]^{2+}$.

Glutaredoxins are the donors of reducing equivalents to ribonucleotide reductase and thus are involved in DNA synthesis together with thioredoxin/thioredoxin reductase (Camier et al., 2007; Gon et al., 2006; Ortenberg et al., 2004; Padovani et al., 2001). Glutaredoxins play important roles in diverse physiological processes like iron homeostasis and heme biosynthesis, maintenance of mitochondrial integrity and prevention of mitochondria-mediated cell death (GRx2), protection of airways from oxidative stress (GRx1and GRx2), protection of cardiac tissue from ischemia-reperfusion injuries, and protection of neurons from dopamine-induced apoptosis (GRx1). Glutathione reductase is the enzyme that keeps GSH in its reduced state by utilizing the reducing equivalents from $NADPH/H^+$. Thus, it is the driving force behind the GSH-dependent antioxidant system which provides a redox buffer and maintains the redox balance within the cell.

2.4.3 Glutathione peroxidase (GPx)

Mammalian GPxs are GSH-dependent peroxidases that reduce H_2O_2 and alkyl hydroperoxides to H_2O and the respective alcohols. Out of seven isoforms (GPx1-7), GPx1-4 and GPx6 (in human) are selenoproteins. GPx5, GPx7 and mouse GPx6 are non-Sec containing Cys homologues. GPx4 is a phospholipid hydroperoxidase and is essential for embryonic development (Garry et al., 2008; Imai and Nakagawa, 2003; Yant et al., 2003) and male fertility (mitochondrial GPx4; Schneider et al., submitted). Recently it has been shown by Seiler et al. that GPx4 is involved in the prevention of lipid peroxidation and is crucial for the viability of cells and neurons (Seiler et al., 2008).

2.5 The thioredoxin/thioredoxin reductase (Trx-TrxR) system

The thioredoxin-dependent system is another NADPH-driven thiol/disulfide oxidoreductase system, ubiquitously presents in the 3 kingdoms, archaea, bacteria and eukarya which is involved in redox regulation and antioxidant defense responses. Additionally, the Trx-TrxR system of bacteria, yeast and mammals is involved in regulating DNA synthesis, gene transcription, cell growth and apoptosis. It consists of thioredoxin, thioredoxin reductase and thioredoxin-dependent

peroxidases (peroxiredoxins) (Hirota et al., 2002; Mustacich and Powis, 2000; Nakamura, 2005). As thiol-disulfide oxidoreductases, all thioredoxins catalyze the reduction of protein disulfides with much higher efficiency than dithiothreitol (DTT) or GSH. Across the phylum, two distinct thioredoxin reductases are found which have different catalytic mechanisms and a mutually exclusive distribution, reflecting a complex evolutionary origin (Figure 4). Most of the archaea, bacteria, eukarya including fungi, plants and the protozoan parasites contain a low molecular weight dimeric thioredoxin reductase (L-TrxR) apparently originating from bacteria. L-TrxR is a specific 35 kDa flavoprotein with a disulfide/dithiol active site (Hirt et al., 2002).

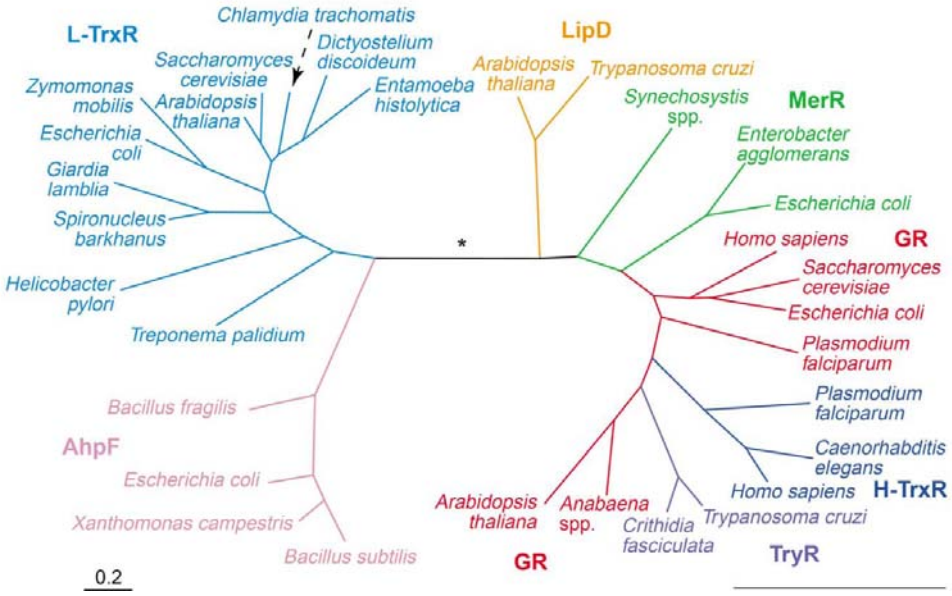

Figure 4. Phylogenetic relationships among members of the oxidoreductase family. H-TrxR: high molecular weight thioredoxin reductase, TryR: trypanothione reductase, GR: glutathione reductase, MerR: mercuric reductase, LipD: lipoamide dehydrogenase, L-TrxR: low molecular weight thioredoxin reductase, AhpF: alkyl hydroperoxide reductase F52A. (Adapted from Hirt et al.; 2002).

By contrast, in higher eukaryotes (including humans, *C. elegans* and Drosophila) and apicomplexan protozoa, this enzyme has been replaced by a high molecular weight thioredoxin reductase (H-TrxR) which also exists as dimer. Unlike L-TrxR, H-TrxR is a larger, 56-65 kDa, selenium-containing flavoprotein with two redox-active catalytic centers and a broad substrate specificity that includes non-disulfide substrates such as hydroperoxides, vitamin C or selenite. H-TrxR is related to glutathione reductase (GR), trypanothione reductase (TyrR), mercuric reductase (MerR), and lipoamide dehydrogenase (LipD), while L-TrxR is related to the alkyl hydroperoxide reductase F52A (AhpF). Although L-TrxR and H-TrxR are homologous proteins, they have

evolved in different ways and probably have converged to the same substrate specificity independently (Hirt et al., 2002).

2.5.1 The mammalian thioredoxin system

The mammalian thioredoxin system is highly complex in organization, regulation and function. It consists of mainly two forms: the well characterized cytosolic form comprises thioredoxin 1 (Trx1) and thioredoxin reductase 1 (TrxR1), while the mitochondrial form is composed of thioredoxin 2 and its respective reductase (TrxR2). Although both systems are general protein disulfide-oxidoreductases, they display some unique functions in their different subcellular compartments. In addition to the mitochondrial and cytosolic thioredoxin reductases, a third thioredoxin reductase, designated thioredoxin/glutaredoxin reductase (TGR), which is predominantly expressed in testis, has been reported in mammals. Due to an additional monothiol glutaredoxin domain extension at its N-terminal end, it can reduce both, Trx as well as GSSG and GSH-linked disulfides in *in vitro* assays (Sun et al., 2001a). The cytosolic thioredoxin system will be described in detail in the following sections with reference to the mitochondrial thioredoxin system.

2.5.2 Thioredoxins

Thioredoxin is a small 10-12 kDa protein, with two redox-active cysteinyl residues organized in a characteristic **thioredoxin fold** with the sequence **-Cyc-Gly-Pro-Cys-** (Martin, 1995). It catalyzes thiol-disulfide exchange reactions (Holmgren, 1985). Thioredoxin was originally purified from *E. coli* in 1964 (Laurent et al., 1964) and identified as electron donor to ribonucleotide reductase. The human thioredoxin was originally cloned as a cytokine-like factor, named adult T-cell leukemia-derived factor, produced by human T-cell leukemia virus type I-transformed cells (Tagaya et al., 1989) and as an autocrine growth factor produced by Epstein-Barr virus-transformed cells (Wollman et al., 1988).

Unlike glutathione and glutathione-dependent enzymes, which are ROS scavengers, thioredoxin plays a crucial role in the redox regulation of gene expression. It shows more than 1000-fold higher activity for the transcription factors NFκB and AP-1 than GSH. Thus, thioredoxin is actively involved in the activation of transcription factors

regulating the expression of stress responsive genes and oxidative stress-induced apoptosis (Nakamura, 2004). In fact, it has been shown that binding of thioredoxin inhibits the kinase activity of ASK-1 (Saitoh et al., 1998), and the oxidation of thioredoxin 1 upon oxidative stress liberates ASK-1 to activate the downstream MAP kinase p38 dependent apoptosis pathway (Nadeau et al., 2007). Trx1 and Trx2 are essential in mammals because genetic disruption of both genes is embryonic lethal (Matsui et al., 1996; Nonn et al., 2003b). Conversely, overexpression of human thioredoxin in transgenic mice not only enhances the longevity (Mitsui et al., 2002), but also confers resistance towards various stress-inducing agents including adriamycin-induced cardiotoxicity, thioacetamide-induced acute hepatic injury and inflammatory cytokine- or bleomycin-induced acute lung injury (Nakamura et al., 2002), and prevents retinal photic injury (Tanito et al., 2002). Conversely, impaired induction of thioredoxin has been associated with increased oxidative stress, immune-dysfunction, cardio-vascular diseases, and hypertension in spontaneous hypertensive rats (Tanito et al., 2004). It has been shown that thioredoxin 1 is secreted by leukocytes and exhibits cytokine-like properties. Truncated thioredoxin (Trx-80), a truncated form of the human cytosolic thioredoxin, is also secreted from cells and even displays greater cytokine-like activity than thioredoxin (Pekkari et al., 2001; Pekkari et al., 2003; Pekkari and Holmgren, 2004). Serum/plasma levels of thioredoxin are elevated after infection, ischemia-reperfusion and oxidative stress and it correlated positively with the severity of cardiac disease (Kishimoto et al., 2001). Increased plasma levels of thioredoxin in HIV-patients are associated with poor prognosis (Nakamura et al., 2001), while in hepatitis C patients increased plasma levels predict clinical responses to interferon therapy (Sumida et al., 2001). Recently it has been shown that thioredoxin 1 interferes with the binding of the CD30 ligand (CD30L) to its receptor and prevents the CD30-induced decrease in cytotoxic effector functions of effector cells (Schwertassek et al., 2007). The role of thioredoxin in cancer is discussed in section 2.7.2.

2.5.3 The mammalian thioredoxin reductases

Several of the proteins involved in antioxidant defense and redox regulations are selenoproteins, including mammalian thioredoxin reductases. The incorporation of selenium as selenocysteine in these proteins is partly responsible for their antioxidant function. Mice lacking the gene encoding selenocysteine (Sec)-specific tRNA are early embryonic lethal (Bosl et al., 1997). Selenium is incorporated co-translationally

in the form of Sec at the C-terminus of TrxR within a tetrapeptide motif (-Gly-Cys-Sec-Gly-COOH). Selenium is essential for TrxR activity since a mutation leading to the exchange of selenocysteine to cysteine causes a marked decrease in the catalytic activity of TrxR (to or below 5%) (Gladyshev et al., 1996; Lee et al., 2000; Nordberg et al., 1998; Tamura and Stadtman, 1996; Zhong et al., 2000; Zhong and Holmgren, 2000). Moreover, TrxR activity is severely impaired in selenium-deficient animals. While addition of nanomolar concentrations of selenium increases TrxR activity several-fold without increasing protein levels significantly in human cancer cells lines (Gallegos et al., 1997) and in the human endothelial cell line EAhy926 (Lewin et al., 2002), TrxR activity in cell lines of lymphoid origin seem to be unaffected by selenium supplementation (Gallegos et al., 1997; Spyrou et al., 1996). In contrast to mammalian TrxR, TrxR from *Drosophila melanogaster* (DmTrxR) is a Cys-containing variant (Bauer et al., 2003); yet its catalytic competence towards Trx is similar to Sec-containing orthologues. Thus, it seems that the role of selenium in TrxR activity is rather complex. Accordingly, it has been proposed that the incorporation of selenium in TrxR increases the number of substrates, improves the enzyme efficiency and sustains enzyme activity in diverse microenvironments (Gromer et al., 2003).

2.5.3.1 The mitochondrial thioredoxin reductase (TrxR2)

The mitochondrial thioredoxin reductase (TrxR2 also known as TR3 or Txnrd2) along with mitochondrial thioredoxin (Trx2) and thioredoxin-dependent peroxidase, peroxiredoxin 3 (Prx3), make up the mitochondrial thioredoxin-dependent antioxidant system. The mouse *Txnrd2* gene was mapped to chromosome 16 (Kawai et al., 2000) and encodes a 57 kDa protein of 527 amino acid residues with a mitochondrial leader sequence. Several splice variants of TrxR2 have been reported with one form encoding a cytosolic version of TrxR2 (Turanov et al., 2006). However, the biological implications of these variations have not been resolved and additional biochemical and structural characterizations of the enzymes are awaited. TrxR2 is highly expressed in liver, heart, hematopoietic system and kidney. The involvement of TrxR2 in the maintenance of mitochondrial integrity and the regulation of mitochondria-dependent apoptosis was revealed by targeted disruption of *Txnrd2* in mice, which resulted in embryonic lethality (E13.5) (Conrad et al., 2004). *Txnrd2* null embryos showed severe anemia due to increased apoptosis of fetal blood cells in the liver, perturbed cardiac development, and growth retardation. *Txnrd2*-deficient

fibroblasts were susceptible to GSH depletion and showed increased ROS levels which can be prevented by NAC supplementation (Conrad et al., 2004). Cardiac tissue-specific deletion of *Txnrd2* led to post-natal death due to biventricular dilated cardiomyopathy and mitochondrial abnormalities in cardiomyocytes.

2.5.3.2 The cytosolic thioredoxin reductase (TrxR1)

2.5.3.2.1 Genomic organization of mouse and human cytosolic thioredoxin reductase

Cytosolic thioredoxin reductase is located on mouse chromosome 10 (Kawai et al., 2000) and encoded by 15 exons (Osborne and Tonissen, 2001). Exon 15 contains the coding region for the C-terminal catalytic center, including the Sec codon UGA, the selenocysteine insertion sequence (SECIS) element, the AU-rich elements, and the translation termination signal. The overall organization of the mouse *Txnrd1* gene is similar to that of the human gene, which is on chromosome 12 and consists of 16 exons (Gasdaska et al., 1996). Alternative splicing of human *TrxR1* gives rise to 21 different transcript variants which differ at the 5´end (Rundlof et al., 2007; Rundlof et al., 2004). Translation of the protein can initiate at two ATG start codons located in exons 3b and 4 of mouse *Txnrd1* that are in the same reading frame (Figure 5). Translation initiation from the ATG in exon 4 produces the originally reported 54.5 kDa protein, while translation initiation at the start codon in exon 3b yields a protein with a predicted molecular mass of 67 kDa (Sun et al., 2001b). The core promoter of the human *TrxR1* gene has a high GC contents, contains binding sites for Oct1, Sp1, and Sp3, and lacks a classical TATA box. This indicates that TrxR1 is a house keeping gene, although it is up-regulated at the mRNA and protein level in response to various exogenous stimuli. The mouse *Txnrd1* promoter lacks binding sites for Oct1, Sp1 and Sp3, but has two conserved AP-1 binding sites (Osborne and Tonissen, 2001). The complex promoter structure and the numerous alternatively spliced transcripts are probably an indication of a tissue-specific gene regulation mediated by various control elements (Rundlof et al., 2000).

Apart from the complex genomic organization and alternative splicing, the mRNA of mouse and human thioredoxin reductase 1 shows non-AU-rich and AU-rich instability elements (AREs) in the 3´UTR (4 in human and 3 in mouse), that mediate rapid degradation of the mRNA (Gasdaska et al., 1999). AREs are typically found in

transcripts that undergo rapid turnover like mRNA encoding for cytokines, proto-oncogenes, growth factors and transcription factors (Chen and Shyu, 1995), and the inactivation of AREs have been implicated in the promotion of cellular transformation and oncogenesis (Aghib et al., 1990). Both human *TrxR1* and mouse *Txnrd1* mRNA have SECIS elements in the 3´UTR that facilitate the incorporation of Sec by the UGA codon.

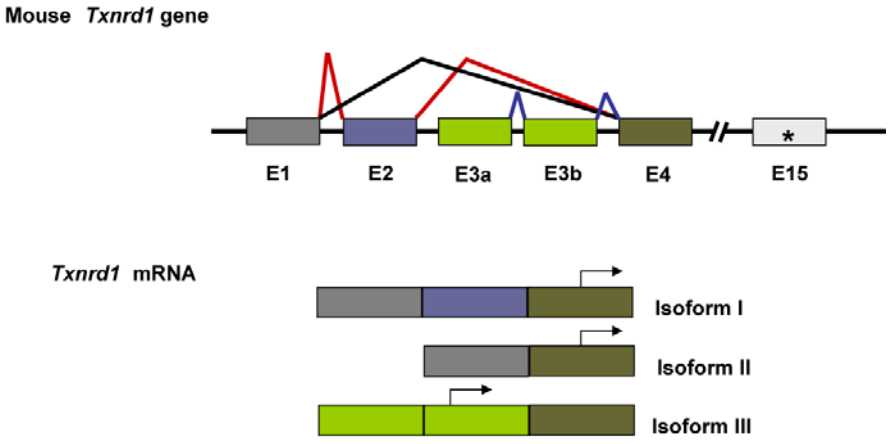

Figure 5. Genomic organization and alternative splicing of the mouse *Txnrd1* gene. Located on chromosome 10, the mouse thioredoxin reductase1 gene consists of 15 exons (1-15). Three isoforms are generated by alternative splicing. Exon 15 encodes the C-terminal catalytic center, including the Sec codon UGA (marked with *), the SECIS element, the AU-rich elements, and the translation termination signal. Arrows indicate translational start codon (Modified from Osborne & Tonissen; 2001)

2.5.3.2.2 Structural organization and catalytic mechanism of TrxR1

The homodimeric selenoprotein TrxR1 consists of two identical subunits of 54 kDa, arranged in a head to tail fashion. Each subunit has one FAD-binding domain, one NADPH-binding site, and an interface domain. There are two redox-active catalytic centers; one located in the N-terminal FAD-binding domain formed by the **-Cys-Val-Asn-Val-Gly-Cys-** sequence and the other is formed by the C-terminal tetrapeptide motif **-Gly-Cys-Sec-Gly-COOH**. The C-terminal catalytic center is exposed and located in a flexible arm and is believed to be responsible for the broad substrate activity of mammalian TrxR1 (Gromer et al., 1998). The catalytically active reaction center is formed by the N-terminal redox active site (C^{59}-XXXX-C^{64}) of one subunit and the C-terminal redox active site (-Cys^{497}-Sec^{498}-) of the other subunit. Thus, each homodimer has two independent, catalytically active centers and the enzyme is only active after dimerization. Catalysis of mammalian thioredoxin reductase shows a ping-pong mechanism, which involves reversible transfer of electrons from

$NADPH/H^+$ via a system of redox-active disulfides (Figure 6B). It is proposed that electrons flow from $NADPH/H^+$ to the FAD, from there to the N-terminal redox-active disulfide in the enzyme and then to the C-terminal catalytic center of the other monomer which finally reduces thioredoxin or other substrates (Holmgren, 1985; Lee et al., 2000; Zhong and Holmgren, 2000). The reaction catalyzed by thioredoxin reductase is readily reversible and $NADPH/H^+$ may be formed from reduced thioredoxin (Trx-$(SH)_2$) and $NADP^+$. Recently, the crystal structure of rat TrxR1 was resolved by Arner´s group (Cheng et al., 2009), which supports the previously proposed mechanism and provided additional insight (Figure 6A).

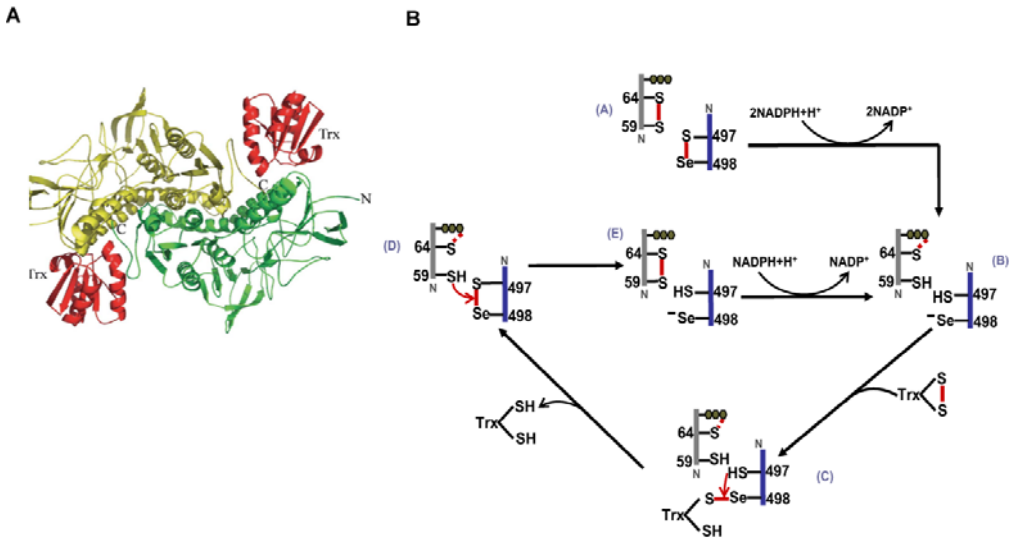

Figure 6. Crystal structure and catalytic mechanism of mammalian thioredoxin reductase. (A) Crystal structure of rat thioredoxin reductase 1. Two subunits are shown in yellow and green, Trx in red (Cheng et al.; 2009). (B) Proposed catalytic mechanism by mammalian TrxR1. Trx is the natural substrate for thioredoxin reductase. Two subunits are shown in gray and blue, catalytic cysteine and selenocysteine are depicted with their amino acid numbers, the flow of electrons is depicted by a red arrow, disulfide bonds are in red, hexagonal boxes represent FAD. Trx: Thioredoxin, TrxR1: Thioredoxin reductase (adapted from Zhong et al.; 2000).

2.5.3.2.3 Physiological function of TrxR1

Mammalian TrxRs are promiscuous enzymes as they reduce diverse classes of physiological substrates including protein-disulfides and non-disulfide substrates such as hydroperoxides (including lipid peroxides), vitamin C (May, 2002; May et al., 1998), selenite (Kumar et al., 1992), α-lipoic acid (Arner et al., 1996), α-tocopherol, ubiquinone, NK-lysin (Andersson et al., 1996), L-cystine (Luthman and Holmgren, 1982), alloxan, and vitamin K as well as non-physiological compounds like DTNB and NBT (Nordberg and Arner, 2001). Since Trx is involved in a large number of physiological functions like antioxidant defense, control of transcription factor activity

(p53, AP-1, NFκB and HIF), growth and proliferation, a majority of biological functions assigned to thioredoxin reductase are actually thioredoxin dependent (as depicted in Figure 7). Also, the expression of Trx in tissues is more abundant than TrxR at the mRNA level (Jurado et al., 2003), and the deletion of the Trxs has more severe effects than when thioredoxin reductases are disrupted (Conrad et al., 2004; Jakupoglu et al., 2005; Matsui et al., 1996; Nonn et al., 2003b). To date it has remained difficult to distinguish between the thioredoxin-dependent and thioredoxin-independent functions of thioredoxin reductases.

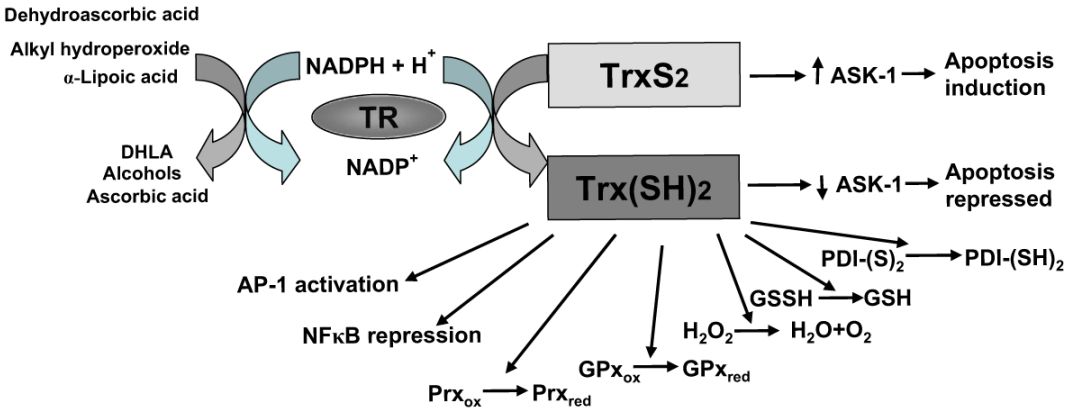

Figure 7. Physiological functions of the mammalian thioredoxin system. As depicted, the majority of the functions of thioredoxin reductase are thioredoxin-dependent. Peroxiredoxins are thioredoxin-dependent peroxidases that play an important role in the removal of H_2O_2. Additionally, thioredoxin reductase plays an important role in the reduction of non-enzymatic antioxidant compounds like dehydroascorbic acid, α-tocopherol and lipoic acid. Prx: peroxiredoxin, GPx: glutathione peroxidase, PDI: protein disulfide isomerase, ASK-1: apoptosis stimulating kinase-1, DHLA: dihydrolipoic acid, TR: thioredoxin reductase (Adapted from Nordberg & Arner; 2001)

Thioredoxin is one of the electron donors for ribonucleotide reductase which maintains the dNTP pool required for DNA synthesis. In all organisms studied so far, loss of Trx and/or TrxR leads to severe proliferation defects, decreased DNA synthesis, and retarded growth. Targeted disruption of thioredoxin reductase 1 in mice resulted in embryonic lethality at E10.5 due to severe growth retardation and widespread developmental abnormalities, indicating that it is indispensable for cell proliferation (Jakupoglu et al., 2005). Additionally, TrxR1 is a direct target of the oncogene *c-myc* (Schuhmacher et al., 2001) and is reported to be up-regulated in various tumors, further emphasizing the role of TrxR1 in cell proliferation. The role of TrxR1 in tumorigenesis is discussed in section 2.7.2

The thioredoxin-dependent system is an important antioxidant system within the cell that provides protection against ROS. The antioxidant function of TrxR1 seems to be dependent on Trx1 as Trx1 has been shown to prevent apoptosis in cells treated with agents known to produce ROS (Spector et al., 1988). TrxR can directly reduce peroxides including hydrogen peroxide and lipid hydroperoxides (Bjornstedt et al., 1995) and act as H_2O_2 scavenger at elevated levels (Zhong and Holmgren, 2000). Furthermore, TrxR1 has an important role in the reduction and recycling of many non-enzymatic antioxidants like ascorbic acid, vitamin E and α-lipoic acid, which, in addition to GSH, contribute to the cellular redox buffer (Nordberg and Arner, 2001). By reducing dehydroascorbate to ascorbic acid, TrxR1 plays an important indirect role in protecting cells from oxidative stress. Since ascorbate is involved in the reduction of α-tocopherol radicals, TrxR1 may play an important role in the antioxidant function of vitamin E. Thus, by scavenging hydroperoxides (especially lipid hydroperoxides), recycling ascorbate and regenerating vitamin E, TrxR1 plays an important role in the protection of membrane from oxidative damage. In fact, the sparing effects of vitamin E and selenium can be attributed to TrxR (Tamura et al., 1995). Owing to its pleiotropic effects, it is not surprising that alterations in TrxR1 function have been implicated in several patho-physiological conditions like rheumatoid arthritis, atherosclerosis, reperfusion injuries, and cancer (Gromer et al., 2004).

2.5.4 Peroxiredoxins

Peroxiredoxins are thioredoxin-dependent peroxidases which are critically involved in H_2O_2 scavenging (Wood et al., 2003a). Mammalian peroxiredoxins are classified into three sub-groups: 1) **2-Cys peroxiredoxins,** 2) **Atypical 2-Cys peroxiredoxins** 3) **1-Cys peroxiredoxin.** 2-Cys peroxiredoxins require 2 redox-active cysteines (a peroxidatic and a resolving cysteine) for catalysis and include the cytosolic isoforms Prx1 and Prx2, the mitochondrial isoform Prx3, whereas Prx4 is located in the endoplasmatic reticulum and may be secreted as well. Atypical 2-Cys peroxiredoxins and 1-Cys peroxiredoxins have only N-terminal redox-active cysteines and are represented by Prx5 and Prx6, respectively (Rhee et al., 2005a).

All Prxs exist as homodimers and contain a conserved N-terminal cysteine residue, which is the primary site for oxidation by H_2O_2. Prxs are involved in reducing hydroperoxide, alkyl hydroperoxides and peroxynitrite. They also regulate peroxide-mediated signaling cascades (Rhee et al., 2005b; Wood et al., 2003b). Prxs have been implicated in c-Myc-mediated transformation and apoptosis. Over-expression of Prxs protects tumor cells against hypoxia (Nonn et al., 2003a), and the over-expression of Prxs in many cancers is correlated with resistance to apoptosis induced by radiation therapy (Park et al., 2000) or the anticancer drug cisplatin (Chung et al., 2001).

2.6 Redundancies between the GSH-dependent and the thioredoxin-dependent antioxidant systems

It is currently not known why there are two separate classes of thiol/disulfide oxidoreductases operating in the same compartment. Although both enzymes, thioredoxin reductase and glutathione reductase, are related evolutionary (Hirt et al., 2002), there is a fundamental difference between the two systems. That is there is a direct link between the reduction of disulfide bonds by thioredoxin and the oxidation of NADPH (The direct targeting model). But the involvement of GSH in the thiol/disulfide reduction by glutaredoxins adds another tier of complexity to the GSH-dependent system (The facilitated targeting model). Although under physiological conditions the reaction rates of GSH and GSSG are too slow to be of great importance, the values of the GSH-GSSG redox potential are close to the midpoint redox potential for GRxs which are ideal candidates for sensing and transducing the signals associated with changes in the GSH-GSSG redox state as they can be GSH-dependent reductases at -240 mV and GSSG-dependent oxidases at -170 mV (Aslund et al., 1997; Lillig et al., 2008). Thus the glutaredoxin-dependent thiol/disulfide reduction is coupled with the change in the glutathione pool, which is the deciding denominator of the efficiency and direction of the glutaredoxin pathway. In all likelihood it is conceivable that the GSH-dependent system is involved in the maintenance of redox homeostasis, while the thioredoxin-dependent system fulfills specialized functions in proliferation, differentiation etc. Both, thioredoxin and glutaredoxin are donors of reducing equivalents to ribonucleotide reductase and thus involved in the maintenance of the dNTP pool and DNA synthesis (Figure 8).

The redundancies between the two pathways are apparent by the fact that in the absence of only one of the pathways, bacterial and yeast strains can survive and grow reasonably well. As reported in yeast, the deletion of both thioredoxins (*Δtrx1 and Δtrx2*) results in slow DNA replication and impaired sulfate assimilation, but viability is only compromised when both cytosolic isozymes thioredoxin and glutaredoxin were lacking (Muller, 1996; Trotter and Grant, 2003; Trotter and Grant, 2005). Limited growth of the triple mutant (*trx1 trx2 glr1* mutant) can be restored under anaerobic condition which showed that although both the systems are involved in the maintenance of the dNTP pool, the lethality is due to perturbation of the redox balance rather than DNA synthesis. This is further supported by the fact that reduced GSH failed to rescue the growth of the triple mutant. Elevated levels of GSSG in *trx1 trx2* mutants showed a link between the thioredoxin system and the redox status of GSH in the cell (Muller, 1996).

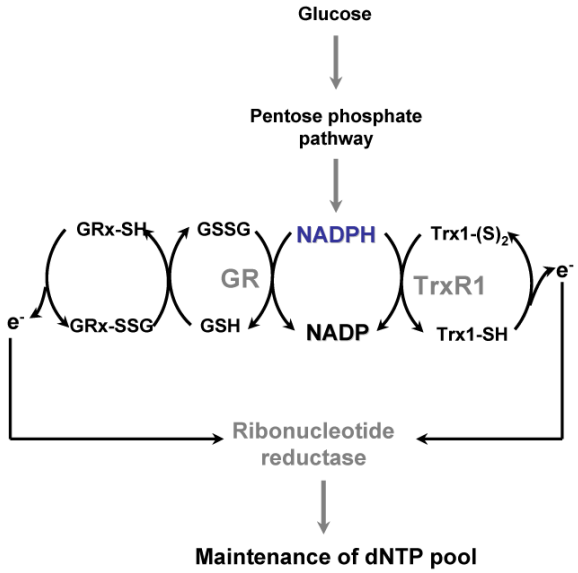

Figure 8. Maintenance of the dNTP pool by thioredoxin and the GSH/glutaredoxin systems. Thioredoxin and glutaredoxin are known donosr of reducing equivalents to the ribonucleotide reductase that maintains the dNTP pool and thus DNA synthesis. Trx: Thioredoxin, TrxR1: Thioredoxin reductase 1, GR: Glutathione reductase, GRx: Glutaredoxin, GSH: Glutathione, GSSG: Oxidized GSH

The redundancy between the two systems in mammals is still unclear and rather complex. The deletion of the thioredoxin system is embryonic lethal (*Trx1, Trx2, Txnrd1, Txnrd2*) in mice. The individual disruption of *Glrx 1, Glrx2 and Gsr* is dispensable but the deletion of *γ-GCS* is lethal in mice. This could be due to the complex organization of the mammalian redox systems. In mice, members of the thioredoxin pathway (*Trx1, Trx2, Txnrd1* and *Txnrd2*) are more regularly

expressed in different organs than mRNA species of the glutathione-dependent pathway (*Glrx1, Glrx2 and Gsr*) (Jurado et al., 2003), indicating a broader involvement of the thioredoxin system in diverse metabolic functions. Hence, both systems appear to have redundant functions, but the extent of redundancy as well as common targets have not been identified yet. A better understanding of these two systems is mandatory for exploring the possibility of targeting these enzymes to treat oxidative stress-associated diseases.

2.7 Interplay of ROS and antioxidants in tumor development

Cancer is a multi-factorial metabolic syndrome characterized by novel acquired capabilities of self-sufficiency in growth with unlimited replicative potential by suppressing the growth-inhibitory pathway or evading the apoptotic machinery (Hanahan and Weinberg, 2000). Whether ROS play a pivotal role in cancer biology is still contentious even though it has been known for a long time that tumor cells in culture produce more ROS than non-transformed cells (Szatrowski and Nathan, 1991). Owing to the chicken/egg nature of the question, it is hard to define a causal link between ROS and tumor formation. Recently, Trachootham et al. showed in an elegant study that the transformation event is followed by an increase in ROS production (Trachootham et al., 2006), presumably due to oncogene-induced replicative stress. Thus, accumulating evidence indicates that ROS are playing a crucial role in tumor initiation, progression, proliferation, and metastasis as well as necrosis and regression as discussed below (Figure 9).

A state of chronic oxidative stress resulting from increased ROS production or loss of antioxidant function can irreversibly inactivate the regulatory circuitry of various signaling pathways and render them constitutively active (like receptor tyrosine kinase signaling, Ras signaling, MAP kinase signaling), which has long been implicated in the causation of various cancers. This self-sufficiency in growth signals drives the cells into continuous proliferation which may eventually lead to cancer.

ROS are notorious for their damaging effects on bio-macromolecules of which DNA damage is most detrimental, because it is stable, cumulative and inheritable. If sub-lethal, these mutations may either cause the activation of proto-oncogenes and/or

inactivation of tumor suppressor genes; thereby increase the likelihood of cancer initiation and progression. The subsequent accumulation of mutations in the genome can result in genomic instability which is one of the hallmarks of cancer (Kopnin, 2007; Rodrigues et al., 2008).

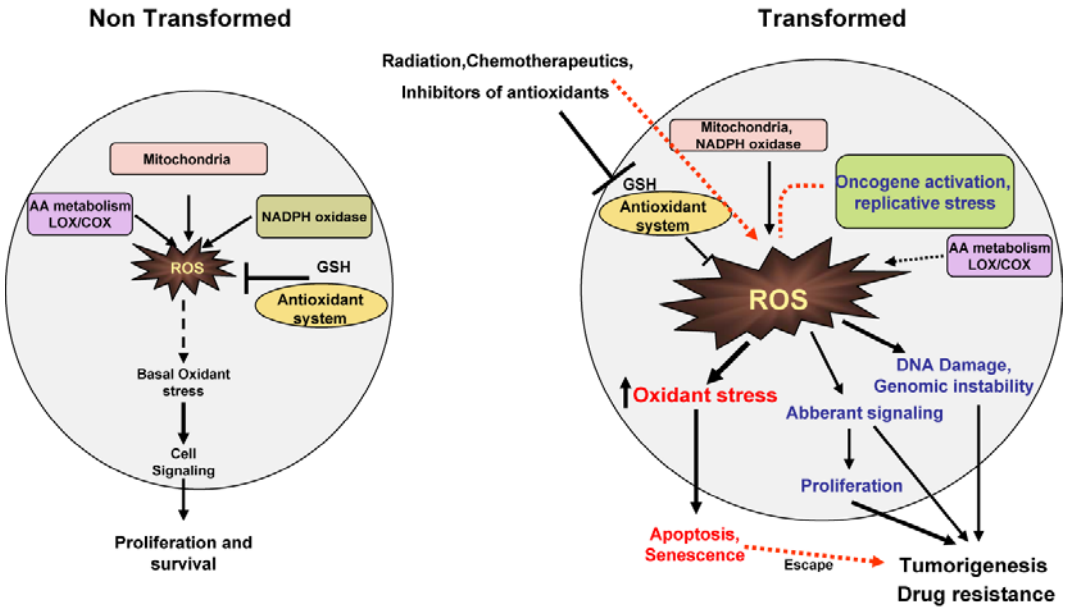

Figure 9. The role of ROS in cancer. By acting as mitogen and/or mutagen, ROS contribute to the formation and progression of tumors. Given that in transformed cells ROS production is higher than in non-transformed cells, agents that inhibit the antioxidant defense system or augment ROS production are novel chemotherapeutics against cancer. Events in red are barriers against cancer while events in blue promote tumorigenesis. Modified from (Schumacker, 2006).

In vivo growing solid tumors contain areas of low oxygen concentration (hypoxia), which was first postulated by Thomlinson and Gray in 1955 (Thomlinson and Gray, 1955). During the course of progression, fluctuations in oxygen concentration put a selective pressure on the cells. By shifting metabolism from aerobic respiration to anaerobic glycolysis, the cells can adapt to and grow in hypoxic conditions, an effect first observed by Warburg 50 years ago (Warburg, 1956). Increased nutritional and oxygen demand in growing tumors induces neo-vascularization. Aberrant blood flow in neo-vascularized tissue causes re-oxygenation, and these cycles of intermittent hypoxia followed by re-oxygenation result in increased ROS levels. The fluctuating microenvironment keeps the tumor cells in a state of persistent oxidative stress. Thus, ROS are thought to play an important role in maintaining the cancer phenotype by stimulating cell growth and proliferation (Hu et al., 2005), increasing genetic instability (Radisky et al., 2005), and facilitating evasion from senescence. Owing to their cancer-promoting effect, increased levels of ROS in cancer cells are often

considered as an adverse prognostic factor. Thus, the role of ROS in tumor development by promoting proliferation and genomic instability is a well-proven and established paradigm in cancer biology.

By contrast, Takahashi et al. reported that ROS have an unexpected role in tumor suppression by inducing and maintaining senescence in tumor cells (Takahashi et al., 2006). If this holds true, then the role of ROS and the redox balance will have an even more complex role in cancer causation and progression. Most likely, the diametrically opposed roles of ROS in tumor causation, growth and maintenance depend on the amount and tempo-spatial production of ROS, the antioxidant status and their interplay within the tumor microenvironment.

2.7.1 Components of the antioxidant system as drug targets for cancer chemotherapy

Selective toxicity against cancer cells is the key for the success of any chemotherapeutic compound. Although tumor cells maintain a high titer of antioxidants, the constitutive oxidative stress caused by the increased production/accumulation of ROS leads to the saturation of the antioxidant system in tumor cells, which can not afford to accommodate further accumulations of ROS. This limited availability of antioxidants in tumor cells may offer novel therapeutic options. A massive outburst of ROS in tumor cells may be achieved selectively by agents that increase ROS production or inhibit the antioxidant system. Thus individual components of the antioxidant system may constitute suitable drug targets for cancer chemotherapy. By targeting the glutathione-dependent antioxidant system with phenyl-ethyl isothiocyanate (PEITC), Trachootham et al. showed that the preferential accumulation of ROS in transformed cells causes oxidative damage to mitochondria, inactivation of redox-sensitive molecules, massive cell death and increased survival of tumor-bearing mice treated with PEITC (Trachootham et al., 2006). Likewise, targeting the thioredoxin-dependent system by knocking-down *Txnrd1* in tumor cells led to a loss of their tumorigenic potential (Yoo et al., 2006). Also Lu et al. has shown that the therapeutic efficacy of arsenic oxide against cancer is based on the inhibition of TrxR1 (Lu et al., 2007). These reports clearly show that components of the antioxidant system are promising targets for the treatment of cancer. Unfortunately, the above studies failed to assess the long term out-come of

inhibiting an antioxidant system. More importantly, the mechanisms of action of the tested compounds are poorly defined. Thus, off-target effects and inhibition of other molecules can not be ruled out at present. Thus, although it is not clear yet what is the molecular role of ROS in tumors, members of the antioxidant defense system seem to be promising candidates for novel therapeutic targets against cancer.

2.7.2 The thioredoxin system in cancer

A number of reports have linked the thioredoxin 1/thioredoxin reductase 1 system to cell proliferation, cancer development, invasiveness, and drug resistance of tumor cells. Previous work in the lab identified TrxR1 and thioredoxin 1 as targets of the proto-oncogene *c-myc* (Schuhmacher et al., 2001). Immunocytochemical and mRNA expression studies revealed high expression of thioredoxin and/or thioredoxin reductase in primary colorectal cancer (Berggren et al., 1996; Raffel et al., 2003), breast cancer (Matsutani et al., 2001; Ueno et al., 2000), gastric cancer (Grogan et al., 2000), small cell and non-small cell lung cancer (Kakolyris et al., 2001; Soini et al., 2001), pancreatic cancer (Han et al., 2002; Nakamura et al., 2000), malignant pleural mesothelioma (Kahlos et al., 2001), adult T-cell leukemia (Wakasugi et al., 1990), hepatocellular carcinoma (Kawahara et al., 1996; Nakamura et al., 1992), invasive mammary carcinomas (Lincoln et al., 2003), and malignant melanomas (Barral et al., 2000; Lincoln et al., 2003). High expression of thioredoxin 1 and/or thioredoxin reductase has been correlated with high proliferative capacity, low apoptosis and elevated metastatic potential of cells (Lincoln et al., 2003), increased drug resistance (Arnold et al., 2004; Iwao-Koizumi et al., 2005; Kawahara et al., 1996; Yokomizo et al., 1995), and decreased patient survival (Raffel et al., 2003). These findings have been corroborated by transfection studies revealing that expression of thioredoxin 1 and TrxR1 increases cell proliferation and confers resistance to cisplatin (Sasada et al., 1996; Sasada et al., 1999) (Sasada et al., 2000), whereas thioredoxin reductase 1 antisense expression sensitizes cells to cisplatin treatment (Sasada et al., 1999). Likewise, a dominant-negative mutant of thioredoxin 1 (C32S/C35S) reverses the transformed phenotype of human breast cancer cells (Gallegos et al., 1996).

It has been shown that Trx1 and its truncated form (Trx80) are secreted by transformed cells and may have growth factor or cytokine-like properties (Pekkari et

al., 2003; Rubartelli et al., 1992; Schenk et al., 1996; Wakasugi et al., 1990). Hypoxic conditions induce the expression of thioredoxin (Hedley et al., 2004; Kim et al., 2003), which, in turn, increases the expression of hypoxia-inducible factor 1α (HIF-1α) and a number of other transcription factors including AP-1. Through this mechanism, thioredoxin increases the production of vascular endothelial growth factor (VEGF) and contributes to tumor angiogenesis (Welsh et al., 2002). Finally, thioredoxin inhibits inhibitors of metalloproteases, TIMP-1 and TIMP-2, and thus shifts the balance between metalloproteases (namely MMP-9) and their inhibitors towards increased activity of MMPs (Farina et al., 2001) that promotes metastasis.

Since Trx1 and TrxR1 are often up-regulated in various tumors, they represent a suitable drug target for the treatment of cancer. Knock-down of *Txnrd1* inhibits self-sufficiency of tumor cells and reverts the malignant phenotype (Yoo et al., 2006; Yoo et al., 2007). Inhibition of TrxR1 inhibits NFκB and AP-1, induces G1-phase growth delay and sensitizes the tumor cells towards the agents that induce oxidative stress like H_2O_2 or ionizing radiation (Smart et al., 2004). Known inhibitors of thioredoxin reductase are nitrosourea, gold compounds (Auranofin, aurothioglucose), cis-platinum complexes (Cisplatin, carboplatin), dinitrohalobenzenes (1-chloro-2,4-dinitobenzene (2,4-CDNB)), arsenicals (Arsenic(III) oxide) and antitumor quinoid compounds (diaziquone, doxorubicin, menadione, plamarumycin CP1), some of which are potent anti-cancer agents (Gromer et al., 2004; Powis et al., 2006). In fact, it has been shown that the therapeutic efficacy of arsenic oxide against cancer is based on the inhibition of TrxR1 (Lu et al., 2007). However, the lack of specificity is a major drawback of this group of drugs as many other flavoenzymes are inhibited as well (Gromer et al., 2004).

Histone deacetylase (HDAC) inhibitors are a new class of anti-cancerous drugs that exert their antitumor effects by preferentially increasing ROS production and inducing polyploidy in transformed cells (Rosato and Grant, 2003; Xu et al., 2005). HDAC inhibitors are supposed to repress the thioredoxin system by up regulating thioredoxin binding protein 2 (Butler et al., 2002; Ungerstedt et al., 2005). HDAC inhibitor-induced cell death is independent of caspases and p53 or p21 status. Due to mutations, p53-dependent functions are compromised in many tumors. Thus, acting through inhibiting the thioredoxin-dependent pathway, HDAC inhibitors can be

effective against those tumors in which p53-dependent apoptosis and/or senescence pathways are defective. Since the thioredoxin/thioredoxin reductase1 system is up-regulated in many tumors and many known anti-tumor compounds act through inhibiting these molecules, thioredoxin/thioredoxin reductase1 are promising drug targets against cancer.

2.8 Aims of the present study

The thioredoxin-dependent system plays pivotal roles in different aspects of cell physiology like cell proliferation, redox regulation of cell signaling, and apoptosis. More importantly, it is up-regulated in many solid tumors and thus a promising novel drug target for cancer chemotherapy. Previous work in the lab has shown that mouse *Txnrd1* is indispensable for cell proliferation (Jakupoglu et al.; 2005). By using a conditional *Txnrd1* knockout mouse and mouse embryonic fibroblast (MEFs) cell lines derived from these mice, the present study was carried out with the following objectives:

1. To address the role of thioredoxin reductase 1 in proliferation and growth.
2. To study the effects of thioredoxin reductase 1 inactivation on cellular redox homeostasis.
3. To study possible redundancies between the thioredoxin- and the GSH-dependent systems.
4. To explore the role of thioredoxin reductase 1 in tumor development.

3. Materials and Methods

3.1 Materials

Reagents	Company	Catalog No.
Acrylamide	Bio-Rad, Munich, Germany	161-0158
Agarose, electrophoresis grade	Invitrogen, Karlsruhe, Germany	15510-027
Agarose, low melting point	Fermentas GmbH, St. Leon-Rot, Germany	R0801
Ammonium persulfate	Sigma-Aldrich GmbH, Taufkirchen, Germany	A3678
Ampicillin	Sigma-Aldrich GmbH, Taufkirchen, Germany	A9518
Arsenic (III) oxide	Sigma-Aldrich GmbH, Taufkirchen, Germany	202673
β-Mercaptoethanol (2-ME)	Roth Carl GmbH & Co., Karlsruhe, Germany	4227.1
Bovine albumin	MP Biomedicals, Eschwege, Germany	840043
Bromophenol blue sodium salt	Merck KGaA, Darmstadt, Germany	111746
Buthionine sulfoximine (BSO)	Sigma-Aldrich GmbH, Taufkirchen, Germany	B2640
t-Butyl hydroperoxide	Sigma-Aldrich GmbH, Taufkirchen, Germany	B-2633
Cadmium chloride	Sigma-Aldrich GmbH, Taufkirchen, Germany	C3141
Calcium chloride	Sigma-Aldrich GmbH, Taufkirchen, Germany	C7902
Chloroquine	Sigma-Aldrich GmbH, Taufkirchen, Germany	C6628
Crystal violet	Sigma-Aldrich GmbH, Taufkirchen, Germany	C3886
DAPI	Invitrogen, Karlsruhe, Germany	D1306
dNTP Mix	Fermentas GmbH, St. Leon-Rot, Germany	R0241
DMSO	Sigma-Aldrich GmbH, Taufkirchen, Germany	D2650
Doxorubicin	Sigma-Aldrich GmbH, Taufkirchen, Germany	D-1515
ECL	GE Healthcare, Freiburg, Germany	RPN2106
EDTA	Sigma-Aldrich GmbH, Taufkirchen, Germany	E9884
Ethanol p.a.	Merck, Darmstadt, Germany	1.00983.2500
Ethidiumbromide	Merck, Darmstadt, Germany	70257083
L-Glutathione oxidized (GSSG)	Sigma-Aldrich GmbH, Taufkirchen, Germany	G4626
Glutathione reductase (Yeast)	Sigma-Aldrich GmbH, Taufkirchen, Germany	G3664
Glycine	MP Biomedicals, Eschwege, Germany	808831
Hydrogenperoxide	Sigma-Aldrich GmbH, Taufkirchen, Germany	H1009
Isopropanol p.a.	Merck, Darmstadt, Germany	1.09634.2511
Luria Broth base	Invitrogen, Karlsruhe, Germany	12795-019
Magnesium sulfate	Sigma-Aldrich GmbH, Taufkirchen, Germany	M2643
Mounting medium	Dako Cytomation, Hamburg, Germany	S3023
MTT	Sigma-Aldrich GmbH, Taufkirchen, Germany	M2128
N-Acetyl-L-Cysteine	Sigma-Aldrich GmbH, Taufkirchen, Germany	A9165

NADPH (reduced)	Sigma-Aldrich GmbH, Taufkirchen, Germany	N6505
Oligonucleotides	Metabion International AG, Martinsried, Germany	
Paraformaldehyde (PFA)	Roth Carl GmbH & Co., Karlsruhe, Germany	0335.3
Phenol	Roth Carl GmbH & Co., Karlsruhe, Germany	0038.3
Phenol/Chloroform	Roth Carl GmbH & Co., Karlsruhe, Germany	A156.2
PhosSTOP	Roche Diagnostics, Mannheim, Germany	04906837001
Protease Inhibitor Cocktail	Roche Diagnostics, Mannheim, Germany	1 697 498
Proteinase K	Roth Carl GmbH & Co., Karlsruhe, Germany	7528.1
Rubidium chloride	Sigma-Aldrich GmbH, Taufkirchen, Germany	83979
SDB-F	Fluka Chemie GmbH, Buchs, Switzerland	46640
Select Agar	Invitrogen, Karlsruhe, Germany	30391-023
Skim milkt powder	Fluka Chemie GmbH, Buchs, Switzerland	70166
Sodium chloride	MP Biomedicals, Eschwege, Germany	194848
Sodium dodecyl sulfate (SDS)	Fluka Chemie GmbH, Buchs, Switzerland	71729
Sodium phosphate tetrabasic	Sigma-Aldrich GmbH, Taufkirchen, Germany	S6422
TEMED	Fluka Chemie GmbH, Buchs, Switzerland	87689
Triethylphosphine gold(I) chloride	Sigma-Aldrich GmbH, Taufkirchen, Germany	288225
Tris-Base	Merck, Darmstadt, Germany	1.08382
Triton X-100	Sigma-Aldrich GmbH, Taufkirchen, Germany	T9284
Trolox®	Fluka Chemie GmbH, Buchs, Switzerland	56510
Tween 20	Sigma-Aldrich GmbH, Taufkirchen, Germany	P5927

Cell culture reagents	**Company**	**Catalog No.**
β-Mercaptoethanol (2-ME)	Invitrogen, Karlsruhe, Germany	31350-010
CD-CHO medium	Invitrogen, Karlsruhe, Germany	10743011
DMEM 1 x	Invitrogen, Karlsruhe, Germany	41966
Doxycycline HCl	Sigma-Aldrich GmbH, Taufkirchen, Germany	D9891
Fetal Bovine Serum	PAA, Pasching, Austria	A15-043
Glutamine (100 x)	Invitrogen, Karlsruhe, Germany	25030
HEPES	Invitrogen, Karlsruhe, Germany	15630056
Hygromycin B	Invitorgen, Karlsruhe, Germany	10687010
OPTI-MEM	Invitrogen, Karlsruhe, Germany	31985
Penicillin-Streptomycin	Invitrogen, Karlsruhe, Germany	15140-122
Puromycin	Sigma-Aldrich GmbH, Taufkirchen, Germany	P7255
Trypan Blue (0.4%)	Sigma-Aldrich GmbH, Taufkirchen, Germany	T8154
Trypsin-EDTA	Invitrogen, Karlsruhe, Germany	25300

Molecular probes	**Company**	**Catalog No.**
Annexin V-FITC	BD Biosciences, Heidelberg, Germany	556419
CM-H2DCFDA	Invitrogen, Karlsruhe, Germany	C-6827
Propidium Iodide (PI)	Sigma-Aldrich GmbH, Taufkirchen, Germany	P4170

Molecular biology products	**Company**	**Catalog No.**
DNA Polymerase I (Klenow)	New England Biolabs GmbH, Frankfurt, Germany	M0210S
Phosphorylated *EcoRI* linker	New England Biolabs GmbH, Frankfurt, Germany	S1078S
Pfx DNA Polymerase	Invitrogen, Karlsruhe, Germany	11708-021
Phosphatase, alkaline	Roche Diagnostics, Mannheim, Germany	713 023
Proteinase K	Roth Carl GmbH & Co., Karlsruhe, Germany	7528.1
Restriction Endonucleases	New England Biolabs GmbH, Frankfurt, Germany	
	MBI Fermentas GmbH, St. Leon-Rot, Germany	
RNase A	QIAGEN GmbH, Hilden, Germany	1007885
T4 DNA Ligase	New England Biolabs GmbH, Frankfurt, Germany	M0202S
Taq DNA Polymerase	Invitrogen, Karlsruhe, Germany	18038-026

Immunologicals	**Company**	**Catalog No.**
α-FLAG (M2) (mouse)	Sigma-Aldrich GmbH, Taufkirchen, Germany	F1804
α-mouse IgG-Cy3 conjugate (goat)	Jackson Immunoresearch Europe Ltd., UK	115-165-003
α-Mouse-HRP conjugate (goat)	Santa Cruz	SC-2031
α-Rabbit-HRP conjugate (goat)	Santa Cruz	SC-2030
α-Rat-HRP conjugate (goat)	Jackson Immunoresearch Europe Ltd., UK	212-165-168
α-Tubulin (mouse)	Sigma-Aldrich GmbH, Taufkirchen, Germany	T8203
phospho-SAPK/JNK (Thr183/Tyr185)	Cell signaling technology	9251S

Disposables and Kits	**Company**	**Catalog No.**
Cell strainer (40 µm Nylon)	BD Falcon (BD Biosciences)	7355837
DC Protein Assay	Bio-Rad, Munich, Germany	500-0112
Gel Extraction Kit	QIAGEN GmbH, Hilden, Germany	28704
Hybond-C super membrane	GE Healthcare, Freiburg, Germany	RPN203G
Hyperfilm	GE Healthcare, Freiburg, Germany	RPN3103K
JETstar Plasmid purification system	Genomed GmbH, Löhne, Germany	220020
LightCycler Capillaries	Roche Diagnostics, Mannheim, Germany	11 909 339 001
LightCycler FastStart DNA Master^{PLUS}		
SYBR Green I	Roche Diagnostics, Mannheim, Germany	03 515 869 001
Millex GP Filter 0.22 µm	Millipore, Carrighwohill, Co. Cork, Ireland	SLGP033RS
Plasmid Maxi Kit	QIAGEN GmbH, Hilden, Germany	12163

PCR Cloning Kit	QIAGEN GmbH, Hilden, Germany	231122
Reverse Transcription System	Promega GmbH, Mannheim, Germany	A3500
RNeasy Mini Kit	QIAGEN GmbH, Hilden, Germany	74104

Equipments	**Company**
Centrifuge 5810R	Eppendorf, Hamburg, Germany
FACS Calibur	BD GmbH, Heidelberg, Germany
GenAmp PCR system 2700	Applied Biosystems, Darmstadt, Germany
Gene Pulser II System	Bio-Rad, Munich, Germany
Gene Pulser Electroporation Cuvettes, 0.4 cm	Bio-Rad, Munich, Germany
Heraeus Biofuge centrifuge	Heraeus Holding GmbH, Hanau, Germany
Heraeus Incubator, Modell B 5060	Heraeus Holding GmbH, Hanau, Germany
Light-Cycler 1.5	Roche Diagnostics, Mannheim, Germany
Microscope Axiovert 135	Carl Zeiss Jena GmbH, Göttingen, Germany
Microscope Axiovert 200M	Carl Zeiss Jena GmbH, Göttingen, Germany
Olympus FV1000	Olympus
OTD Combi Ultracentrifuge	Sorvall, Langenselbold, Germany
Photometer Bio	Eppendorf, Hamburg, Germany
PowerPac 200 Power Supply	Bio-Rad, Munich, Germany
Spectrophotometer	DU-64 Beckman Coulter GmbH, Krefeld, Germany
Tecan spectrophotometer	Tecan, Austria
UZ-PA-38,5-1 Ultracentrifuge Tubes	Kisker GbR, Steinfurt, Germany

Oligonucleotides	**Sequence**
Genotyping primers	
TR1floxf1:	5’-TCC ACC TCA CAG GAG TGA TCC C-3’
TR1floxr1	5’-TGC CTA AAG ATG AAC TCG CAG C-3’
Delete-PCR primers	
TR1wtforw2	5’-GGTCTGAGCTAGCGTGAAGTGTTCC-3’
Neopromrev1	5’-ACGTGCTACTTCCATTTGTCACGTCCTGC-3’
Cloning primers	
5’ Puro fw	5’-CCACAACCATGACCGAGTACAAGCCCACGGTG-3’
3’ Puro BsrG1 rev	5’-CTAGCTGTACAGCGTCAGGCACCGGGCTTGCGGGTC-3’
Lenti-Linker 1a	5´-GATCCTTCGAAGAATTCTCTAGAACGCGTCTCGAGACCGGTTAC-3´

Lenti-Linker 1b (rev)	5´-GTAACCGGTCTCGAGACGCGTTGTATAGAATTCTTCGAAG-3´
Oligo-Nhe1-Txnrd1 for1	5'-ATGATGCTAGCAATGGCTCCAAAGATCCCCCTG-3'
Oligo-Xba1-Txnrd1 rev	5'-ACGTCTAGACAGGAAAAGGTTGAGCTCAACAG-3'
Oligo Txnrd1 CT for	5'-CAGGTCGAAGGAGGCTGCAGCATCGCACTG-3'
Oligo Txnrd1 CT rev	5'-CAGTGCGATGCTGCAGCCTCCTTCGACCTG-3'
Oligo Txnrd1 C59S for	5'-CTCGGAGGAACGTCCGTGAATGTGGGTTG-3'
Oligo Txnrd1 C59S rev	5'-CAACCCACATTCACGGACGTTCCTCCGAG-3'
Oligo Txnrd11 C64S for	5'- GAATGTGGGTTCCATACCTAAGAAGCTG-3'
Oligo Txnrd1 C64S rev	5'- CAGCTTCTTAGGTATGGAACCCACATTC-3'
Oligo Txnrd1 CS for	5'- CTCCAGTCTGGCTCCTGAGGTTAAGCCCCAGT-3'
Oligo Txnrd1 CS rev	5'- ACTGGGGCTTAACCTCAGGAGCCAGACTGGAG-3'
Oligo Txnrd1 UC for	5'- CTCCAGTCTGGCTGCTGCGGTTAAGCCCCAGT-3'
Oligo Txnrd1 UC rev	5'- ACTGGGGCTTAACCGCAGCAGCCAGACTGGAG-3'
Oligo Txnrd1 US for	5'- CTCCAGTCTGGCTGCTCCGGTTAAGCCCCAGT-3'
Oligo Txnrd1 US rev	5'- ACTGGGGCTTAACCGGAGCAGCCAGACTGGAG-3'
Oligo Txnrd1 UAA for	5'- TCCAGTCTGGCTGCTAAGGTTAAGC-3'
Oliog Txnrd1 UAA rev	5'- GCTTAACCTTAGCAGCCAGACTGGA-3'

RT-PCR primers

18 S for	5'-GGACAGGATTGACAGATTGATAG-3'
18 S rev	5'-CTCGTTCGTTATCGGAATTAAC-3'
Aldolase A	5'-GGTCACAGCACTTCGTCGCACAG-3'
Aldolase B	5'-TCCTTGACAAGCGAGGCTGTTGGC-3'
Gclc for	5'-TGGGCAACTGCTGTCTCCAG-3'
Gclc rev	5'-GGCTCCAGGCCTCTCTCCTC-3'
Gclm for	5'-GCTTCGCCTCCGATTGAAGA-3'
Gclm rev	5'-TCTGGTGGCATCACACAGCA-3'
Gsr for	5'-ATCGCGGGCATCCTCTCTGC-3'
Gsr rev	5'-TCATGGTCGTGGTGGGCTTCC-3'
Gss for	5'-GTGCTGAAGCCCCAGAGAGA-3'
Gss rev	5'-CAGGCCGTAGCAAGCAATTC-3'
Txnrd1-E13f	5´-TTGGCCATTGGAATGGACAGTCC-3´
Txnrd1-E15r	5´-AGCACCTTGAATTGGCGCCTAGG-3´
Txnrd1-59	5´-CGAAGACACAGTGAAGCATGACTGGG-3´
Txnrd1-60	5´-TCCCCTCCAGGATGTCACCGATGGCG-3´
xCT for1	5'-GGCACCGTCATCGGATCAGGCATC-3'
xCT rev1	5'-CACGAGCTTGATTGCAAGTTCAGG-3'

Sequencing

T7 promoter	5'-TAATACGACTCACTATAGGG-3'
Sp6 promoter	5'-ATTTAGGTGACACTATAGAA-3'
LTR 3'-for1	5'-GCTCACAACCCCTCACTC-3'
IRES rev1	5'-CTTCGGCCAGTAACGTTAGG-3'

All DNA-oligonucleotides were obtained from Metabion GmbH, Martinsried, Germany.

Biologicals

Plasmids	Vector Type	Source
pBJ3Ω *c-myc*	Expression	Hartmut Land
pUC EJ6.6 *Ha-ras*^{V12}	Expression	Hartmut Land
pHC-BZ-SVpuro	Expression	In house
pHL 2823	Expression	In house
pHL 2823 Ds Red C1	Expression	Present work
391 K73 pEcoEnv-IRES-puro	Expression	Tim Schröder
392 pRSV_Rev	Expression	Tim Schröder
393 pMDLg_pRRE	Expression	Tim Schröder
441 pRRL.PPT.SF.IRES-golgiVENUS	Expression	Tim Schröder
442 pRRL.PPT.SF.IRES-VENUSnucmem	Expression	Tim Schröder
443 pRRL.PPT.SF.IRES-mitoVENUS	Expression	Tim Schröder
441 PL	Intermediate	Present work
442 PL	Intermediate	Present work
443 PL	Intermediate	Present work
441 L1 IRES-golgiVENUS	Expression	Present work
442 L1 IRES-VENUSnucmem	Expression	Present work
443 L1 IRES-mitoVENUS	Expression	Present work
442 L1 IRES-puro	Expression	Present work
441 L1 *Ha-ras*^{V12}-IRES-golgiVENUS	Expression	Present work
443 L1 *c-myc* IRES-mitoVENUS	Expression	Present work
442 L1-SF-IRES puro	Expression	Present work
442 L1-SF-Txnrd1 wt (2ATG) IRES puro	Expression	Present work
442 L1-SF- Txnrd1 C59S IRES puro	Expression	Present work
442 L1-SF- Txnrd1 C64S IRES puro	Expression	Present work
442 L1-SF- Txnrd1 C497S IRES puro	Expression	Present work
442 L1-SF- Txnrd1 U498C IRES puro	Expression	Present work
442 L1-SF- Txnrd1 U498S IRES puro	Expression	Present work
442 L1-SF- Txnrd1 U498 STOP IRES puro	Expression	Present work

pdrive	Cloning	Qiagen PCR cloning kit
pdrive Puro	Intermediate	Present work
pdrive Txnrd1 wt (2ATG)	Intermediate	Present work
pcDNA3.0 SF-TAP	Expression	Johannes Gloeckner
pcDNA3.0 SF-TAP ASA	Intermediate	Present work
pSF- Txnrd1 wt (2ATG)	Intermediate	Present work
pSF- Txnrd1 C59S	Intermediate	Present work
pSF- Txnrd1 C64S	Intermediate	Present work
pSF- Txnrd1 C497S	Intermediate	Present work
pSF- Txnrd1 U498C	Intermediate	Present work
pSF- Txnrd1 U498S	Intermediate	Present work
pSF- Txnrd1 U498 Stop	Intermediate	Present work
pRTS-1(pRTS-GL-SVH-rtTA)	Expression	In house
pRTS-1-SF-Txnrd1 wt (2ATG)	Expression	Present work

Bacterial strains

XL-1 Blue competent cells (Stratagene USA Catalogue# 200249).

E.coli K12 GM2163 *Dam*$^{-}$ and *Dcm*$^{-}$ competent cells (New England Biolabs GmbH, Frankfurt, Germany Catalogue# E4105S).

Cell lines

HEK 293-T cells were used as packaging cell line for lentivirus production.

The cell lines used in the present study were isolated and established from mouse embryonic fibroblasts (MEFs) derived from conditional *Txnrd1* knockout mice. The conditional *Txnrd1* knockout mice harbor two loxP sites flanking exon 15 (fl). loxP is a 34 base pair sequence which is recognized by Cre recombinase and depending up on orientation of the two loxP sites, the loxP-flanked part of a gene can either be deleted or inverted. E12.5 embryos, isolated from the breeding of conditional *Txnrd1* knockout mice were used to generate the following cells lines and their derivatives:

Floxed (fl) *Txnrd1* cell lines: *Txnrd1*$^{fl/fl}$ (Üa51 and Üa53) and *Txnrd1*$^{+/fl}$ (Üa46).

***Txnrd1* deleted cell lines**: *Txnrd1*$^{-/-}$ (51ΔD4 and 53ΔE1) and *Txnrd1*$^{+/-}$ (46ΔB5) were derived from the floxed cell lines (mentioned before) after Tat-Cre treatment and single cell cloning.

Transformed cell lines: The above cell lines were transformed by transducing them with lentiviruses encoding the *c-myc* and *Ha-ras*^{V12} oncogenes. The following transformed cell lines were generated after single cell cloning: 46MRA3, 51MRB3 and 53MRC4. As mentioned above, *Txnrd1* was deleted in these cell lines by Tat-Cre treatment and the respective knockout cell lines were generated after single cell cloning. One heterozygous cell line 46MRA3Δ1C6 and two knockout cell lines 51MRB3ΔF1 and 53MRC4ΔE3 were used in this study.

Mouse strains/mouse lines

C57BL/6 (Charles river).

Conditional *Txnrd1* knockout mice (Jakupoglu et al., 2005).

Miscellaneous reagents

The Tat-Cre fusion protein was a kind gift from Dr. Wolfgang Hammerschmidt (Gene Vector Group, Helmholtz Zentrum München).

Anti-human thioredoxin reductase 1 antibody was generously provided by Dr. Gladyshev (Director Redox Biology Center, Department of Biochemistry, University of Nebraska, Lincoln, USA).

3.2 Methods

3.2.1 Cloning techniques

Preparation of competent bacteria

Chemically competent XL-1 *E. coli* bacteria were produced using the rubidium chloride method. A single cell colony on an agar plate was used to inoculate 3 ml of LB medium without antibiotic. The suspension was incubated overnight at 37°C with constant shaking. This starter culture was used to inoculate 250 ml of LB medium, containing 20 mM magnesium sulfate and kept at 37°C under constant shaking until

the $OD_{\lambda 600}$ reached 0.4-0.6. Subsequently, the cells were harvested at 4,500 rpm for 5 min at 4°C. All subsequent steps were performed at 4°C with pre-chilled pipettes, tubes and flasks. The pellet was resuspended in 100 ml of ice-cold TFB1 and was incubated for 5 min on ice. Then, the cells were centrifuged again at 4,500 rpm for 5 min at 4°C. Finally, the pellet was resuspended gently in 10 ml TFB2 and incubated for 30 min on ice. The chemically competent cells were snap-frozen in liquid nitrogen in 200 µl aliquots and stored at -80°C. The efficiency of transformation was determined by transforming the bacteria with serial dilutions of a plasmid.

Buffer TFB1: 30 mM Potassium acetate, 10 mM $CaCl_2$, 50 mM $MnCl_2$, 100 mM RbCl, 15 % glycerol. pH adjusted to 5.8 with1 M acetic acid

Buffer TFB2: 10 mM MOPS/PIPES, 75 mM $CaCl_2$, 10 mM RbCl, 15 % glycerol. pH adjusted to 6.5 with 1 M KOH.

Transformation of bacteria

Transformation of bacteria was achieved by heat shock treatment. Frozen competent cells were thawed on ice, mixed with 10 µl of the ligation mixture or 100 ng to 1 µg of plasmid DNA, and the mixture incubated for 10 min on ice. Heat shock was performed by incubating the bacteria at 42°C for 2 min followed by 10 min incubation on ice. 500 µl LB medium without antibiotics was added to the cell suspension and the mixture was incubated for 45 min at 37°C with shaking. The transformation mixture was plated on an LB plate containing the appropriate antibiotic. Agar plates were incubated for 12-16 h at 37°C until single cell colonies became visible.

Preparation of plasmid DNA

The plasmid DNA was isolated from the bacteria using the JETstar plasmid purification system. For screening purposes, single cell colonies were picked from LB plates and grown as suspension cultures at 37°C for 6 h with shaking in 2 ml LB medium containing the appropriate antibiotic. The cells were harvested by centrifugation at 10,000 x g for 1 min and resuspended in 200 µl of buffer E1 containing RNaseA by vortexing. 200 µl of cell lysis buffer E2 was added to the cell suspension and mixed gently by inverting the tube and then incubated for 5 min at room temperature. Next, 200 µl of the denaturation buffer E3 was added. After mixing gently by inverting, the mixture was centrifuged for 6 min at 10,000 x g. To

remove proteins and lipids, 400 µl of phenol-chloroform was added to the supernatant. After mixing, centrifugation was carried out at 10,000 x g for 5 min. The upper aqueous phase containing the plasmid DNA was collected carefully in a separate Eppendorf microfuge tube. 500 µl isopropanol was added to the supernatant. The plasmid DNA was precipitated by centrifugation for 12 min at 4°C at 10,000 x g. The DNA pellet was washed once with 70% ethanol, air dried and resuspended in 50 µl 1 x TE buffer pH 8.0. Analytic restriction digestions were carried out with suitable restriction endonucleases to check the correctness of the plasmid. After screening, the correct clone was taken for higher scale preparation using the JETstar maxi-prep kit. The concentration of the plasmid DNA was determined by measuring the absorbance at 260 nm wavelength (A_{260}) in a spectrophotometer.

E1: 50 mM Tris, 10 mM EDTA, pH 8,0

E2: 200 mM NaOH, 1% w/v SDS

E3: 3.1 M potassium acetate, adjust to pH 5.5 with acetic acid

1 x TE: 10 mM Tris HCl, 1 mM EDTA. pH adjusted to 8.0

Restriction digestion

Restriction digestion was performed with the corresponding endonucleases according to manufacturers' instructions (New England Biolabs GmbH or MBI Fermentas GmbH). The DNA fragments were separated by electrophoresis in a 1% agarose gel at 100 V in 1 x TAE buffer. For cloning purposes, the fragments were separated in 0.8% low melting point (LMP) agarose (MBI Fermentas GmbH, St. Leon-Rot, Germany). The fragment of appropriate size was excised from the gel with a scalpel. 50 µl of solution A was added to the gel piece and the final volume was adjusted to 500 µl with H_2O. The mixture was kept at 60°C for 10 min for melting. 300 µl of phenol was added to the mixture, vortexed vigorously and centrifuged at 10,000 x g for 7 min at room temperature. The upper phase was collected and extracted with butanol several times until the volume of the mix was reduced to 50 µl. Then, 150 µl of 100% ethanol p.a. was added to the samples and centrifuged at 10,000 x g for 10 min at 4°C. Finally, the sample was washed with 70% ethanol and air dried. The pellet was suspended in 25 µl of 1 x TE.

Solution A: 1 M NaCl, 10 mM Tris HCl, 1 mM EDTA, pH 7.5

TAE (50 x): 2 M Tris Acetate (2 M Tris base, 5.71% acetic acid (v/v), 50 mM EDTA/NaOH). pH adjusted to 8.0

Phenol-chloroform extraction and ethanol precipitation of DNA

Purification of DNA fragments after restriction digestion was done by phenol-chloroform treatment followed by ethanol precipitation. An equal volume of phenol-chloroform was added to the digestion reaction, briefly mixed and centrifuged for 6 min at 10,000 x g. The upper aqueous phase was recovered and DNA was precipitated by adding 2.5 x volumes of ethanol and NaCl at a final concentration of 50 mM, followed by centrifugation at 10,000 x g at 4°C. The precipitated DNA was washed once with 70 % ethanol, centrifuged as above and air dried. The dried DNA pellet was dissolved in 30 µl of 1 x TE.

Klenow fragment fill-in reaction

In order to generate blunt-end DNA fragments, single-stranded 5' overhangs generated by restriction enzyme digests (sticky ends) were filled-in with DNA Polymerase I (Klenow fragment) according to the manufacturer's instructions (New England Biolabs GmbH). The Klenow fragment has retained the 5´-3´ polymerase activity and the 3'-5' exonuclease activity, but is devoid of the 5'-3' exonuclease activity of DNA polymerase I. Hence, the Klenow fragment forms blunt ends by either filling-in 5'-overhangs or by removing 3'-overhangs. DNA fragments were purified by phenol-chloroform extraction as described above.

Dephosphorylation of linearized plasmid DNA

To prevent religation of the vector, vector DNA was dephosphorylated with calf intestine alkaline phosphatase according to manufacturer's instructions (Roche Diagnostics). After dephosphorylation, DNA fragments were purified by phenol-chloroform extraction as described above.

DNA ligation

The ligation of the insert with the plasmid back-bone was conducted by using T4 DNA ligase according to the manufacturer's instructions (New England Biolabs

GmbH). A typical ligation mixture contained 2 µl vector, 4 µl insert, 1 µl 10 x T4 ligase buffer and 1 µl T4 DNA ligase in a final reaction volume of 10 µl; the ligation was carried out at 16°C overnight. Subsequently, the ligation mixture was used for the transformation of competent bacteria.

Annealing of synthetic oligonucleotides

Sense and anti-sense synthetic oligonucleotides were mixed in equimolar ratios, heated to 95°C in a waterbath, and allowed to cool down slowly to room temperature by turning off the heating. The annealed DNA duplex was then ligated into suitable vectors.

Isolation of RNA and cDNA synthesis

Total RNA from mammalian cells was isolated using the RNeasy Mini Kit (Qiagen) according to manufacturer's instructions. Approximately $1x10^6$ cells were lysed on the plate by the addition of 600 µl buffer RLT, containing 10 µl β-mercaptoethanol/ml RLT buffer. The samples were stored at -80°C if needed. To avoid DNA contamination, on-column DNaseI digestion was performed. RNA was eluted from the column with 30 µl elution buffer. The RNA concentration was determined by measuring the absorbance at 260 nm wavelength (A_{260}) in a spectrophotometer. For cDNA synthesis, 1 µg of the isolated RNA was used. cDNA synthesis was performed by using the Reverse Transcription System (Promega) according to manufacturer's instructions with random primers at 42°C in a reaction volume of 20 µl. The first-strand cDNA synthesis reaction mix was finally diluted to 100 µl with nuclease-free water and subjected to RT-PCR.

Quantitative RT-PCR

The quantitative RT-PCR was carried out by using the LightCycler FastStart DNA MasterPLUS SYBR Green I Kit in combination with the LightCycler 1.5 System (Roche diagnostic, Mannheim, Germany). For each RT-PCR reaction, 6 µl H_2O, 1 µl primer mix, 2 µl Master Mix and 1 µl cDNA were mixed in a pre-cooled LightCycler Capillary. RT-PCR primers were designed with software Primer3 (Rozen and Skaletsky, 2000), with a product size of 150-300 base pairs. The house-keeping

gene *aldolase* or *S18* was used for normalization. The specificity of the RT-PCR reaction was monitored by determining the melting point, which was done by running a melting curve program.

3.2.2 Methods of gene delivery into target cells

Electroporation of MEFs

Logarithmically growing mammalian cells were harvested by trypsinization and washed in PBS. Approximately $3x10^6$ cells in 500 µl PBS were used per electroporation. The cells were mixed with 20-30 µg of plasmid DNA in 0.4 cm cuvettes and electroporated using the GenePulser II apparatus (Bio Rad, Munich, Germany) with standard settings of 240 Volt and 950 µF capacitance. The transfected cells were seeded on a 10 cm cell culture dish in standard DMEM medium with 10% FCS. The selection of transfected cells was initiated 24 h after electroporation with the appropriate selection marker (puromycin (up to 2 µg/ml) or hygromycin B (up to 300 µg/ml)), with gradually increasing doses. Stably transfected transgene-expressing cells lines were obtained after long term selection over suitable selection markers.

Transduction of cells using lentiviruses

Lentiviral-transduction is a fast and efficient method of gene delivery into cells. Due to the high infection rates of even non-dividing and hardly transfectable cells, the absence of adverse effects on target cells, and the stable transgene expression after provirus integration, this method was used to transduce primary MEFs. The HIV-based 3rd generation ecotropic lentiviral vector system was used for the *in vitro* delivery of genes of interest into different mouse cell lines. In order to avoid any recombination events, all necessary proteins for lentivirus production including Env, Gag, Pol and Rev are encoded by three different plasmids. To ensure maximum bio-safety, the natural promoter is replaced by promoters from other viruses (e.g. Rous sarcoma virus), the 5´and 3´-LTRs are truncated, all the accessory genes are removed, and the virus is pseudotyped with glycoproteins from other viruses.

Lentiviral vector system and their modifications

The lentiviral vector system consists of the following components:

Packaging vectors:

391 K73 pEcoEnv-IRES-puro

392 pRSV_Rev

393 pMDLg_pRRE

Transfer vectors:

441 pRRL.PPT.SF.IRES-golgiVENUS

442 pRRL.PPT.SF.IRES-VENUSnucmem

443 pRRL.PPT.SF.IRES-mitoVENUS

The aforementioned transfer vectors 441, 442, and 443 were modified by deleting the *EcoRI* and *XhoI* restriction sites to generate pre-linker (PL) intermediates. These were digested with *BamHI* and *SnaBI.* Subsequently, the lenti-linker 1 was inserted that contains multiple unique restriction sites to generate the 441 L1, 442 L1 and 443 L1 transfer vectors. The puromycin acetyltransferase gene was amplified by PCR from pHC-BZ-SVpuro. *SnaBI* and *BsrG1* sites were attached to the ends of the PCR product by the primers used for amplification. The *SnaB1*and *BsrGI* digested PCR fragment was cloned into the *MscI*- and *BsrGI*-digested 442 L1 nucmembVENUS plasmid to generate the 442 L1 IRES Puro vector (Figure 10).

Cloning of the Ha-ras and c-myc oncogenes into the lentiviral vectors

pBJ3Ω *c-myc* and pUC EJ6.6 *Ha-ras*^{V12} were obtained from Dr. Hartmut Land. A 1.7 kb fragment covering the mutated (Val12) Ha-ras coding sequence was amplified by PCR using pUC EJ6.6 *Ha-ras*^{V12} as template. Two *EcoRI* sites were introduced by the primers used for amplification. Then, the 1.7 kb fragment was digested with *EcoRI* and cloned into the same site of 441 L1 golgiVENUS to generate 441 L1 *Ha-ras*^{V12} golgiVENUS. The pBJ3Ω c-myc vector was digested with *Ecl136II* and an *EcoRI* linker (New England Biolabs GmbH, Frankfurt, Germany) was inserted. Then, the plasmid was digested with *EcoRI* and the excised 1.3 kb fragment containing the

c-myc coding sequence was cloned into the 443 L1 mitoVENUS plasmid to generate 443 L1 *c-myc* mitoVENUS.

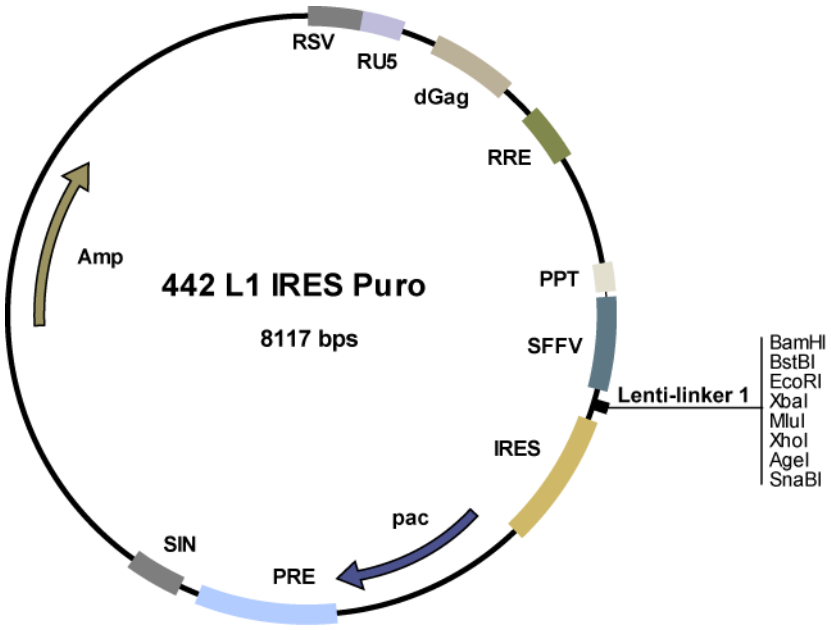

Figure 10. Schematic representation of the HIV-based lentiviral vector. The transfer vector carries the gene of interest and consists of the truncated genome of the virus that is needed for infection and integration. The transgene is expressed from the SFFV promoter. By incorporating the sequence for an internal ribosomal entry site (IRES), bicistronic messages are created. RSV: Rous sarcoma virus promoter, PPT: polypurine tract, SFFV: spleen foci forming virus, pac: puromycin acetyltransferase (resistance gene), PRE: Post-transcriptional regulatory element, RRE: Rev-responsive element, SIN: self-inactivating. Several restriction sites are incorporated into the lenti-linker 1 to facilitate the insertion of the gene of interest.

Cloning of mouse thioredoxin reductase 1 gene into the lentiviral vector

Mouse *Txnrd1* (transcript variant 2 or 2ATG, Accession number: NM_001042513.1) containing the SECIS element was amplified from brain cDNA by PCR using Pfx DNA polymerase and the following primers: Oligo-Nhe1-Txnrd1 for1 (5'-TGATGCTAGCAATGGCTCCAAAGATCCCCCTG-3') and Oligo-Xba1-Txnrd1 rev (5'-ACGTCTAGACAGGAAAAGGTTGAGCTCAACAG-3´). This PCR product was cloned into the pDrive vector using the PCR cloning kit (Qiagen, Hilden, Germany) generating pDrive-Txnrd1 wt (2ATG). The sequencing of the amplified product revealed a T to C nucleotide exchange in the non-coding SECIS sequence, which was reverted by site-directed mutagenesis. Subsequently, the plasmid pDrive-Txnrd1 was digested with *NheI* and *OliI*, the *Txnrd1* fragment isolated and cloned into the pcDNA3.1 SF-TAP ASA vector, which was generated by site-directed mutagenesis from pcDNA3.1 SF-TAP. The pcDNA3.1 SF-TAP ASA vector was digested with *XhoI*,

treated with Klenow enzyme, and then digested with *NheI*. The *NheI*/*OliI*-digested *Txnrd1* fragment was cloned into this vector to generate pSF-Txnrd1. From this plasmid, the *Txnrd1* fragment was cloned as an *EcoRI-XbaI* fragment into the 442 L1 IRES-Puro (Puro = puromycin acetyltransferase) plasmid to generate 442 L1 SF-Txnrd1 wt (2ATG) IRES-Puro.

Site-directed mutagensis of Txnrd1

Thioredoxin reductase1 has two catalytic centers: one at the N-terminus containing 2 cysteine residues (C59 and C64) and the second at the C-terminus formed by cysteine and selenocysteine (C497 and U498). All three cysteine residues and the Sec were individually mutated to serine and cysteine, respectively. The following mutants were created by site-directed mutagenesis using the respective pairs of oligonucleotides. The mutated bases are depicted in red.

wt (N-terminal)	**GGA GGA ACG TGT GTG AAT GTG GGT TGC ATA**
C59S	GGA GGA ACG T**CC** GTG AAT GTG GGT TGC ATA
C64S	GGA GGA ACG TGT GTG AAT GTG GGT T**C**C ATA

wt (C-terminus)	**CTC CAG TCT GGC TGC TGA GGT TAA GCC CC**
C497S	CTC CAG TCT GGC T**C**C TGA GGT TAA GCC CC
U498C	CTC CAG TCT GGC TGC TG**C** GGT TAA GCC CC
U498S	CTC CAG TCT GGC TGC T**CC** GGT TAA GCC CC
U498STOP	CTC CAG TCT GGC TGC T**AA** GGT TAA GCC CC

All mutations were carried out with the pDrive-Txnrd1 wt (2ATG) plasmid. From these plasmids, the different C-terminal mutant DNA fragments were isolated with *Eco47III* and *XbaI* and inserted into the 442 L1 SF-Txnrd1 wt (2ATG) IRES Puro plasmid digested with the same enzymes. For generating the N-terminal mutants (C59S, C64S and SS), the *BclI* and *Eco47III* restriction enzymes were used to exchange the wild-type for the mutated sequences.

Lentiviral production and transduction of target cells

HEK 293-T cells were used for virus production. $5x10^6$ HEK 293-T cells were seeded in a 10 cm cell culture dish and incubated for 12 h prior to transfection. Cells were grown to 70% confluency and then used for transfection. The packaging cell line was transfected simultaneously with four plasmids by the calcium phosphate method.

A typical transfection mix for one 10 cm plate consisted of:

2 µg pEcoEnv-IRES-puro

5 µg pMDLg_pRRE

10 µg pRSV_Rev

5 µg transfer vectors

The above vectors were mixed with 50 µl of 2.5 M calcium chloride in water to a final volume of 500 µl. To this mixture, 500 µl of 2 x HeBS (HEPES buffered saline, pH 7.5) was added while air was bubbled through the mixture and then kept for 20 min at room temperature. 10 ml of transfection medium containing 25 µM chloroquine was added to the cell monolayer. 1 ml of the transfection mix was added to each plate and the cells were incubated for 8-12 h. After incubation, the transfection medium was replaced with 8 ml of fresh transfection medium without chloroquine and the cells were incubated for further 36 h (Figure 11). The supernatant containing the virus particles was collected after 36 h, filtrated through a 0.22 µm sterile filter, and concentrated by ultracentrifugation at 8000 rpm for at least 16 h. The virus pellet was resuspended in 200 µl of cell culture medium and stored at -80°C until further use. For transduction, $1x10^5$ MEFs were infected with 10 µl of virus suspension for 24 h. The transduction efficiency was analyzed by FACS 48 h thereafter by monitoring VENUS expression (in case of 441 L1 *Ha-ras*^{V12} IRES golgiVENUS and 443 L1 *c-myc* IRES mitoVENUS). Stable cell lines were generated by transducing the cells with viruses carrying the puromycin resistance gene (for 442 L1 IRES-Puro) and subsequently selected with puromycin, starting form 0.5 µg/ml to the final concentration of 2 µg/ml.

Chloroquine (1000 x): 25 mM chloroquine in PBS

Calcium chloride: 2.5 M in water

HeBS (2 x): 50 mM HEPES, 280 mM NaCl, 1.5 mM Na_2HPO_4, pH 7.05 adjusted with NaOH

TF medium: Standard DMEM, 20 mM HEPES

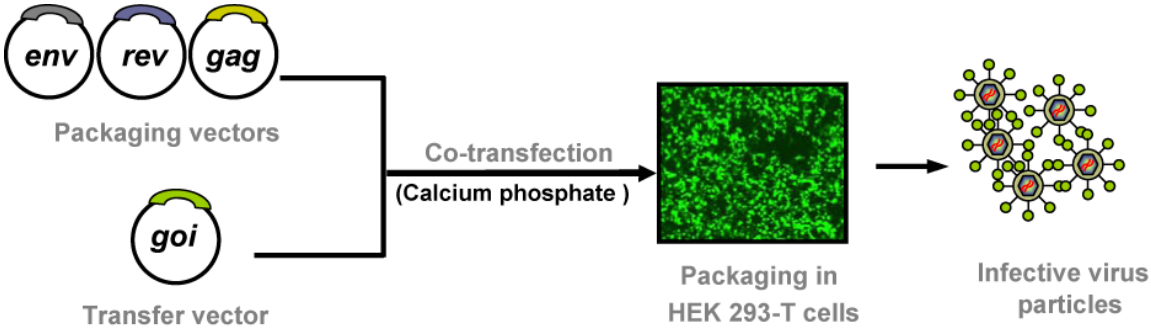

Figure 11. Lentivirus production in packaging cell lines. All four plasmids were co-transfected in HEK 293-T cells using the calcium phosphate method. The supernatant was collected after 36 h. The virus particles were recovered by ultra-centrifugation and then used for the transduction of target cells. *env*: gene encoding for the viral envelope, *gag*: gene coding for the viral glycoprotein, *rev*: gene encoding the reverse transcriptase, *goi*: gene of interest.

3.2.3 Immunoblotting and immunocytochemistry

Antibody generation against mouse thioredoxin reductase 1

A monoclonal antibody against mouse thioredoxin reductase 1 was generated by Dr. Elisabeth Kremmer, Helmholtz Zentrum München. Rats were immunized with a mouse thioredoxin reductase 1-specific peptide (N-VTKRSGGDILQSGC-) coupled to ovalbumin (OVA)/Keyhole limpet hemocyanin (KHL). The peptide was obtained from Peptide Specialty Laboratories (Heidelberg, Germany). After screening 40 hybridoma clones, clone 1E12 was found to be immunoreactive against mouse Txnrd1. The antibody-rich supernatant of hybridoma clone 1E12 was then used in the present study.

Western blot

Whole cell lysates were prepared by incubating cells for 15 min on ice with LCW Lysis Buffer, containing Protease Inhibitor Cocktail (Roche Diagnostics, Mannheim, Germany). Subsequently, the cell debris was removed by centrifugation for 15 min at 4°C at 10,000 x g. The protein concentration of the supernatant was determined by the DC Protein Assay kit (Bio-Rad), according to manufacturer's instructions. 30 µg of protein was mixed with 6 x Laemmli buffer and boiled for 3-5 min at 95°C. Proteins

were size-separated in a 12 % SDS-PAGE gel. Stacking was done at 80 V, while separation was carried out at 125 V in a Mini-PROTEAN 3 Electrophoresis Cell. Proteins were transferred from the gel onto a Hybond-C super nitrocellulose membrane in Blotting Buffer by submerge blotting at 130 V, 400 mA for 75-90 min. Membranes were blocked with 5% skim milk powder in TBS-T for 60 min and hybridized with a primary antibody at 4°C overnight. Membranes were washed three times in TBS-T for 5 min each. Then, the membrane was incubated with the HRP-conjugated secondary antibody for 90 min. After that, the membranes were washed repeatedly in TBS-T (3 x 5 min) and proteins were visualized by the ECL detection system (GE Healthcare, Freiburg, Germany). For re-blotting, the membranes were stripped in 0.4 M NaOH for 10 min. prior to the incubation with the second antibody; the membranes were blocked with 5% skim milk powder in TBS-T for 60 min as described above.

LCW Lysis Buffer: 0.5% TritonX-100, 0.5% Sodium deoxocholate salt, 150 mM NaCl, 20 mM TRIS, 10 mM EDTA, 30 mM Na-pyrophosphate, pH 7.5

12% Separating gel: 3.3 ml water, 4 ml Acrylamide bis-acrylamide (29:1), 2.5 ml 1.5 M Tris HCl pH 8.8, 100 µl 10% SDS, 100 µl 10% Ammonium persulfate (APS) and 4 µl TEMED

5% Stacking gel: 4.1 ml water, 1ml Acrylamide bis-acrylamide (29:1), 750 µl 1 M Tris HCl pH 6.8, 60 µl 10% SDS, 60 µl APS, 8 µl TEMED

Sample Loading Buffer (6 x): 375 mM TrisHCl pH 6.8, 9% SDS, 50% Glycerol, 0.3% Bromophenol Blue, 9% 2-ME

Running Buffer (10 x): 250 mM TRIS-Base, 1% SDS, 2.5 M Glycine

Blotting Buffer: 4.5 g Tris base, 21 g Glycine, 300 ml Methanol, 1.2 l water

TBS-T: 25 mM TRIS, 125 mM NaCl, 0.1% Tween-20, pH 8.0

Blocking buffer: 5% BSA or skimmed milk in TBS-T

Stripping solution: 0.4 M NaOH in water

Immunocytochemistry and confocal microscopy

For immunocytochemistry, cells were plated onto UV-sterilized cover slips in 6-well cell culture dishes. The cells were fixed for 5 min in a 2% para-formaldehyde (PFA) solution after aspirating the medium. The cover slips were washed 3 x with PBS and

permeabilized for 15 min with 0.1% Triton X-100 in PBS. Subsequently, the cells were blocked for 2 h with 10% normal goat serum in PBS. For detection of SF-Txnrd1, the cover slips were incubated overnight with the α-FLAG antibody (clone M2 mouse monoclonal, Sigma-Aldrich GmbH, Taufkirchen, Germany) at 4°C in a humidified chamber. The cover slips were washed 3 x with PBS/Tween and subsequently incubated with the α-mouse-Cy3-conjugated secondary antibody for 45 min in the dark. The cover slips were washed 3 x with PBS/Tween and then incubated for 2 min in DAPI solution. The cover slips were briefly rinsed in PBS and then mounted onto microscope slides, using mounting medium (Dako Cytomation, Hamburg, Germany). The slides were dried overnight at 4°C, protected from light and eventually sealed with nail polish. Pictures were taken by confocal microscopy with the Olympus FV1000 microscope and image was analyzed by FV10-ASW 1.6 viewer software.

PFA solution: 4% (w/v) PFA in PBS, pH 7.4 adjusted with HCl

α-FLAG antibody: 1:200 in PBS/10% normal goat serum

α-mouse IgG-Cy3: 1:500 in PBS/10% normal goat serum

DAPI-solution: 1 µg/ml DAPI diluted in PBS (5 mg/ml stock solution in H_2O)

PBS/Tween: 0.1% (v/v) Tween 20 in PBS

Triton X-100 solution: 0.1% (v/v) Triton X-100 in PBS

3.2.4 Cell culture related techniques

Isolation of MEFs and establishment of cell lines

MEFs were isolated from the conditional knockout mice at E12.5 embryos. Embryos were dissected from the uterus. After removing the appendages and visceral organs, the remaining parts were minced with forceps and incubated with trypsin/EDTA for 10 min. Finally, the cell suspension was incubated with cell culture medium and allowed to grow in culture for 2 days. Then, they were splitted every 3rd day. All the cell lines were genotyped for *Txnrd1* and were cryo-preserved for future use in liquid nitrogen. Immortalized cell lines were established after passaging the primary cell lines for at least 20 passages at 5 % oxygen, because cultivation of MEFs at normal

atmospheric oxygen concentration severely limits the replicative potential of the cells (Parrinello et al., 2003).

PBS (without Ca^{2+}, Mg^{2+}): 80.0 g NaCl, 2.0 g KCl, 14.4 g Na_2HPO_4, 2.4 g KH_2PO_4 in 1 l H_2O, pH 7.4

Standard DMEM: DMEM 1 x, 10% FCS, 1% glutamine, 50 U/ml penicillin G, 50 µg/ml streptomycin

Measurement of cell proliferation/viability

Trypan Blue dye exclusion method

Trypan blue dye exclusion method was used for measuring the viability of MEFs. Trypan blue is excluded from viable cells due to intact plasma membrane while dead cells stain blue. The cells were trypsinized and an equal volume of medium was added to the cell suspension to neutralize trypsin. 10 µl of cell suspension was mixed with 40 µl of 0.4% trypan blue, and cells were counted using a Neubauer haemocytometer. Viable cells were counted in 4 WBC-counting chambers.

Trypan blue: 0.4% solution (Sigma-AldrichGmbH, Taufkirchen, Germany)

MTT assay

MTT assay was performed to measure the proliferation of the transformed cells and their response to different cytotoxic agents in 96-well plates as described by Mosmann, T. (Mosmann, 1983) with some modifications. 10,000 cells/well were plated in quadruplicate in 100 µl of cell culture medium. The cells were incubated with 50 µg of MTT for 4 hours at 37°C to measure the proliferation. For cytotoxic assay, 10,000 cells/well were plated in quadruplicate in 50 µl of cell culture medium and allowed to settle for 4-6 hrs after plating. Then 50 µl of cell culture medium containing the required concentration of different drugs was added to the cells. The cells were treated with drugs for 72 h. Subsequently, cells were incubated with 50 µg of MTT for 4 hrs at 37°C. Finally, 200 µl of acidified isopopanol was added to each well to dissolve the formazan crystals. Absorbance was measured at 570 nm (670 nm as reference wavelength) in a Tecan spectrophotometer and data was acquired by Magelan software version 4. To evaluate the cytotoxic effect, the OD value of

untreated cells was taken as 100% viable and data was normalized against this value and expressed as percentage viability.

MTT (Thiazolyl blue) reagent:

Stock solution (5mg Thiazolyl blue) in PBS, filter sterilized and stored in dark at 4°C.

Working solution: 1:1000 dilution in cell culture medium.

0.04 M HCl in isopropanol: 1.57 ml 32% HCl, 398.43 ml isopropanol.

Flow cytometry (FACS analysis)

Cell cycle analysis

The cells cycle analysis of transformed *Txnrd1* knockout cells was done by the PI method which measures the DNA content of the cells. PI intercalates into DNA. Since the DNA content of cells in G2/M phase is twice as that of G0/G1 phase, they can be distinguished from each other in FACS due to difference in amount of PI intercalated into DNA. $1x10^6$ cells from asynchronously proliferating cell cultures were harvested by trypsinization, washed twice with ice-cold PBS, and fixed in ice-cold 70% ethanol overnight. Then, the cells were washed again twice in ice-cold PBS and treated with DNase free RNase A (50-100 µg) for 30 min at room temperature. Subsequently, 10-20 µg of PI was added to each sample, and the cell suspensions were incubated for additional 15 min at room temperature in the dark. Then the samples were analyzed by FACS (BD FACS Calibur) in FL3 channel and data was analyzed by ModFitLT V3.0 software.

PI: 1 mg/ml in water

DNase free RNase A: 100 mg/ml

Ethanol p.a: 70%

Intracellular peroxide detection

Intracellular peroxide levels were detected by DCF staining. The acetylated forms of DCF, such as CM-H2DCFDA, are non-fluorescent until the acetyl groups are removed by intracellular esterases and oxidation occurs inside the cell. $1x10^5$ cells were loaded with 1 µM CM-H2DCFDA for 60 min at 37°C in DMEM without FCS. After staining, cells were harvested by trypsinization, followed by centrifugation (1200

rpm, 5 min) and 3 x washing with PBS. Finally, the cells were resuspended in 200 µl PBS. Samples were analyzed in a flow cytometer (BD FACS Calibur) in which cells were excited with 488 nm UV line argon ion laser and emission was recorded on channel FL1 at 530 nm. Data was analyzed by BD CellQuest^{TM} Pro software (BD Biosciences).

DCF solution: 1 µM CM-H2DCFDA in ethanol

Annexin V-PI staining for the detection of cell death

Annexin V-PI staining is a classical method to discriminate between apoptotic and necrotic cell death. In apoptotic cells, the membrane phospholipid phosphatidylserine (PS) is translocated from the inner to the outer leaflet of the plasma membrane. Annexin V binds PS with high affinity in a Ca^{2+}-dependent fashion. PI is excluded by cells with intact membranes. So the combination of annexin V-PI allows distinguishing apoptosis from necrosis. While Annexin-V positive and PI-negative cells are defined as apoptotic cells, double-positive cells are either late apoptotic or necrotic. For Annexin V-PI analysis, the cells were washed twice with cold PBS and resuspended in 100 µl annexin-binding buffer. Then the cells were incubated with 5 µl of Annexin V-FITC (BD PharMingen, Heidelberg, Germany) and 5 µl of PI (20 mg/ml stock solution, Sigma-Aldrich GmbH Taufkirchen, Germany) for 15 min in the dark at room temperature. The cells were then analyzed by FACS (BD FACS Calibur) and data was analyzed by the BD CellQuest^{TM} Pro software (BD Biosciences)

Annexin V-binding buffer: 10 mM N-(2- hydroxyethyl)piperazin-N'-(propansulfonicacid)/ NaOH, pH 7.4, 140 mM NaCl, 2.5 mM CaCl2

PI solution: 1 mg propidium iodide in PBS

Soft-agarose assay

To assess the effect of *Txnrd1* knockout on the colonigenic potential of *myc-ras*-transformed cells, soft-agarose assays were performed. Approximately 500 cells/well were plated in 0.3% soft agarose prepared in cell culture medium in a 6-well cell culture plate. The agarose was allowed to cool by keeping it at 4°C for 15 min and then the plate was returned to the incubator. The cell culture medium was replaced at a 3 days interval. The single cell colonies appeared after 10 days. The colonies were

fixed in methanol and stained with crystal violet. They were allowed to dry and then counted visually.

Crystal violet: 0.5% in PBS

3.2.5 Biochemical techniques

Measurement of L-cystine uptake activity

Cystine uptake activity in xCT over-expressing *Txnrd1* knockout cells was measured by uptake of radio-labelled cystine in collaboration with Dr. Hideyo Sato (Yamagata University, Japan). Uptake of cystine was measured by techniques essentially as described by Sagara et al. and Novogrodsky et al. (Novogrodsky et al., 1979; Sagara et al., 1993). About 2 x 10^6 cells were washed in PBS and resuspended in 0.125 ml of pre-warmed PBS containing 0.1% glucose and 0.01% $Ca^{2+}$and Mg^{2+}. 125 µl of isotope labeled cystine (0.1 µCi/sample) (L- [14C (U)] Cystine (250 mCi/ mmol/ 0.02 mCi/ ml) (Perkin Elmer Life Sciences, Inc., Boston, USA) in uptake solution was added to the cell suspension and the suspension was incubated at 37°C. 100 µl aliquots were taken after the given time intervals and layered on a mixture of mineral oil and di-n-butyl phthalate 15:85 (vol/vol; total 200 µl) previously put in a small plastic tube. After centrifugation at 13,000 rpm for 10 sec in a microfuge, the tip of the tube containing the cell pellet was cut off, and the cells were solubilized in 200 µl of 0.5 M NaOH in a scintillation vial overnight at 37°C. Afterwards 3 ml of scintillation liquid and 100 µl of Tris-HCl were added to the vials and the radioactivity was determined using a scintillation counter (Beckman Instruments, LIQUID SCINTILATION SYSTEM, LS 5000 TA, Fullerton, CA). To compare basic activity of uptake solution with uptake activity of the cells, 5 µl of isotope labeled uptake solution was taken and mixed with 200 µl of 0.5 M NaOH for the determination of specific activity.

Uptake solution (for 10 samples): 1% (w/v) Ca^{2+}, Mg^{2+}

50 µl [14C] $(Cys)_2$ (0.1 µCi/sample) $MgCl_2$ x 6 H_2O 1 g

5 mM $(Cys)_2$ 15 µl * $CaCl_2$ x 2 H_2O 1.324 g

5 x PBS 50 µl dissolved in 100 ml of H_2O

10% (w/v) glucose 2.5 µl

1% (w/v) Ca^{2+}, Mg^{2+} 2.5 µl

H_2O 130 µl

*5 mM $(Cys)_2$ dissolved in 0.05 M HCl under stirring for a few hours at room temperature

Measurement of GSH concentration by HPLC

The total GSH (GSH+GSSG), reduced GSH and oxidized GSH (GSSG) concentration in transformed *Txnrd1* knockout cells were measured by the isocratic high-performance liquid chromatography (HPLC) method described for the estimation of total homocysteine (Feussner et al., 1997) with slight modification. This method is based on the derivatization of thiol group with a thiol-specific fluorogenic marker, 7-fluoro-benzo-2-oxa-1,3-diazole-4-sulphonate (SBD-F), which can be separated isocratically by reversed-phase HPLC using a Superspher 100 RP-18 column as stationary phase.

In brief, about $1x10^6$ cells were plated on a 10 cm dish 36 h before determination. Cells growing in log phase of growth were washed twice with PBS, then harvested by cell scrapers and collected in 6 ml of PBS. Cells were pelleted by centrifugation for 10 min at 2000 rpm at 4°C. Cells were resuspended in 300-500 µl of 2 M borate buffer (containing 5 mM Na_2EDTA, pH 9.5). Then the suspension was sonicated to lyse the cells. For reduction of disulfide bonds (in order to measure oxidized GSH), 200 µl of sample was mixed with 20 µl of tri-n-butylphosphine and incubated for 30 min at 4°C. To measure the reduced GSH 200 µl of samples were treated with 20 µl of Borate buffer. The reaction was stopped by adding 200 µl of 4 M percholric acid. Then the samples were centrifuged at 10,000 rpm for 10 min at 4°C. Finally, 100 µl samples or standard solution was mixed with 250 µl of Borate buffer (pH 10.5) and 100 µl of SBD-F and incubated for 1 h at 60°C in a water bath. After derivatization with SBD-F, samples were cooled to 4°C. 50 µl of the samples were applied on a HPLC column (Separation column - LiChroCART 250-4 and precolumn -LiChrospher 60 RP-select B (5 µM), MERCK KGgA (Darmstadt, Germany); Beckman detector System Gold, Pump Model 126 and Beckman counter Autosampler System Gold 508). The mobile phase consisted of a 30 mmol/l ammonium-formiate – 40 mmol/l ammonium-nitrate buffer (pH 3.65 adjuste with formic acid) and acetonitrile (95 + 5, by vol) at a flow rate of 1 ml/min. The column effluent was monitored by fluorescence detection (Fluorescence Detector RF 10Axl (Shimadzu, Japan)) with an excitation

wavelength of 385 nm and an emission wavelength of 515 nm. Standard samples were prepared by 2-fold serial dilution of 250 µmol/l of GSH in 0.1 mol/l Borate buffer, containing 2 mmol/l Na_2EDTA, for the calibration. The concentration of GSH was determined for the peak area in the chromatogram.

Borate buffer: 2 M Borate buffer containing 5 mM Na_2EDTA, pH 10.05

SDB-F: 1 mg/ml in borate buffer

Estimation of glutathione reductase activity

Glutathione reductase (GR) together with its co-factor, $NADPH/H^+$, catalyzes the reduction of oxidized glutathione (GSSG) to reduced glutathione (GSH). In this assay the oxidation of NADPH to NADP+ is monitored by the decrease in absorbance at 340 nm (Equation (I)).

$$\mathbf{GSSG + NADPH+H^+ \xrightarrow{GR} 2\ GSH + NADP^+} \qquad \text{(I)}$$

This rate of decrease in absorbance at 340 nm is directly proportional to the glutathione reductase activity in the sample, because the enzyme is present at rate-limiting concentrations. The unit definition for glutathione reductase activity may be expressed in terms of the oxidation of $NADPH/H^+$ or the reduction of GSSG since their molar ratio is 1:1. One unit of glutathione reductase oxidizes 1 µmol of $NADPH/H^+$ per minute at 25°C, pH 7.5.

The GR activity in transformed *Txnrd1* knockout cells was measured by the assay mentioned above. Briefly, $1x10^6$ exponentially growing cells were trypsinized, washed twice with ice-cold PBS, and then lysed in 200-300 µl of lysis buffer and further incubated for 30 min on ice. The lysate was kept for 30 min on ice and then centrifuged at 10,000 x g for 15 min at 4°C. The protein concentration was measured by the BCA method, adjusted to 2.5 mg protein/ml, and 25 µg of protein was used for measuring GR activity at 340 nm wavelength in a Tecan spectrophotometer with UV filter. Reading was taken every 2 min and the decrease in absorbance was monitored for 10 min. Yeast GR was used to prepare a standard curve which allowed

determining GR activity in the samples. The change in absorbance/min was used to calculate the GR activity in the sample from the standard curve of Yeast GR.

Lysis buffer: 0.2 M potassium phosphate buffer, 100 µM PMSF, 20% Triton X-100

Solution A: 0.2 M potassium phosphate buffer, 10 mM EDTA, pH 7.2

Solution B: 30 mM oxidized glutathione in water

Solution C: 0.8 mM NADPH in solution A

Solution D: 1% BSA in solution A

3.2.6 Tumor transplantation protocol

Implantation of transformed cells in mice

To investiagte the effects of Txnrd1-deficiency on the tumorigenic potential of *myc-ras* transformed cells; cells were transplanted in *C57BL/6* mice. $1x10^6$ transformed cells in a final volume of 100 µl were injected subcutaneously into *C57BL/6* mice, and tumors were allowed to develop. After 10 days the mice were sacrificed and the tumor volume and tumor mass were determined.

Treatment of Txnrd1-deficient tumor-bearing mice with BSO

To analyze the effectiveness of BSO treatment on Txnrd1-deficient tumor, $1x10^5$ transformed *Txnrd1* knockout cells were implanted subcutaneously into both flanks of *C57BL/6* mice. Tumors were allowed to grow for 3 days. After 3 days BSO (20 mM) was provided in drinking water for 10 days. Untreated group was provided with drinking water without BSO. Parental cell line was injected and treated similarly. At the end of the experiments mice were sacrificed and tumor mass and tumor volume was determined.

4. RESULTS

4.1 Analysis of thioredoxin reductase 1 function *ex vivo*

4.1.1 Establishment of mouse embryonic fibroblast cell lines from conditional Txnrd1 knockout mice

Thioredoxin reductase 1 (*Txnrd1*) has been implicated in cell proliferation and growth, and is indispensable for embryonic development (Bondareva et al., 2007; Jakupoglu et al., 2005). Using an siRNA knock-down approach in established cell lines, Yoo et al. reported that Txnrd1 is not essential for the survival of the cells *in vitro* (Yoo et al., 2006). As all attempts of establishing MEFs directly from knockout embryos invariably failed (Jakupoglu et al., 2005), the conditional *Txnrd1* knockout mouse generated by Jakupoglu et al., and cell lines derived there from, were used in the present study.

MEFs cell lines were established from conditional *Txnrd1* knockout mice, in which the knockout of *Txnrd1* can be achieved by expressing Cre recombinase. The strategy used for conditional disruption of *Txnrd1* is depicted in figure 12A. The procedure for the *in vitro* induction of the *Txnrd1* knockout is illustrated in figure 12B. MEFs were isolated from E12.5 embryos, obtained from the breeding of $Txnrd1^{fl/fl}$ mice with $Txnrd1^{+/fl}$ mice. $Txnrd1^{fl/fl}$ and $Txnrd1^{+/fl}$ MEFs cell lines were established and their genotype was confirmed by PCR (Figure 12C). Two $Txnrd1^{fl/fl}$ (Üa51 and Üa53) and one $Txnrd1^{+/fl}$ (Üa46) cell line were immortalized by cultivating them for at least 20 passages at 5% oxygen (Parrinello et al., 2003). *In vitro* deletion of *Txnrd1* was achieved by treating the cells with a Tat-Cre fusion protein (kindly provided by Dr. W. Hammerschmidt). Briefly, $5x10^4$ cells were incubated with 1 µg Tat-Cre protein for 16 h in CHO medium, and then the medium was exchanged for normal cell culture medium. After 24 hours the cells were washed, trypsinized, and single cell-cloned in 96-well plates by limiting dilution. Single cell clones were individually expanded and screened for deletion of *Txnrd1* by PCR (Figure 12C). The two knockout clones 51ΔD4 and 53ΔE1 and the heterozygous clone 46ΔB5 were expanded to establish cell lines. These three cell lines together with the respective parental cell lines Üa51, Üa53 and Üa46 were used throughout the present study. The presence/absence of Txnrd1 in these cell lines was verified by Western blotting (Figure 12D) using an antibody against human TrxR1.

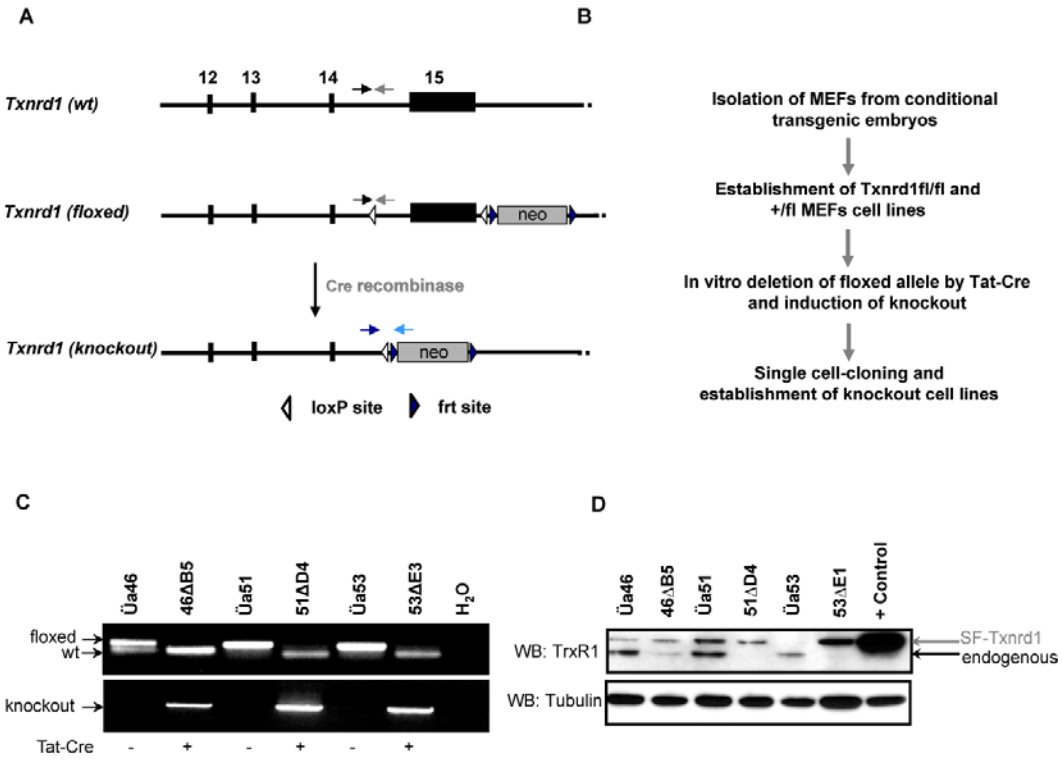

Figure 12. Disruption of thioredoxin reductase 1 in MEFs by Cre recombinase *ex vivo*. A) Schematic representation of the generation of *Txnrd1* conditional knockout mice (Jakupoglu et al.; 2005). Exon 15 of the *Txnrd1* gene, harboring the C-terminal catalytic center, was flanked by two *lox*P sites (shown as white triangles), which can be targeted by Cre recombinase. Primer pairs used for genotyping of mice and cells are depicted as black and gray arrows. **B)** Outline of procedure to establish the *Txnrd1* knockout cell lines. **C)** Genotype of different MEFs cell lines. Successful deletion of the gene was verified by PCR using the deletion-specific primer pairs (depicted in blue and cyan arrows in A). The 66 bp band corresponds to the wild-type allele, the 130 bp band corresponds to the floxed allele, and the 320 bp band is obtained after successful deletion of the *lox*P-flanked allele. **D)** Deletion in these cell lines was confirmed by immunoblotting using an antibody raised against human TrxR1 in rabbit. The SF-Txnrd1 expressing cell line was used as positive control. Anti-human TrxR1 antibody was a kind gift form Dr. Gladyshev (University of Nebraska, Lincoln, USA).

4.1.2 Txnrd1 knockout cells are highly susceptible to GSH depletion

Mitochondrial thioredoxin reductase (*Txnrd2*) knockout cells were previously shown to be highly susceptible to GSH depletion induced by BSO (Conrad et al., 2004). To test whether *Txnrd1* knockout cells are equally susceptible to BSO, *Txnrd1* knockout cells were treated with increasing concentrations of BSO; the viability of cells was assessed 72 h later by the trypan blue dye exclusion method. As shown in figure 13, *Txnrd1* knockout cells (53ΔE1) were highly sensitive to BSO treatment. While the heterozygous control cell line died in a similar manner with increasing BSO concentrations as the parental cell lines (46ΔB5 v/s Üa46), the knockout cell line (53ΔE1) died already at lower BSO concentrations than the respective parental cell

line (Üa53). Thus, like *Txnrd2* knockout cells, viability of *Txnrd1* knockout cells was severely compromised after BSO-mediated GSH depletion. The same results were obtained with a second pair of cell lines (Üa51 and 51ΔD4) (data not shown).

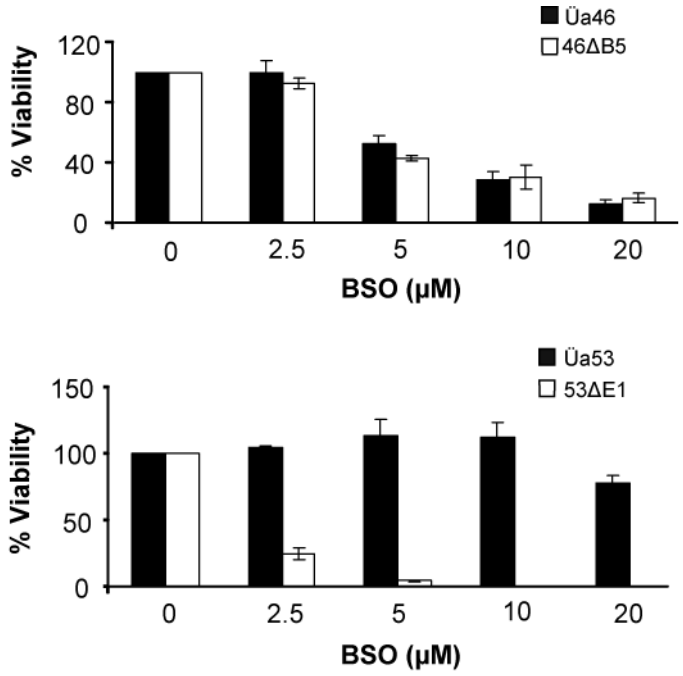

Figure 13. *Txnrd1* knockout cells were susceptible to experimental GSH depletion. *Txnrd1* knockout cells 53ΔE1 and heterozygous control cells 46ΔB5 were treated with the indicated concentrations of BSO for 72 h, and the viability was determined by the trypan blue exclusion method. *Txnrd1* knockout cells (53ΔE1) were highly susceptible to BSO as compared to the parental cell line Üa53 (4.14±0.46 % v/s 113.56±12.41 % at 5 μM BSO). The heterozygous control cell line 46ΔB5 behaved similar to the parental cell line Üa46 (30.22±7.65 % v/s 28.7±4.7 % at 10 μM BSO) (mean ± SD). Data shown here is representative of two independent sets of experiments. This was confirmed with another knockout cell line, yielding the same results (data not shown).

4.1.3 Reconstitution of Txnrd1 expression restored resistance against BSO

To prove that the above finding was due to the loss of function of *Txnrd1*, the Strep-FLAG-tagged mouse *Txnrd1* cDNA, including the SECIS element (SF-Txnrd1 wt (2ATG)), was stably expressed in *Txnrd1* knockout cells by lentiviral transduction (Figure 14A). In parallel, various mutant forms of *Txnrd1*, in which the Sec (U498) and the three cysteines (C59, C64 and C497) involved in Txnrd1 catalysis, were mutated individually to cysteine and serine (for U498) and serine (for C59, C64 and C497), respectively, by site-directed mutagenesis. Those were then stably expressed in the *Txnrd1* knockout cells to elucidate their catalytic significance *in vivo*. Different

cell lines expressing either wild-type or mutated *Txnrd1* genes were established by puromycin selection. Expression of the tagged Txnrd1 (SF-Txnrd1) was confirmed by Western blotting using an antibody against FLAG (Figure 14B).

The different cell lines were treated with 15 µM of BSO, and cell viability was determined 72 h later. As shown in figure 14C, the expression of SF-Txnrd1 wt (2ATG) provided rescue against BSO-mediated toxicity (38.79±7.35%) as compared to the mock control (0.36±0.56%). The functionality of different Txnrd1 mutant forms was compared with wild-type Txnrd1. As shown in figure 14C, the N-terminal Cys mutants (C59S, C64S) provided rescue in comparable fashion to the wild-type protein (38.75±22.75% and 34.04±7.96%), while the C-terminal mutants were less efficient in compensating the loss of Txnrd1 function. The C497S mutant was functionally almost inactive and did not rescue knockout cells from cell death induced by GSH depletion (3.6±5.09%). With about 25% remaining viability (24.23±11.23%), the U498C mutant was able to partially rescue the phenotype, whereas the U498S and U498STOP mutants were less active and only a small proportion survived BSO treatment (8.6±8.9% and 12.79±3.09%, respectively). These results suggested that mutation of one of the N-terminal Cys residues has little impact on enzyme function. The C-terminal cysteine residue C497 is the most critical cysteine residue involved in catalysis as it is the releasing cysteine.

The subcellular localization of SF-Txnrd1 wt (2ATG) and the various mutants was determined by confocal microscopy using an anti-FLAG antibody (Figure 14D). Although Txnrd1 has been reported to be located in the cytosol, the wt (2ATG) protein was also detected in the nucleus. Also the U498STOP mutant and to a lesser extent the C497S mutant displayed nuclear localization. By contrast, all other mutants were predominant cytosolic in distribution. The staining pattern for C64S and C497S exhibited granularity, so localization to other sub-cellular compartments can not be ruled out at the moment and further studies are needed to firmly establish the intracellular localization of these mutants.

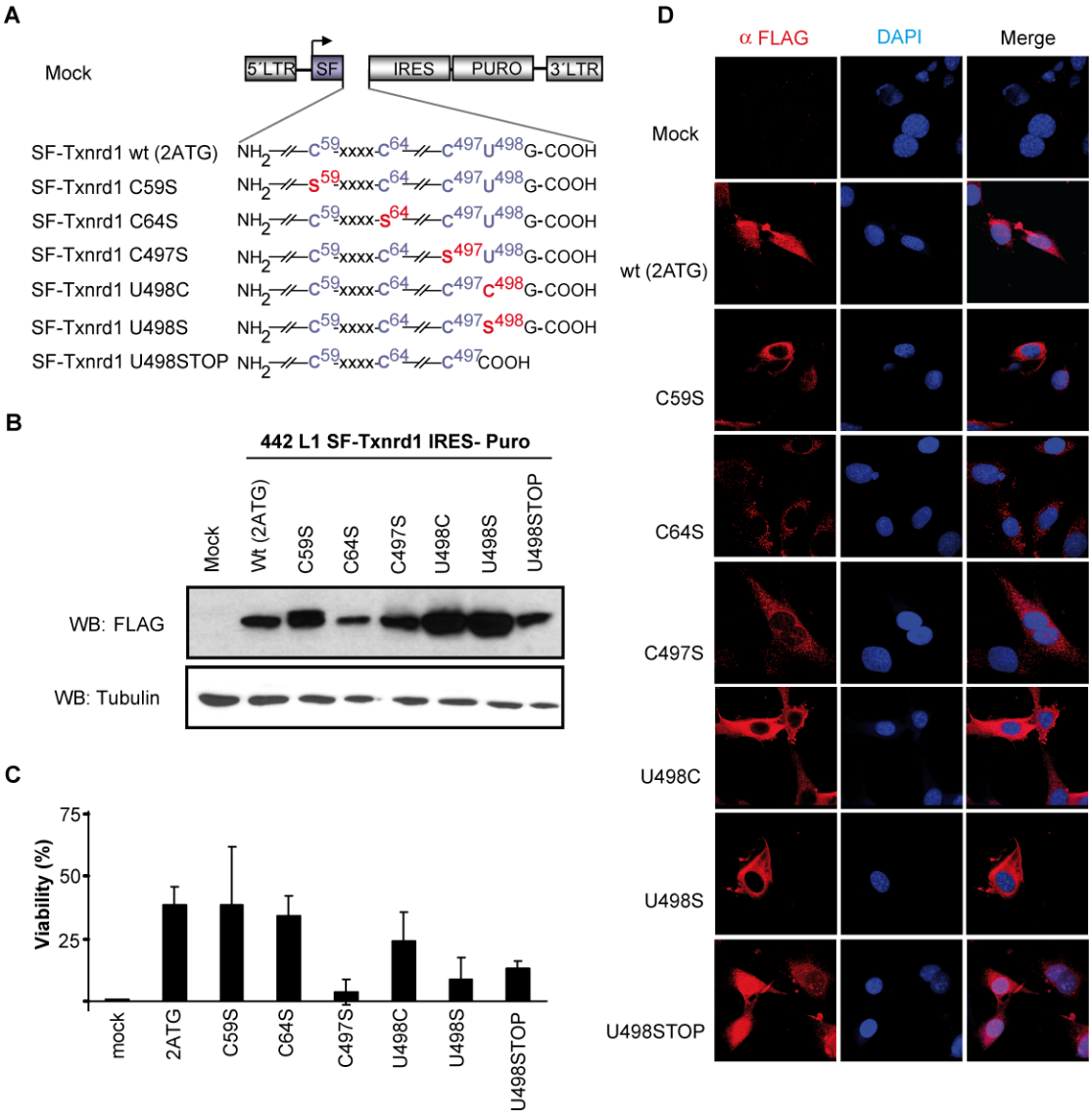

Figure 14. Reconstitution of Txnrd1 function provided rescue against BSO-mediated GSH depletion. A) Schematic representation of various strep-FLAG-tagged mouse Txnrd1 (SF-Txnrd1) constructs which were stably expressed in knockout cells by lentiviral transduction. **B)** Expression of the different forms was analyzed by Western blotting using a FLAG-specific antibody. Immunoblotting revealed differential expression in the cells although they were expressed from the same promoter. **C)** The viability was determined for each form after 72 h of BSO treatment. The % viability was calculated by setting the cell number in the untreated controls as 100%. The reconstitution of Txnrd1 provided substantial rescue against BSO-mediated cell death (38.79±7.35% as compared to the mock control 0.36±0.56%). Data is pooled from two sets of experiments (mean±SD). Out of all the mutants tested, the C497S mutant was functionally inactive, while the C-terminal mutants were less efficient in complementing the loss of endogenous Txnrd1. **D)** Sub-cellular localization of the different constructs was confirmed by immunocytochemistry and confocal microscopy. Although Txnrd1 has been reported to be a cytosolic enzyme, the wild-type protein was localized in the nucleus as well (600 x magnification).

4.1.4 Txnrd1 knockout cells were not rescued by antioxidants

It has been shown that mitochondrial thioredoxin reductase (*Txnrd2*) knockout cells can be rescued from BSO-mediated GSH depletion by antioxidant supplementation like NAC (Conrad et al., 2004)(Tamara Perisic, unpublished observation). Moreover, *γ-GCS* knockout cells, which are devoid of endogenous GSH synthesis, can be grown in culture in the presence of thiol-containing compounds (Shi et al., 2000). These reports suggested that the requirement of GSH for cell survival and proliferation can be bypassed by antioxidant supplementation. To test whether the decrease in cell viability following BSO-mediated GSH depletion in *Txnrd1* knockout cells can be antagonized by antioxidants, the *Txnrd1* knockout cell line 53ΔE1 and the heterozygous control cell line 46ΔB5 were treated with 10 μM BSO in the presence or absence of the antioxidants NAC, Trolox® and 2-mercaptoethanol (2-ME) for 72 h. Subsequently, cell numbers were determined using trypan blue. As shown in figure 15, all antioxidants tested antagonized the BSO-induced decline in cell viability in wild-type (Üa53 and Üa46) and heterozygous control (46ΔB5) cell lines, but they invariably failed to rescue the *Txnrd1* knockout cells (right panel Figure 15). These experiments were repeated in another knockout cell line yielding similar results (data not shown). These findings indicated that the GSH requirement can not be bypassed by antioxidants in the absence of *Txnrd1*. Thus, either *Txnrd1* is required for the utilization of the antioxidants, or in the absence of GSH, viability of *Txnrd1* deficient cells cannot be sustained by antioxidant supplementation.

4.1.5 Txnrd1 knockout cells underwent necrosis or oxidative stress-induced cell death upon BSO treatment

To study the mode of cell death following BSO-mediated GSH depletion, the knockout cell lines 53ΔE1 and 51ΔD4 were treated with 10 μM BSO. Since the heterozygous cell line 46ΔB5 was more resistant towards BSO as compared to the knockout cell lines (Figure 13), these cells were treated with 20 μM BSO to study the cytotoxic effect within the same time period. The cells were treated with BSO in the presence or absence of antioxidants for 24 hours and then stained with annexin V and PI. The samples were analyzed by FACS and the data was quantified by Cell Quest™ Pro software (BD Bioscience).

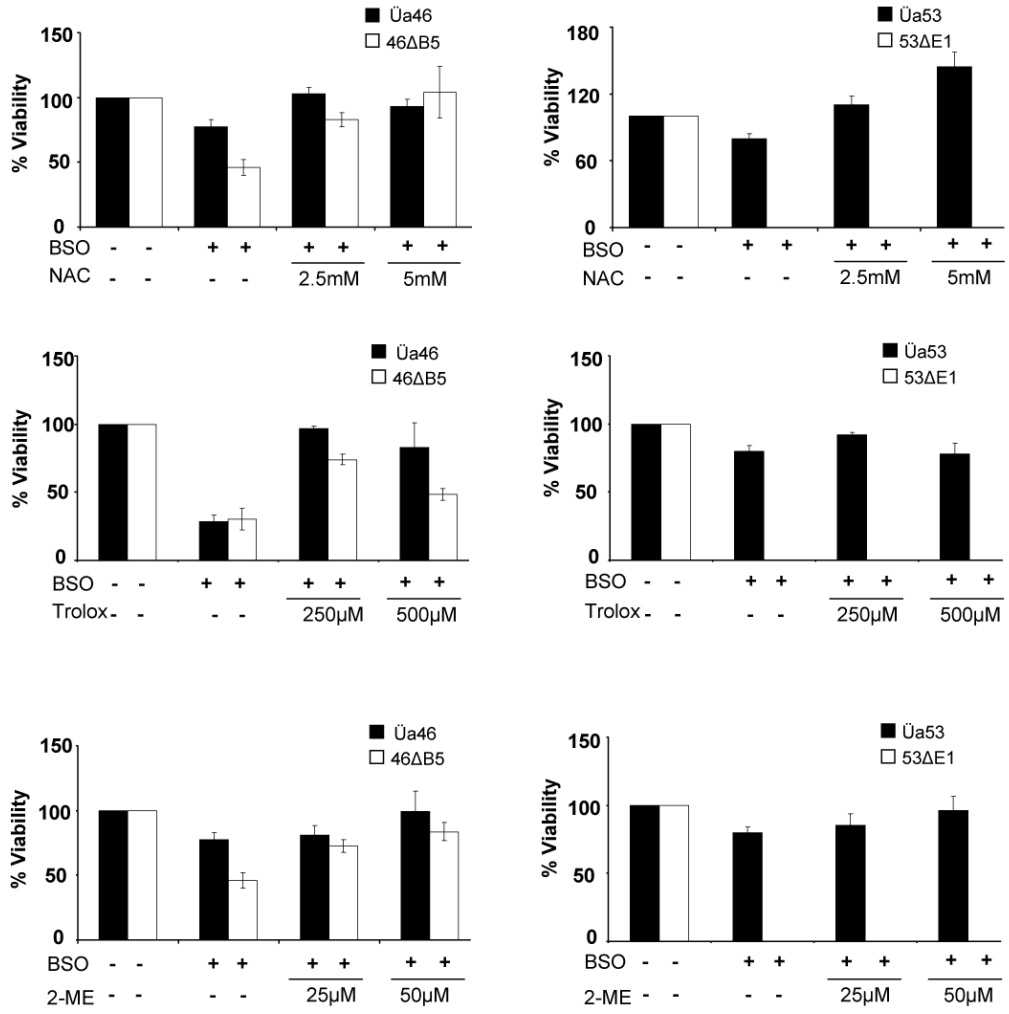

Figure 15. Antioxidant supplementation was unable to rescue the *Txnrd1* knockout cells against BSO-mediated GSH depletion. Three antioxidants NAC, Trolox® and 2-ME were tested at the given concentrations for rescuing cells from cell death induced by treatment with 10 µM BSO. While they provided resistance against BSO in wild-type (Üa53 and Üa46) and heterozygous (46ΔB5) cell lines, they failed to rescue the knockout (53ΔE1) cells from cell death induced by BSO-mediated GSH depletion. While the viability of BSO-treated Üa53 wild-type cells was 79% compared to untreated cells, Üa53 cells were efficiently rescued from BSO-induced cell death with 2.5mM NAC (109.97% viability), 5mM NAC (144.5%), 250 µM Trolox® (92%), 500 µM Trolox® (78%), 25 µM 2-ME (85%), and with 50 µM 2-ME (96% viability). Knockout cells could not be rescued from BSO-induced cell death by any of these antioxidants. The data is representative of two sets of experiments, which was further confirmed in another knockout cell line with similar findings (mean±SD).

BSO-treated knockout cells exhibited very late apoptotic or necrotic characteristics (Annexin V-positive and PI-positive) and underwent rapid cell death presumably due to massive oxidative stress. As shown in figure 16, BSO treatment of the control cell line (46ΔB5) resulted in 18.7% Annexin V- and PI double-positive cells which was reduced to 1.8%, 4.3% and 4% when the cells were simultaneously treated BSO plus either 5 mM NAC, 250 µM Trolox® or 50 µM 2-ME, respectively.

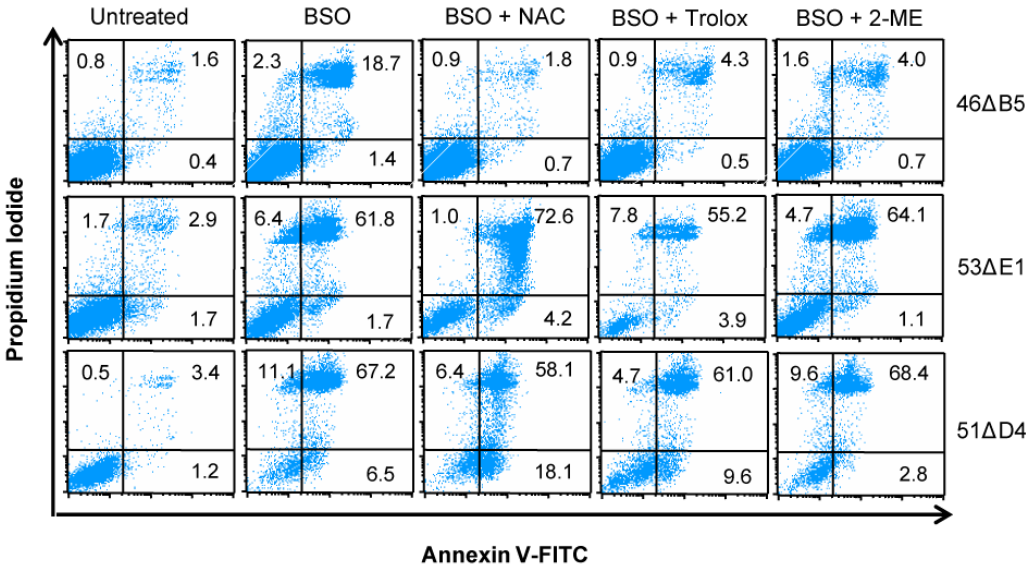

Figure 16. Antioxidant supplementation failed to rescue the *Txnrd1* knockout cells from BSO-induced cell death. Cells were treated with BSO with or without antioxidant supplements for 24 h and then stained with Annexin V and PI and analyzed by FACS. The tested antioxidants were able to rescue the heterozygous control cell line 46ΔB5 (18.7% Annexin V-PI positive cells in case of BSO alone v/s 1.8% with NAC, 4.3% with Trolox® and 4.0% with 2-ME), but were ineffective in preventing BSO-induced cell death in the knockout cell lines 53ΔE1 (61.8% BSO alone, 72.6% with BSO plus NAC, 55.2% with BSO plus Trolox® and 64% with BSO plus 2-ME) and 51ΔD4 (67% with BSO alone, 58% with BSO plus NAC, 61% with BSO plus Trolox® and 68.4% with BSO plus 2-ME).

But in the case of both knockout cells lines (53ΔE1 and 51ΔD4), none of the antioxidants was able to prevent BSO-induced cell death (72.6% with NAC, 55.2% with Trolox® and 64.1% with 2-ME as compared to 61.8% Annexin V and PI double-positive cells with 10 µM BSO alone). Thus, these antioxidants were ineffective in rescuing *Txnrd1* knockout cells from BSO-induced cell death.

4.1.6 xCT over-expression failed to rescue Txnrd1 knockout cells from GSH depletion

Previous work in the lab had shown that over-expression of xCT, the substrate-specific subunit of the cystine/glutamate antiporter system $\mathbf{X_c^-}$, confers high resistance to oxidative stress in Burkitt's lymphoma cells (Banjac et al., 2008), and effectively bypasses GSH-deficiency in γ-*GCS* knockout cells (Seiler, 2008). System $\mathbf{X_c^-}$ facilitates the uptake of cystine, $(Cys)_2$, from the extracellular space, which is rapidly reduced to cysteine (Cys) within the cell by a still unknown mechanism. Thus, by increasing the cellular uptake of cystine and strongly boosting the intracellular and

extracellular cysteine levels, xCT over-expression bypasses the requirement for GSH. To test whether xCT over-expression rescues *Txnrd1* knockout cells, the *Txnrd1* knockout cells 53ΔE1 and the heterozygous control cell line 46ΔB5 were transfected with the mouse xCT expression plasmid 141pCAG-3SIP-xCT. An eGFP-expression plasmid (141pCAG-3SIP-eGFP) and empty vector (141pCAG-3SIP) were used as controls. The following cell lines were established after puromycin selection: 53ΔE1-mock, 53ΔE1-eGFP, 53ΔE1-xCT, and 46ΔB5-mock, 46ΔB5-eGFP, and 46ΔB5-xCT. Over-expression of *xCT* in these cell lines was confirmed by qRT-PCR. Compared to 53ΔE1-eGFP cells, 53ΔE1-xCT cells showed a 22-fold increase in the *xCT* mRNA levels, which resulted in a 7-fold higher uptake of radiolabelled cystine (0.208±0.022 versus 1.385±0.347 nmol cystine/min/mg protein) (Figure 17A and B). Even though the control cell line 46ΔB5-xCT showed a 4-fold increase in *xCT* transcripts, the cystine uptake in these cells was only marginally increased (0.182±0.05 nmol cystine/min/mg protein) compared to the 46ΔB5-eGFP control cells (0.141±0.03 nmol cystine/min/mg protein).

These cells were then challenged with BSO to assess whether xCT over-expression is able to rescue *Txnrd1* knockout cells from BSO-induced cell death as previously shown for Burkitt's lymphoma cells and γ-*GCS* knockout cells. As illustrated in figure 17C, xCT over-expressing cells (53ΔE1-xCT) not only died at a much lower concentration of BSO (2.5 µM) than eGFP-transfected cells (53ΔE1-eGFP) (10 µM), they also died at a much faster rate (Figure 17D). Although xCT was only marginally over-expressed in the heterozygous control cell line (46ΔB5-xCT), it conferred resistance against BSO in a dose-dependent manner (at 10 µM BSO 79.84±4.8% of the cells were viable as compared to 30.43±1.45% for eGFP-transfected cells) (Figure 17C). This was reflected in a marginal growth advantage provided to the 46ΔB5-xCT control cell line when cultivated in presence of 10 µM BSO (Figure 17D).

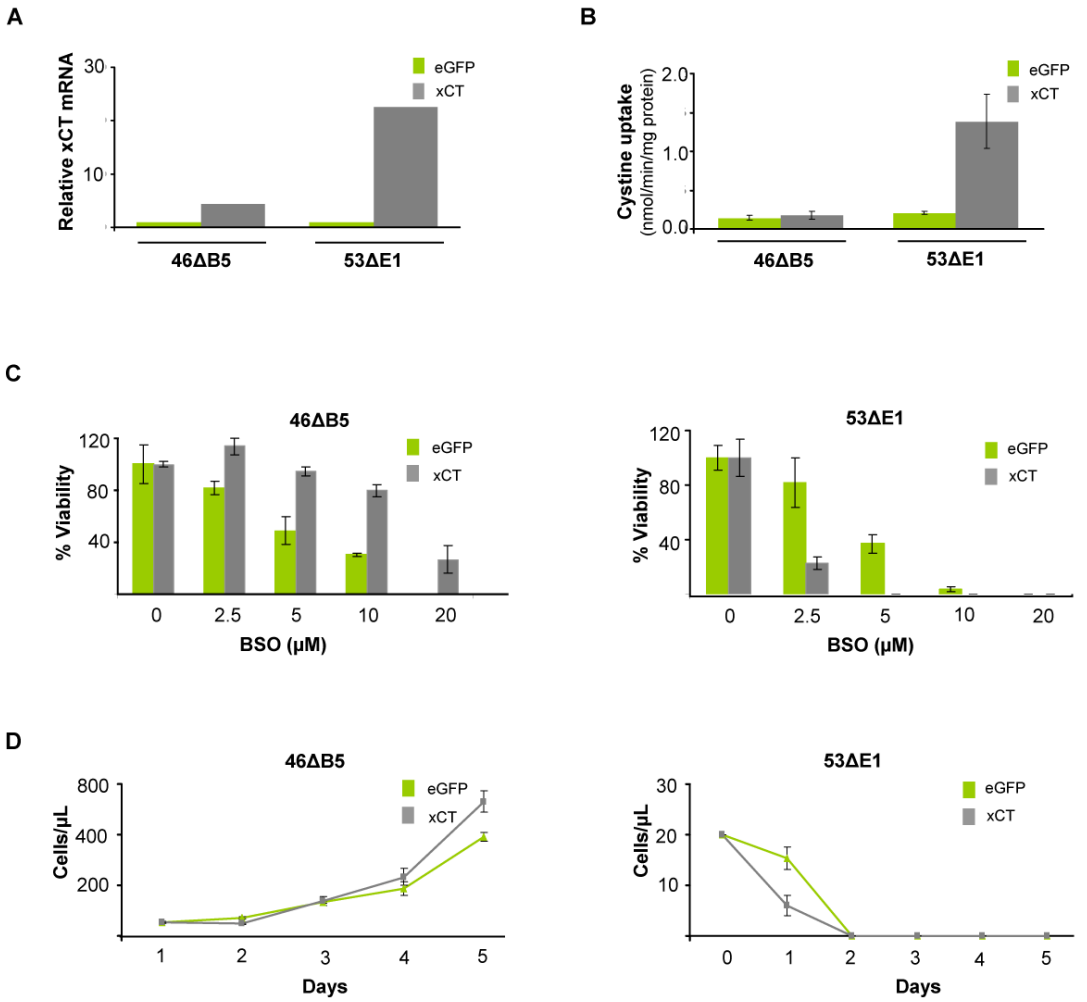

Figure 17. Enforced expression of xCT in *Txnrd1* knockout cells was ineffective in rescuing the cells from BSO-induced cell death. xCT over-expression was confirmed by **(A)** qRT-PCR and **(B)** specific cystine uptake activity. As compared to eGFP-transfected 53ΔE1-eGFP control cells, the xCT over-expressing cells 53ΔE1-xCT showed a 22-fold increase in *xCT* mRNA and a 7-fold increase in cystine uptake activity. Only a 4-fold increase in *xCT* mRNA levels in 46ΔB5-xCT cells resulted in a marginal increase in cystine uptake (0.182±0.05 v/s 0.141±0.03 nmol cystine/min/mg protein). **(C)** Even the marginal increase in cystine uptake caused increased resistance towards BSO in the heterozygous cell line 46ΔB5-xCT compared to 46ΔB5-eGFP control cells (80% v/s 30% at 10 μM BSO) and in addition **(D)** provided a growth advantage to the cells in a time-dependent manner. In stark contrast, xCT over-expression in *Txnrd1* knockout cells 53ΔE1-xCT failed to rescue knockout cells against BSO-induced cell death. Data is representative of two separate sets of experiments (mean±SD).

4.1.7 xCT over-expressing Txnrd1 knockout cells underwent rapid cell death as compared to mock-transfected control cells upon GSH depletion

The above experiments showed that xCT over-expressing *Txnrd1* knockout cells (53ΔE1-xCT) died rapidly and at a much lower concentration of BSO than eGFP-expressing cells (53ΔE1-eGFP). For further quantification of cell death, 53ΔE1-mock and 53ΔE1-xCT cells were treated with 10 μM of BSO for 24 h and then stained with

Annexin V and PI, and analyzed by FACS. Compared to mock-transfected cells (53ΔE1-mock) (7.5±0.8%), xCT over-expressing *Txnrd1* knockout cells were more susceptible to induction of cell death by BSO (53ΔE1-xCT) (23.8±5.4) (Figure 18). These results suggested that BSO treatment of xCT over-expressing *Txnrd1* knockout cells causes induction of cell death at a faster rate compared to mock-transfected cells. Thus, rather than conferring resistance against BSO-induced cell death, xCT over-expression in *Txnrd1* knockout cells accelerated the induction of BSO-induced cell death.

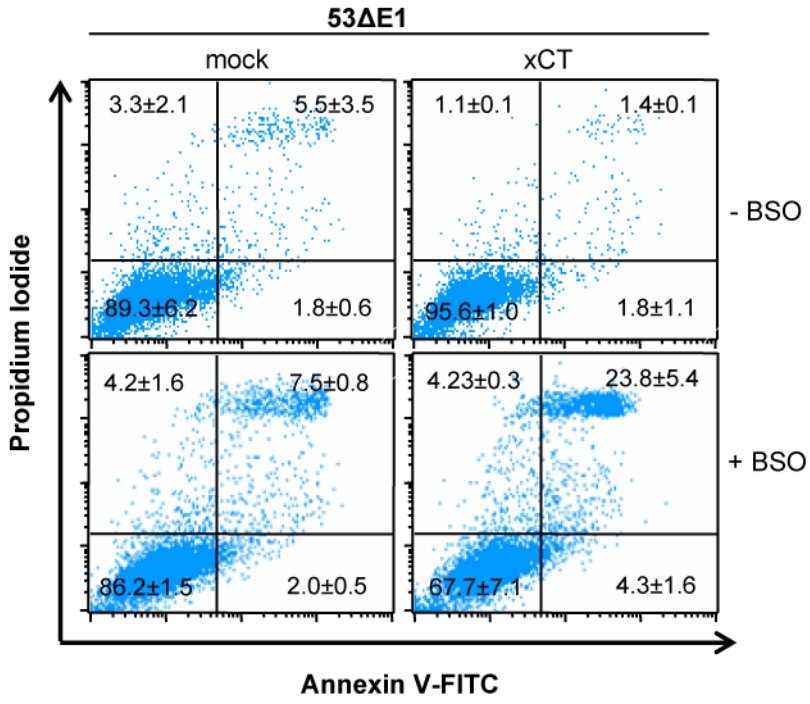

Figure 18. Over-expression of xCT in *Txnrd1* knockout cells induced rapid cell death upon BSO treatment. Mock-transfected and xCT over-expressing cells were treated with 10 μM of BSO for 24 h, subsequently stained with Annexin V and PI, and analyzed by FACS. As compared to 53ΔE1-mock cells (7.5±0.8%), 53ΔE1-xCT cells revealed a higher percentage of dying cells (23.8±5.4%). Pooled data from two separate experiments is represented with the mean±SD in percentage.

4.1.8 xCT over-expressing Txnrd1 knockout cells suffered from severe oxidative stress upon GSH depletion

If the induction of cell death is the sole effect of GSH depletion, xCT over-expressing *Txnrd1* knockout cells should undergo cell death at the same pace as the control cell line. Based on the above findings, it was speculated that the accumulation of imported cystine leads to or mimics the state of massive oxidative stress due to the

high abundance of disulfide. It has also been known that under oxidative stress, proteins undergo mixed disulfide formation, which positively correlates with the extent of oxidative stress.

4.1.8.1 ROS accumulation in xCT over-expressing *Txnrd1* knockout cells was comparable to that in mock-transfected cells

To investigate whether BSO-treatment leads to increased accumulation of ROS in xCT-over-expressing *Txnrd1* knockout cells as compared to mock-transfected controls, cells were treated with 10 µM BSO for 24 h. These were subsequently stained with DCF and analyzed by FACS to detect the level of soluble ROS. As shown in figure 19A and B, ROS accumulation in xCT over-expressing Txnrd1 knockout cells 53ΔE1-xCT (mean fluorescent intensity MFI=190.9±87.7) was comparable to that in mock transfected *Txnrd1* knockout cells (53ΔE1-mock) (MFI=177.5±61.5) after BSO treatment. Furthermore, a lower level of ROS was detected in heterozygous cells over-expressing xCT (46ΔB5-xCT) (MFI=22.35±5.8) and mock-transfected cells (46ΔB5-mock) (MFI=26.8±8.4) upon BSO treatment. The result of the above experiment led to the conclusion that the accelerated cell death induced by BSO-induced cell death in xCT-over-expressing *Txnrd1* knockout cells was not due to increased ROS accumulation upon GSH depletion. It suggested a contribution of “disulfide stress” due to an accumulation of imported cystine.

4.1.8.2 Activation of the SAPK/JNK pathways led to execution of rapid cell death in xCT-over-expressing *Txnrd1* knockout cells

The SAPK/JNK and p38 MAPK pathways are stress-induced signalling pathways. Upon various kinds of stress stimuli, SAPK/JNK and p38 become phosphorylated at serine/threonine residues and induce the downstream target genes responsible for induction of cell death. As it was hypothesized that rapid induction of cell death in xCT over-expressing *Txnrd1* knockout cells was due to disulfide overload-mediated oxidative stress, the phosphorylation status of these SAPK/JNK was determined by Western blot using phospho-specific antibodies raised against Thr183/Tyr185 amino acid residues of human SAPK/JNK. xCT over-expressing cells along with control cell lines were treated with 10 µM BSO for 10-12 h and cell lysate was prepared in LCW buffer in the presence of PhosSTOP phosphatase inhibitor cocktail (Roche

diagnostics) and protease inhibitor cocktail (Roche diagnostics) and analyzed by immunoblotting. As shown in figure 20, there was a preferential activation of the SAPK/JNK pathway in xCT over-expressing *Txnrd1* knockout cells upon GSH depletion than in eGFP expressing control cells, as more accumulation of phospho-SAPK/JNK was detected by western blot.

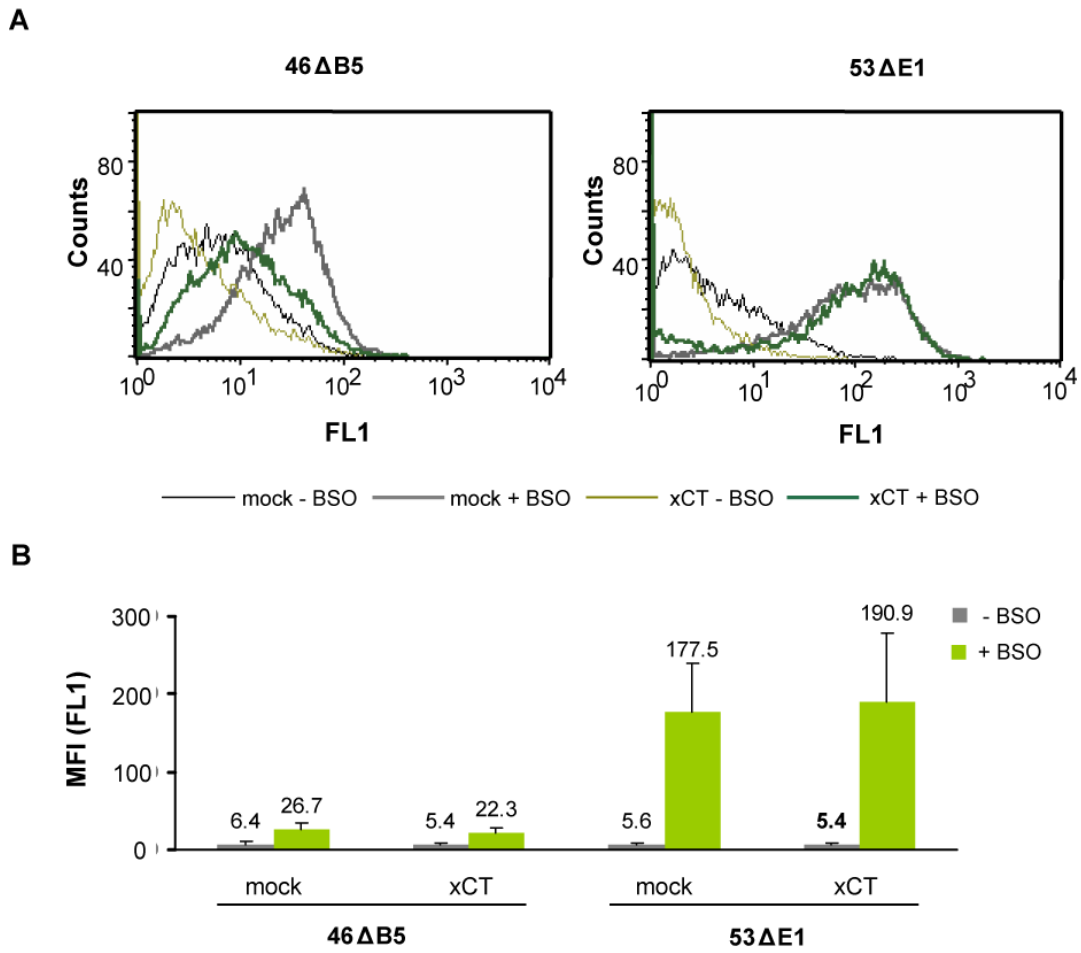

Figure 19. Accumulation of ROS in xCT over-expressing *Txnrd1* knockout cells upon BSO treatment. Cells were treated for 24 h with BSO and stained with DCF to detect soluble ROS. **(A)** Histogram showing ROS accumulation after BSO treatment. As indicated by a shift in the histogram to the left, xCT-over-expressing heterozygous cells (46ΔB5-xCT) showed less ROS accumulation (thick green line) than mock-transduced cells (thick grey line). Knockout 53ΔE3 cells accumulated significantly more ROS than heterozygous 46ΔB5 cells and there was no left shift in the histogram in case of xCT-over-expressing *Txnrd1* knockout cells, **(B)** Mean fluorescence intensity (MFI) in FL1. The accumulation of soluble ROS in xCT over-expressing *Txnrd1* knockout cells was comparable to that in mock transfected cells (MFI=190.9±87.7 v/s 177.5±61.5). Pooled data from two sets of experiments is shown as mean fluorescent intensity of FL1±SD.

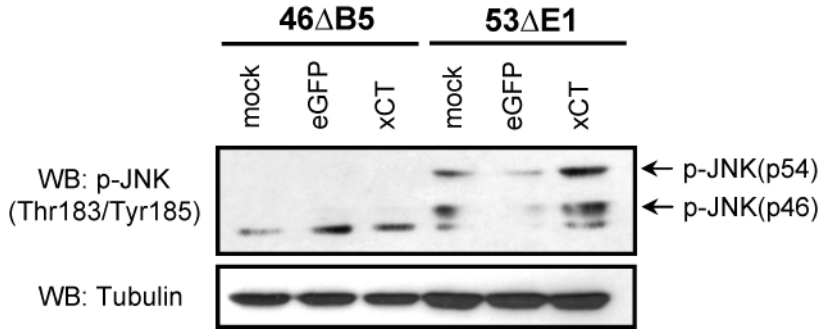

Figure 20. Preferential activation of SAPK/JNK in xCT over-expressing *Txnrd1* knockout cells after BSO treatment. The higher level of phospho- SAPK/JNK may be indicative of increased oxidative stress due to an accumulation of imported cystine ("Disulfide overload").

4.1.9 Co-culture of Txnrd1 knockout cells with xCT over-expressing cells failed to prevent BSO-induced cell death

xCT overexpressing Burkitt´s lymphoma, *γ-GCS* knockout cells, and *Txnrd2* knockout cells take up cystine very efficiently, reduce it intracellularly and secrete large amounts of cysteine into the medium (Perisic, T., unpublished and (Banjac et al., 2008; Seiler, 2008)). It was found previously in our lab that xCT over-expressing cells, by providing cysteine and generating a reducing extra-cellular environment, can serve as feeder cells and render co-cultivated control cells that are otherwise dependent on a thiol-containing compound, independent from antioxidant supplementation to the medium. The secreted cysteine is then taken up by the control cells, and by providing the reducing equivalents, maintains the reducing intracellular environment. Thus, the GSH or NAC requirement of eGFP-transfected *γ-GCS* knockout cells could be bypassed by co-culture with xCT over-expressing *γ-GCS* knockout cells (Seiler, 2008). Under GSH depletion, the major redox buffer GSH can thus be replaced by the readily available cysteine in xCT over-expressing cells. Yet, the mechanism of intracellular reduction of cystine to cysteine is unknown.

Since over-expression of xCT failed to rescue the *Txnrd1* knockout cells, it was hypothesized that *Txnrd1* knockout cells may fail to reduce the imported cystine. If cystine can not be reduced, xCT over-expression would apparently not prove beneficial to these cells. However, culturing *Txnrd1* knockout cells in a reducing extra-cellular milieu that is already conditioned with cysteine might improve their survival. To test this possibility, eGFP-expressing *Txnrd1* knockout cells or heterozygous control cells were co-cultured at a 1:1 ratio (Figure 21A) with xCT over-

expressing *Txnrd2* knockout cells. These xCT over-expressing *Txnrd2* knockout cells had been shown to be capable to protect eGFP-transfected *Txnrd2* knockout cells from BSO-induced cell death (Perisic, T., unpublished results).

The co-cultures were treated with BSO for 48 hours and subsequently analyzed by FACS for the presence of eGFP-positive cells. The results of the co-culture experiment revealed that xCT over-expressing *Txnrd2* knockout cells were unable to rescue *Txnrd1* knockout out cells from cell death induced by BSO-mediated GSH depletion (Figure 21B). In contrast, BSO-induced cell death was prevented in the heterozygous control cell line 46ΔB5-eGFP and the eGFP-transfected *Txnrd2* knockout cells (34% and 45% eGFP-positive cells, respectively). Hence, it was concluded from these experiments that cells devoid of *Txnrd1*, upon GSH depletion, are unable to exploit neither the beneficial effects of imported cystine nor that of freely available cysteine in the culture medium. Thus, *Txnrd1* knockout cells can neither be rescued from GSH depletion-induced cell death by antioxidants, by xCT over-expression nor by co-culture with xCT-over-expressing cells that condition the medium with cysteine.

4.1.10 Reconstitution of Txnrd1 expression in xCT over-expressing Txnrd1$^{-/-}$ cells provided resistance against BSO

To demonstrate that the aforementioned phenotype was exclusively caused by the loss of Txnrd1, knockout cells were reconstituted with exogenous Txnrd1 by lentiviral transduction. 53ΔE1-xCT and 53ΔE1-eGFP cells were infected with SF-Txnrd1 wt (2ATG) recombinant virus, which also expresses puromycin acetyltransferase to select for transduced cells. The over-expression of SF-Txnrd1 wt (2ATG) in these cells was evaluated by Western blotting using a human TrxR1-specific antibody (Figure 22A). Empty virus expressing cells were taken as mock control.

As compared to mock-transduced cells (53ΔE1-xCT mock or 53ΔE1-eGFP mock), SF-Txnrd1 wt (2ATG)-transduced cells (53ΔE1-xCT-SF-Txnrd1) showed increased resistance towards BSO over a wide range of concentrations (up to 40 µM BSO). Furthermore, 53ΔE1-xCT-SF-Txnrd1 wt (2ATG) cells exhibited higher viability compared to 53ΔE1-eGFP- SF-Txnrd1 wt (2ATG) cells (Figure 22B). This

observation indicates that xCT over-expression protects the cells from GSH depletion when Txnrd1 is restored. In addition, restoration of Txnrd1 abrogated JNK/SAPK pathway activation in xCT over-expressing cells treated with BSO (Figure 23). Thus, reconstitution of Txnrd1 expression fully revert the BSO-induced phenotype. These results suggested that the requirement for GSH can only be bypassed by antioxidant supplementation or xCT over-expression in the presence of functional Txnrd1.

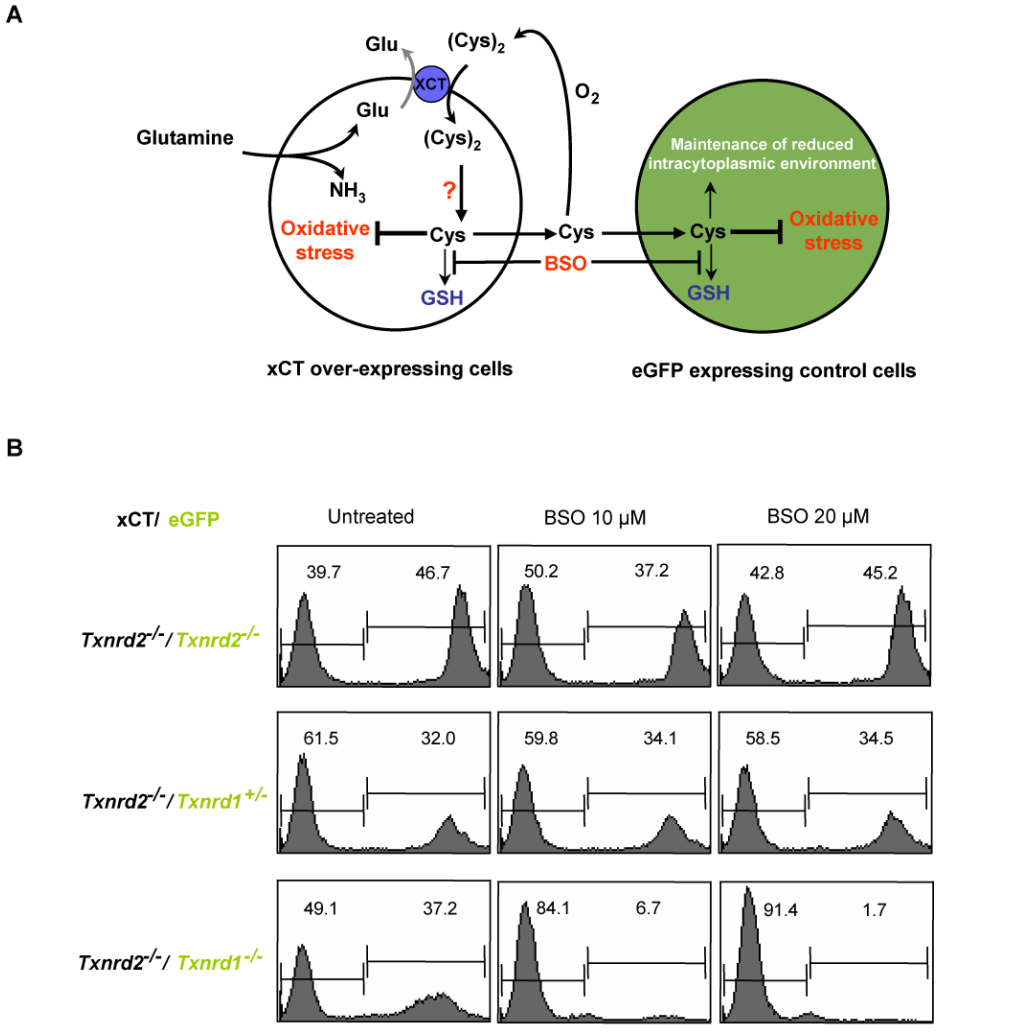

Figure 21. Co-culture of *Txnrd1* knockout cells with xCT over-expressing *Txnrd2* knockout cells. **A)** Schematic outline of the co-culture experiment. Under GSH deficiency xCT over-expression rescues the cells by boosting the intracellular and extracellular cysteine concentration. **B)** The co-culture experiments showed that culture of *Txnrd1* knockout cells in a reducing extra-cellular condition, provided by the xCT over expressing *Txnrd2*$^{-/-}$ cells had no beneficial effect and failed to rescue the *Txnrd1* knockout cells from BSO-mediated cell death (1.7 % eGFP positive cells). In contrast, co-cultures of eGFP-expressing heterozygous *Txnrd1* cells and *Txnrd2* knockout eGFP control cells with xCT over-expressing *Txnrd2* knockout cells rescued the control cells from BSO- induced cell death (34.5% and 45.2% respectively at 20 µM BSO). xCT over-expressing *Txnrd2* knockout cells thus provide a feeder effect and protect co-cultured eGFP-transfected Txnrd2$^{-/-}$ or *Txnrd1*$^{+/-}$ cells from BSO-induced cell death.

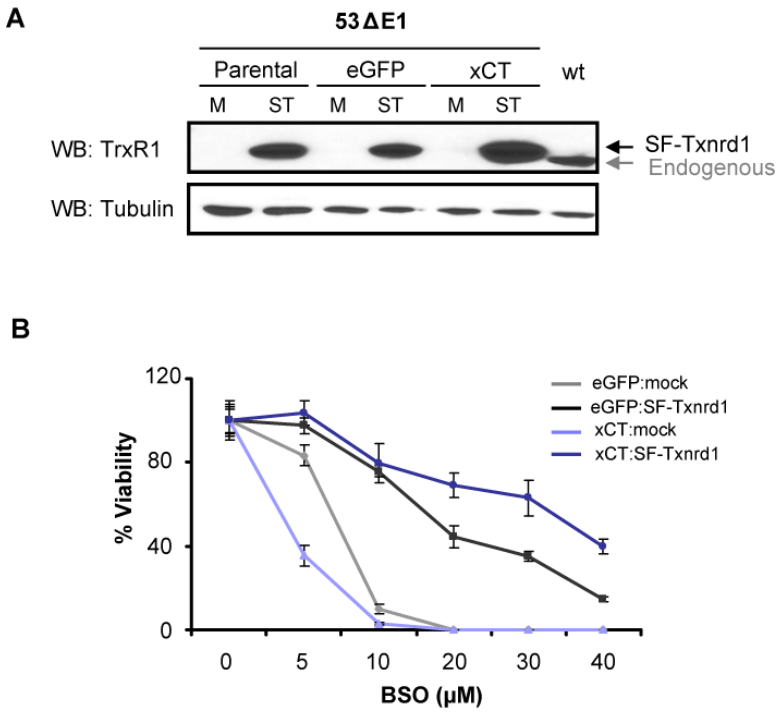

Figure 22. Re-expression of Txnrd1 in xCT over-expressing *Txnrd1*$^{-/-}$ cells confers resistance to BSO-mediated toxicity. xCT over-expressing *Txnrd1* knockout cells were transduced with empty virus (mock control) and a SF-Txnrd1 wt (2ATG) expressing lentivirus. **(A)** Over-expression of SF-Txnrd1 was analyzed by Western blotting using an antibody against human TrxR1 raised in rabbit (a kind gift from Dr. Gladyshev). **(B)** Over-expression of *Txnrd1* rescued xCT over-expressing *Txnrd1* knockout cells over a wide range of BSO concentrations (39% viability at 40 µM BSO) as compared to mock-transduced cells (2.8% viable cells at 10 µM BSO). M: 442 L1 puro (mock lentivirus), ST: 442 L1 SF-Txnrd1 wt (2ATG) puro (SF-Txnrd1 expressing lentivirus).

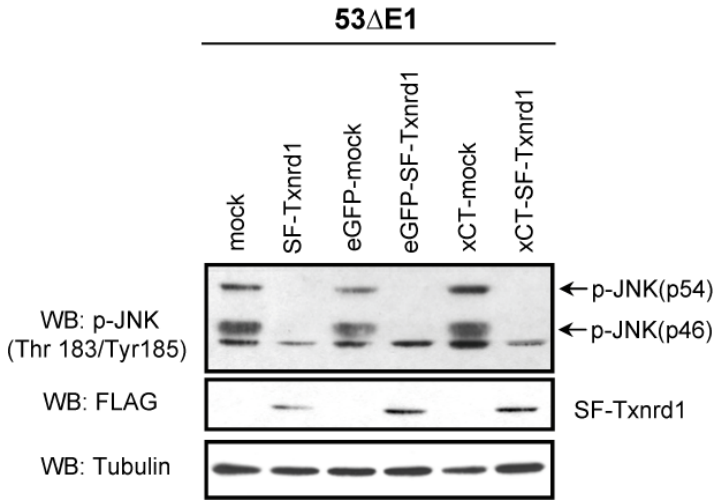

Figure 23 Reconstitution of Txnrd1 prevented SAPK/JNK activation in xCT over-expressing *Txnrd1*$^{-/-}$ cells upon GSH depletion. Lentiviral add-back of Txnrd1 fully rescued xCT over-expressing *Txnrd1* knockout cells due to effective reduction of imported cystine and diminished oxidative stress upon GSH depletion.

4.2 Analysis of Txnrd1 function in oncogene-transformed cell lines

4.2.1 In vitro transformation of MEFs using the c-myc and Ha-ras^{V12} oncogenes

The transformation of primary cells is dependent on the activation of oncogenes. The *c-myc* and *Ha-ras^{V12}* oncogenes are well known to synergize in this process (Land et al., 1983). In order to establish transformed cell lines, the conditional *Txnrd1* knockout MEFs cell lines Üa46, Üa51 and Üa 53 were transduced with lentiviruses expressing the *c-myc* and *Ha-ras^{V12}* oncogenes. While *c-myc* or *Ha-ras^{V12}* alone were not able to transform primary MEFS (Figure 24A), the cells were efficiently transformed when MEFs were co-transduced with *c-myc* and *Ha-ras^{V12}* expressing lentiviruses. Cell transformation is characterized by unlimited growth potential, loss of contact inhibition, and anchorage independence. The *c-myc* and *Ha-ras^{V12}* co-transduced MEFs showed a higher rate of proliferation, grew in multilayered fashion, and formed single cell colonies in soft agar. When implanted into mice, these cells formed aggressive tumors (see section 4.2.14), which confirmed their transformed status. To establish clonal tumor cell lines, 500 *c-myc*- and *Ha-ras^{V12}*-transduced cells were plated per well of a 6-well plate in 0.3% soft agar. After 10-14 days, individual single cell colonies were picked and expanded to establish transformed cell lines. The cell lines 46MRA3, 51MRB3, and 53MRC4 were used in the present study. Expression of c-Myc and Ha-ras^{V12} in these clones was confirmed by Western blotting (Figure 24B).

4.2.2 Induction of Txnrd1 knockout in transformed cells using Tat-Cre protein

4.2.2.1 Single cell cloning and the generation of knockout cell lines

The *Txnrd1$^{+/fl}$* transformed cell line 46MRA3 and two independent *Txnrd1$^{fl/fl}$* transformed cell lines, 51MRB3 and 53MRC4, were treated with Tat-Cre protein as described in section 4.1.1. Clonal cell lines were generated by limiting dilution in 96-well plates. Out-growing clones were expanded and the *Txnrd1* knockout was confirmed by PCR for the deleted *Txnrd1* allele (Figure 25), semi-quantitative RT-PCR, and Western blotting (Figure 26A and B).

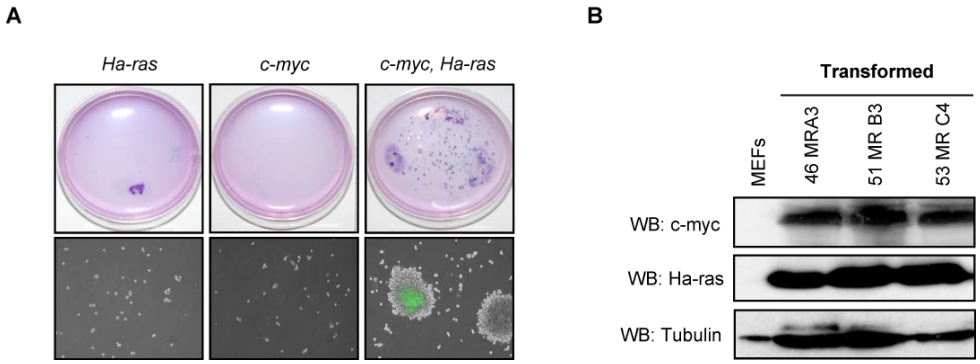

Figure 24. *In vitro* transformation of MEFs by *Ha-ras*^{V12} and *c-myc* oncogenes. **(A)** Soft agar assay (upper panel) and 10 x microscopic view (lower panel). C-myc and Ha-ras^{V12} transformed cells formed colonies in soft agar as they acquired anchorage-independence growth property after transformation. **(B)** Western blot result showed over-expression of c-myc and Ha-ras^{V12} in the transformed cell lines as compared to non-transformed MEFs.

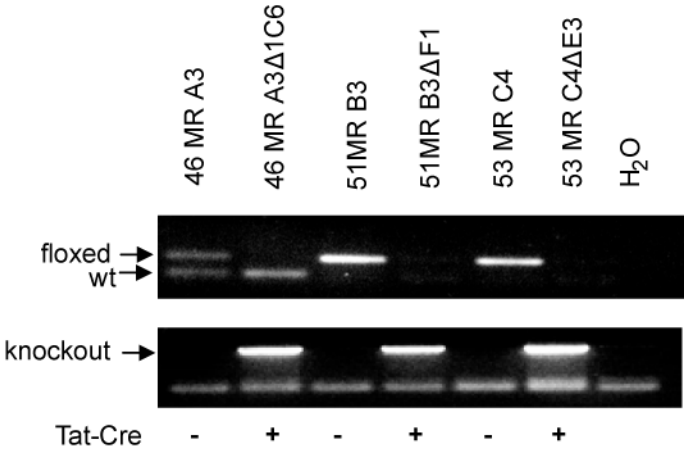

Figure 25. Genotyping of *c-myc* and *Ha-ras*^{V12} transformed *Txnrd1* MEFs cells. The genotype of different MEFs cell lines was confirmed by PCR. The lower band corresponds to the wild-type allele (wt), the upper to the floxed allele (upper panel). The loss of the floxed allele(s) after Tat-Cre treatment indicated the knockout of the *Txnrd1* gene. The successful knockout of *Txnrd1* was confirmed by the specific amplification of a PCR product only obtained after deletion of the loxP-flanked *Txnrd1* allele (lower panel). The cell line 46MRA3 is *Txnrd1*$^{+/fl}$ while 51MRB3 and 53MRC4 are *Txnrd1*$^{fl/fl}$. After Tat-Cre treatment the derived cell lines were either heterozygous (46MRA3Δ1C6) or knockout (51MRB3ΔF1 and 53MRC4ΔE3) for *Txnrd1*.

4.2.2.2 Confirmation of the *Txnrd1* knockout in transformed single cell clones

After verifying the *Txnrd1* deletion in the single cell clones at the genomic level by PCR, the clones were additionally analyzed for the deletion of *Txnrd1* at the mRNA level and at the protein level. No RT-PCR amplification product was obtained after Tat-Cre treatment of the cells with the primer pairs *Txnrd1 13-15* that are located in exon 13 and exon 15, which confirmed the deletion of the gene at the mRNA level.

However, when the upstream primer pair *Txnrd1 59-60* was used, the same RT-PCR amplification products were obtained before and after Tat-Cre treatment, indicating that truncated mRNA transcripts were synthesized in knockout clones (Figure 26A), confirming the previously described results obtained in *Txnrd1* knockout embryos (Jakupoglu et al., 2005). Therefore, a putative expression of a truncated Txnrd1 protein was assessed by Western blotting. These experiments showed that no truncated version of Txnrd1 was expressed in these cells (Figure 26B).

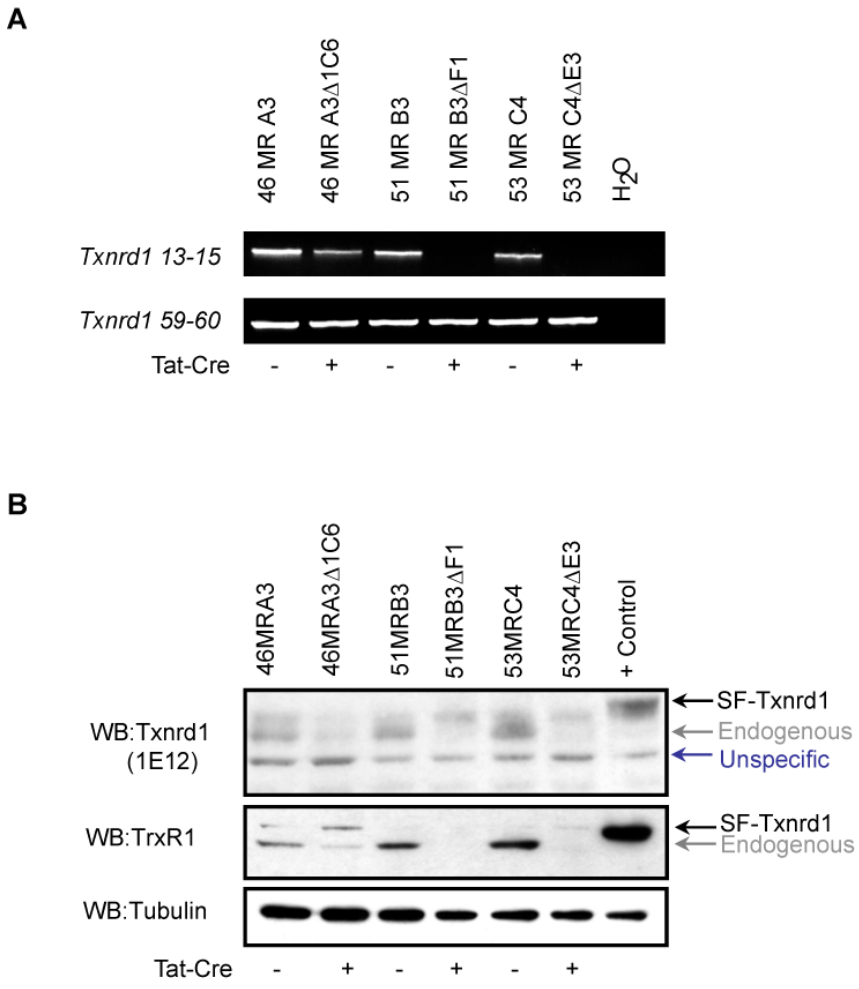

Figure 26. Confirmation of the *Txnrd1* knockout in transformed single cell clones. (A) RT-PCR amplification using primer pair *Txnrd1 13-15* yielded no product, confirming the deletion of *Txnrd1* at the mRNA level. The upstream primer pair *Txnrd1 59-60* generated product in all cases, indicating the production of truncated mRNA transcripts. **(B)** Western blotting results using Txnrd1-specific antibodies ruled out the generation of any truncated protein. The monoclonal antibody 1E12 was raised against the C-terminal portion of mouse Txnrd1. As the C-terminal portion was deleted and the antibody was raised against the C-terminus, the knockout was further confirmed by using a polyclonal anti-human TrxR1 antibody raised in rabbit. The anti-human TrxR1 antibody was a kind gift of Dr. Gladyshev (University of Nebraska, Lincoln, USA).

4.2.3 Effect of Txnrd1 knockout on the proliferation of transformed cells

Several previous reports proposed an indispensable role for Txnrd1 in proliferation and tumorigenesis (Gan et al., 2005; Lu et al., 2007; Yoo et al., 2006; Yoo et al., 2007). However, as shown above, *c-myc* and *Ha-ras*^{V12} transformed Txnrd1-deficient cell lines could be successfully established and grown in culture. Therefore, these cells were compared to their respective parental cell lines in terms of proliferation, clonogenicity and tumorigenicity. The proliferation of the cells was measured by MTT assays over a period of 4 days in 96-well plates. Surprisingly, no difference in the proliferation of knockout and parental cell lines was observed (Figure 27).

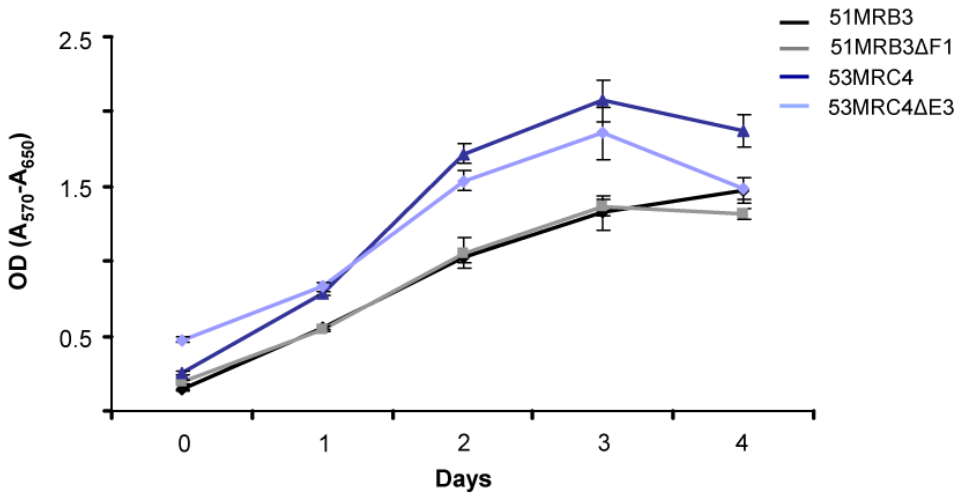

Figure 27. Loss of *Txnrd1* had no apparent effect on the proliferation of transformed cells. Proliferation of cells was measured by MTT assay carried out in 96-well plates. There was no alteration in the proliferation of *Txnrd1* knockout cells with respect to the parental cell line. Two knockout cell lines (51MRB3ΔF1 and 53MRC4ΔE3) showed a similar proliferation rate as the respective parental cell lines.

4.2.4 Txnrd1 knockout cells displayed no substantial alterations in cell cycle distribution

Since Txnrd1 has been implicated in cell proliferation and is known to provide reducing equivalents to ribonucleotide reductase, we hypothesized that the cell cycle phases might be altered in *Txnrd1* knockout cells. Therefore, cell cycle analysis was performed by staining the DNA of knockout and parental cell lines with PI. $1x10^6$ cells from asynchronously proliferating cell cultures were harvested by trypsinization, washed twice with cold PBS, and was fixed in ice-cold 70% ethanol overnight. Then

the cells were washed, treated with DNase-free RNase A and stained with PI. The samples were analyzed by FACS and data was analyzed by ModFitLT V3.0 software.

As shown in figure 28, there was no alteration in either DNA content or cell cycle distribution of transformed *Txnrd1* knockout cells (33.85±4.7% cells were in G0/G1 phase, 52.33±0.8% in S phase, and 13.81±3.8% in G2/M phase) as compared to the parental cell line (34.55±1.1% in G0/G1 phase, 48.76±2.3% in S phase, and 16.68±3.5% cells in G2/M phase).

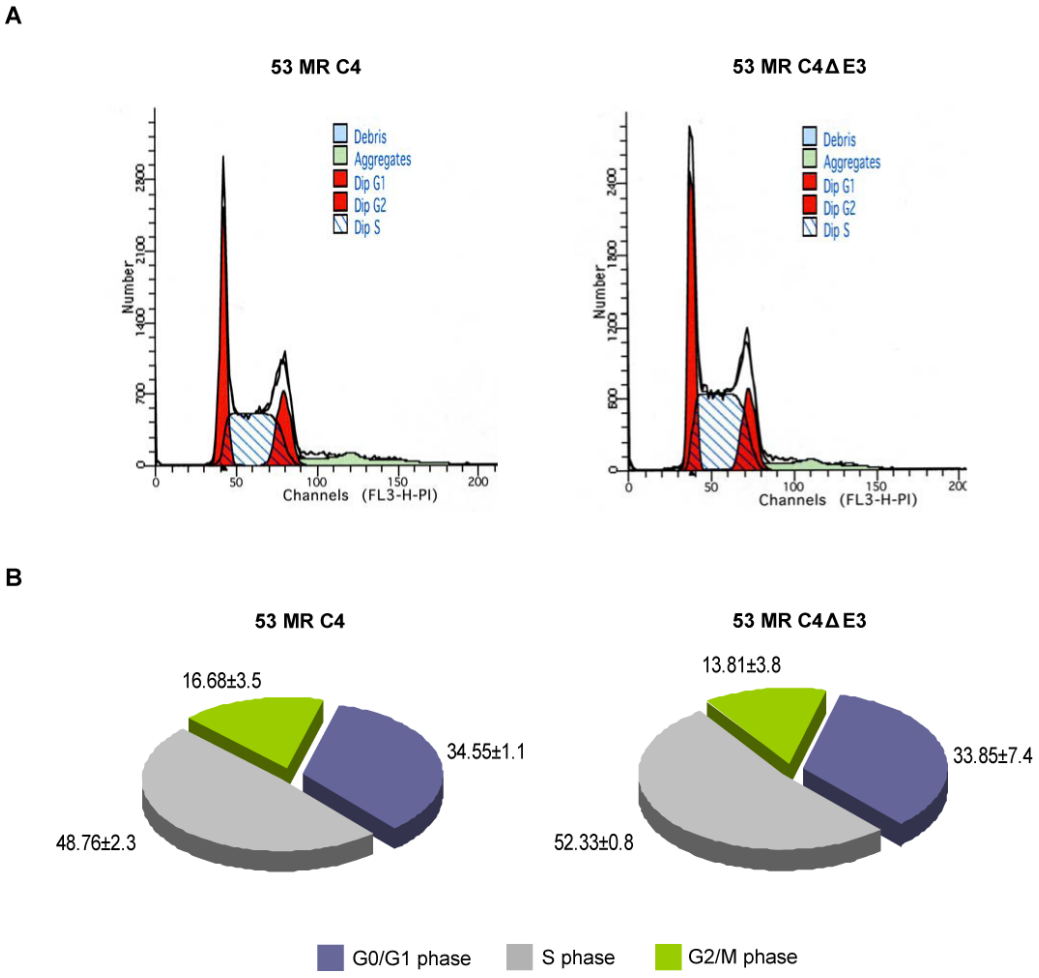

Figure 28. Transformed *Txnrd1* knockout cells showed a similar cell cycle phase distribution as the parental cell line. Asynchronously growing cells were used for cell cycle analysis by PI staining. **(A)** Cell cycle analysis showed no difference in cell cycle distribution of transformed *Txnrd1* knockout cells as compared to the parental cell line. G0/G1, S and G2/M phase distribution for 53MRC4ΔE3 cells (33.85±4.7%, 52.33±0.8% and 13.81±3.8%) were similar to that of the parental cell line 53MRC4 (34.55±1.1%, 48.76±2.3% and 16.68±3.5% respectively). **(B)** The pie diagram represents the pooled data from two independent experiments (mean±SD in %).

These results indicated that cells can survive and proliferate normally in the absence of Txnrd1. In stark contrast to the previous findings on the important role of Txnrd1 in cell proliferation (Bondareva et al., 2007; Jakupoglu et al., 2005; Yoo et al., 2007), these results implicated that cells apparently can compensate for the loss of Txnrd1 function by possibly up-regulating alternative pathways that render Txnrd1 dispensable for proliferation and growth of transformed cells.

4.2.5 Cellular response of transformed Txnrd1 knockout cells to oxidizing agents

Since thioredoxin reductase 1 is an antioxidant enzyme involved in redox regulation, loss of Txnrd1 function may lead to an increased susceptibility towards oxidative stress. To address this, transformed *Txnrd1* knockout cells were challenged with increasing concentrations of hydrogen peroxide and t-butyl hydroperoxide. As shown in figure 27, the viability of neither knockout nor wild type cells was impaired by hydrogen peroxide (Figure 29A) or t-butyl hydroperoxide (Figure 29B) at the tested concentrations.

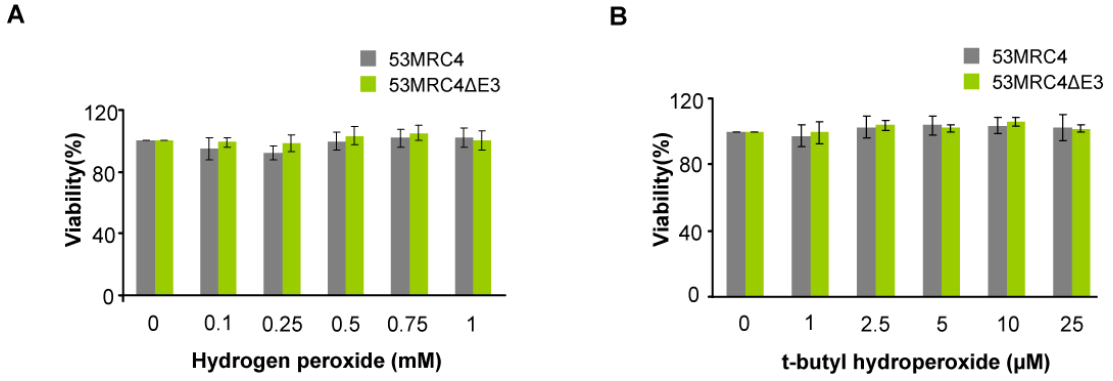

Figure 29. Transformed *Txnrd1* knockout cells were not susceptible to oxidants. Transformed *Txnrd1* knockout cells were challenged with **(A)** hydrogen peroxide and **(B)** t-butyl hydroperoxide. Cells were treated for 72 h with H_2O_2 and t-butyl hydroperoxide, and the viability was measured by MTT assay. % viability was calculated by taking the OD value of untreated cells of the respective cell lines as 100%. At the highest concentration of H_2O_2 (1 mM) and t-butyl hydroperoxide (25 µM) the viability of *Txnrd1* knockout cells 53MRC4ΔE3 was 100.03±6.3% and 101.88±2.14%, respectively as compared to the parental cell line 53MRC4 (101.88±6.2% and 102.65±7.87%), showing no difference at the tested concentrations (mean±SD in %).

4.2.6 Transformed Txnrd1 knockout cells were moderately resistant to chemical inhibitors of Txnrd1

Several chemical compounds and chemotherapeutic agents are known inhibitors of Txnrd1. Consequently, if the cytotoxic effects of these agents were due to specific inhibition of Txnrd1, then the *Txnrd1* knockout cells may be more resistant to these drugs. A number of heavy metals-containing compounds like arsenic (Lin et al., 2001; Lu et al., 2007), platinum (Arner et al., 2001; Witte et al., 2005), organotellurium (Engman et al., 2003) and gold (Engman et al., 2006; Marzano et al., 2007) have been reported or proposed as Txnrd1 inhibitors at least in *in vitro* enzyme activity assays. Therefore, *Txnrd1* knockout cells were challenged with increasing amounts of arsenic (III) oxide and the gold compound TEP Au and the viability of the cells was measured 72 h later. As shown in figure 30A and B, the knockout cells 51MRB3ΔF1 were in fact slightly more resistant to both arsenic (III) oxide (63.34±2.44% viability at 10 µM of arsenic oxide) and TEPAu (59.34±1.8% at 7.5 µM TEPAu) than the parental cell line 51MRB3 (27.62±1.03% at 10 µM arsenic (III) oxide and 17.52±2.04% at 7.5 µM TEPAu). The decreased susceptibility of the knockout cells towards these agents suggested that Txnrd1 is indeed a target of these compounds. However, these cells became susceptible when higher concentrations of these drugs were used, suggesting that these substances most likely also affect other cellular enzymes, among those presumably Txnrd2.

4.2.7 Response of transformed Txnrd1 knockout cells to DNA damage–inducing chemotherapeutics

Cisplatin and doxorubicin are commonly used chemotherapeutic agents for cancer treatment and their effects are known to mainly induce severe DNA damage. It has been reported by Witte et al. that cisplatin also inhibits Txnrd1 but not glutathione reductase (Witte et al., 2005). In addition, it has been reported that Txnrd1 confers resistance towards cisplatin and that knockdown of *Txnrd1* sensitizes the cells towards cisplatin (Sasada et al., 1999). By contrast, the anthracyclin anticancer agent doxorubicin is a poor inhibitor of Txnrd1 (Witte et al., 2005). Therefore, the transformed *Txnrd1*$^{-/-}$ cells were challenged with both compounds and the viability was measured after 72 h by MTT assay.

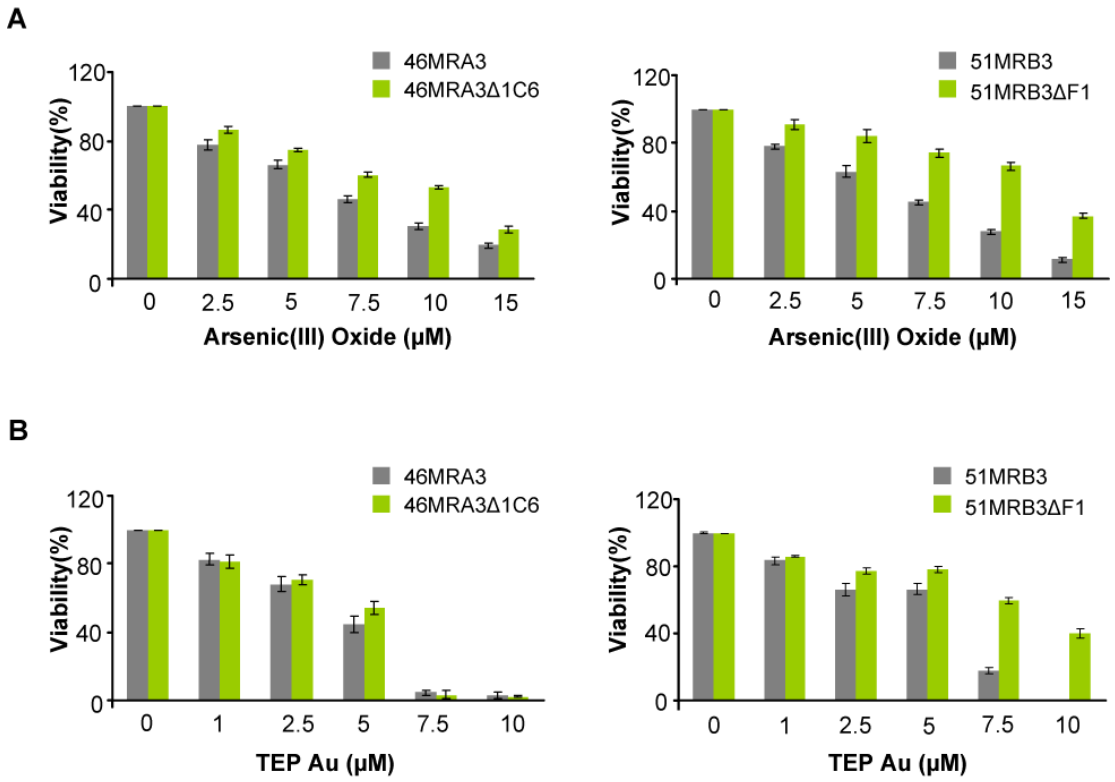

Figure 30. Transformed *Txnrd1* knockout cells were less susceptible to thioredoxin reductase 1 inhibitors. (A) In response to 10 μM Arsenic(III) oxide *Txnrd1* knockout cells 51MRB3ΔF1 showed higher viability (66.34±2.4%) as compared to the parental cell line 51MRB3 (27.62±1.03%) **(B)**. A similar pattern of response was observed with 10 μM TEPAu as knockout cells showed 39.63±2.78% viability as compared to 0% viability of parental cells. The heterozygous cell line 46MRA3Δ1C6 showed marginal resistance towards these two reagents as compared to parental cell line 46MRA3 (mean±SD in %).

As shown in figure 31A, transformed *Txnrd1* knockout cells 51MRB3ΔF1 were moderately resistant against 3.5 μM cisplatin (42.31±1.8%) as compared to the parental cell line (51MRB) (20.27±0.27%), but were equally susceptible to doxorubicin (Figure 31B). The heterozygous control cell line 46MRA3Δ1C6 behaved like the parental cell line.

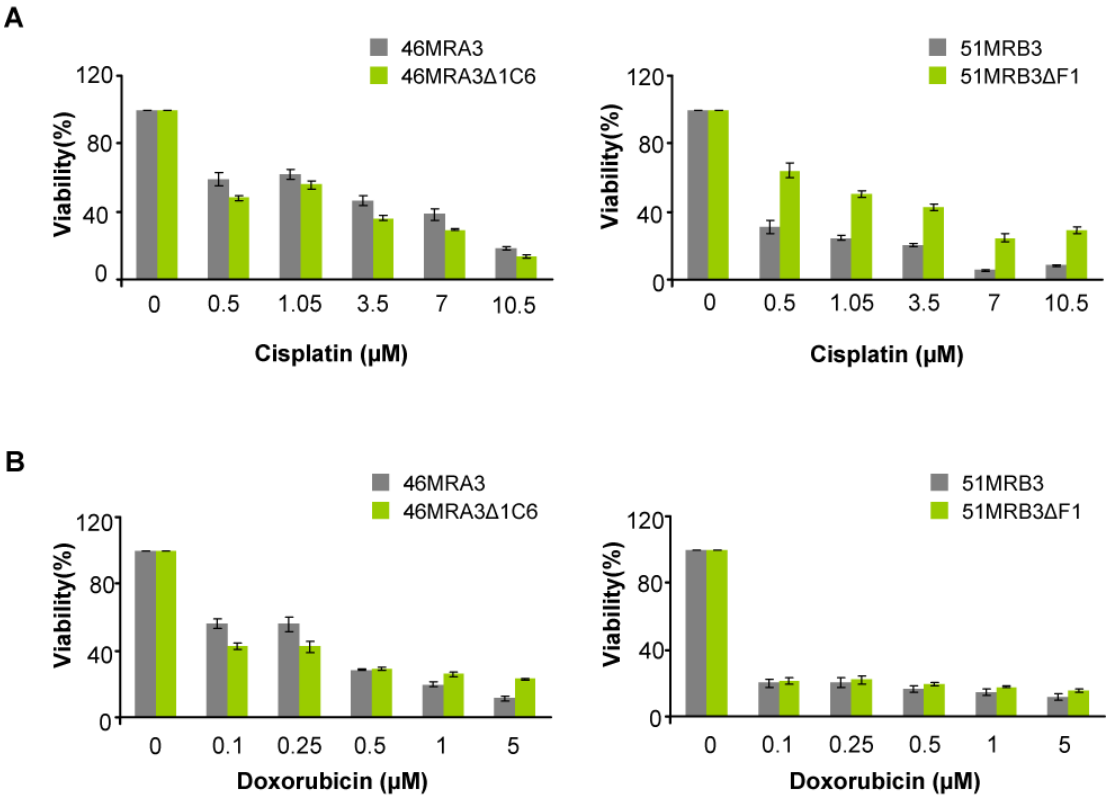

Figure 31. Transformed *Txnrd1* knockout cells were partially resistant towards cisplatin but not to doxorubicin. (A) Transformed *Txnrd1* knockout cells 51MRB3ΔF1 were found to be moderately resistant against 3.5 μM cisplatin (42.31±1.8%) as compared to the parental cell line (51MRB) (20.27±0.27%). **(B)** With respect to doxorubicin there was no difference between the knockout and wild-type cell lines (15.42±0.95 % v/s 11.58±1.84 % at 5 μM doxorubicin) (mean±SD in %).

4.2.8 Response of transformed Txnrd1 knockout cells to agents that inhibit members of the GSH-dependent pathways

Txnrd1 knockout cells were highly susceptible to GSH depletion induced by BSO (Figure 13), which suggested that the GSH-dependent pathway could be a compensatory mechanism. To address whether a similar mechanism is also responsible for rendering *Txnrd1* dispensable for tumor cells, the members of the GSH-dependent pathway were examined in detail in transformed *Txnrd1* knockout cells (discussed in detail in the following sections). Chemical agents known to inhibit the GSH-dependent pathways including BSO (inhibitor of γ-GCS), cadmium chloride (known to cause oxidative stress and preferentially oxidize and inhibit glutaredoxins) (Chrestensen et al., 2000; Liu et al., 2009) and phenylethyl isothiocyanate (PEITC, a naturally occurring compound known to induce ROS accumulation by inhibiting GSH-

dependent pathways) (Trachootham et al., 2006) were tested on transformed *Txnrd1* knockout cells.

As already observed for immortalized *Txnrd1* knockout MEFs (Figure 13), transformed *Txnrd1* knockout cells were highly susceptible to BSO treatment (Figure 32A and B). The result confirmed that GSH is essential for the proliferation and survival of transformed *Txnrd1* knockout cells as well.

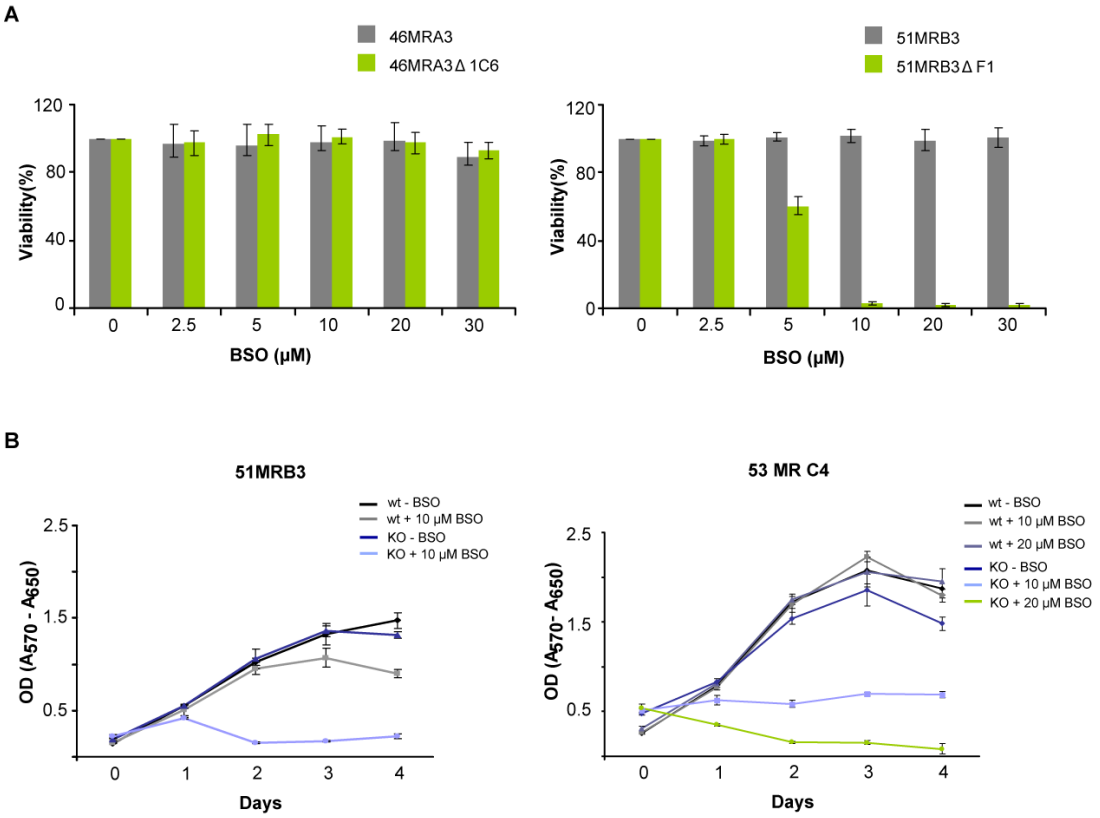

Figure 32. Transformed *Txnrd1* knockout cells were highly susceptible to BSO treatment. Viability of transformed *Txnrd1* knockout cells (51MRB3ΔF1 and 53MRC4ΔE3) was severely compromised upon BSO treatment. **(A)** Dose response experiments revealed that knockout cells were dead already at 10 μM of BSO at which parental wild-type cells were still fully viable. The heterozygous cell line (46MRA3Δ1C6) responded in a similar manner as its parental cell line without showing any impairment in viability due to loss of one allele (93.23±4.9% v/s 89.13±8.13% at 30μM of BSO) (mean±SD in %). **(B)** Proliferation curves of two knockout cell lines confirmed the results obtained in (A).

In contrast to the clear effect of BSO, transformed *Txnrd1* knockout cells were marginally more resistant towards cadmium chloride (27.74±2.67% v/s 16.85±2.65% at 10 μM $CdCl_2$) (Figure 33A) and PEITC (50.16±3.12% v/s 40.94±1.53% at 2.5 μM PEITC) (Figure 33B) as compared to the corresponding parental cell lines. Although

Nishimoto et al. reported that siRNA-mediated knockdown of TrxR1 in Hela cells sensitizes the cells to low dose of cadmium but provided resistance to higher toxic concentration (Nishimoto et al., 2006), the mechanism of action of these compounds is still obscure and it is difficult at present to draw conclusions from the existing data.

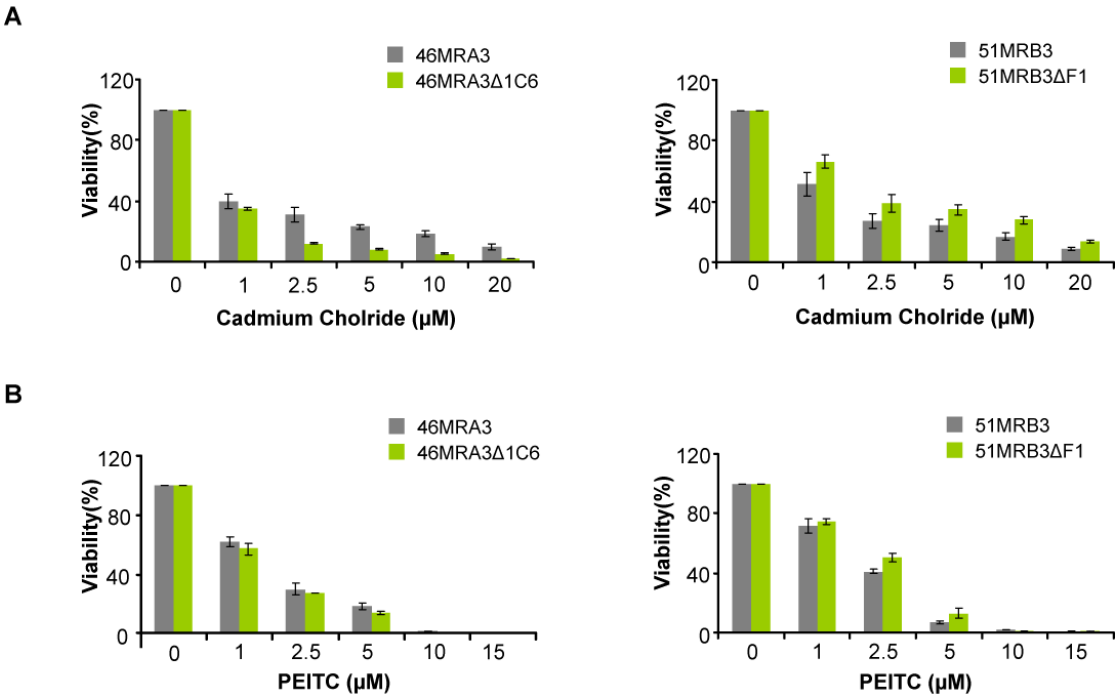

Figure 33. Transformed *Txnrd1* knockout cells were marginally resistant against cadmium chloride and PEITC. *Txnrd1* knockout cells (51MRB3ΔF1) were marginally resistant to **(A)** cadmium chloride (27.74±2.67% v/s 16.85±2.65% at 10 μM $CdCl_2$) and **(B)** PEITC (50.16±3.12% v/s 40.94±1.53% at 2.5 μM PEITC) as compared to the parental cell lines (mean±SD in %).

4.2.9 Reconstitution of thioredoxin reductase 1 expression in transformed Txnrd1 knockout cells reverted the effects of GSH depletion

To confirm that the above observed effects were caused by specific disruption of *Txnrd1*, strep-FLAG tagged mouse Txnrd1 (SF-Txnrd1 wt (2ATG)) was over-expressed in transformed *Txnrd1* knockout cells using a tetracycline-inducible expression vector (Bornkamm et al., 2005). The tetracycline-inducible expression vector has the advantage of inducing the trangene expression in a dose-dependent and time-dependent manner by addition of tetracycline or doxycycline. Moreover, the expression of the transgene can be abrogated by the withdrawal of

tetracycline/doxycycline. The SF-Txnrd1 wt (2ATG) gene was cloned into the doxycycline-inducible expression vector (pRTS1 SF-Txnrd1 wt (2ATG) (Figure 34A).

Transformed *Txnrd1* knockout cells were transfected with this expression vector by electroporation. Transfection efficiency was monitored by co-transfecting the cells with a DS-red C1 reporter plasmid and found to be <5% (data not shown). Therefore, the cells were selected for two weeks with hygromycin B starting at 50 µg/ml and then gradually increasing the final concentration to 300 µg/ml. After two weeks of hygromycin B selection, the expression of SF-Txnrd1 wt (2ATG) was confirmed by Western blotting using antibodies against FLAG (Figure 34B). These cells were then challenged with BSO in the presence (1 µg/ml) or absence of doxycycline. As shown in figure 34C and D, transformed *Txnrd1* knockout cells survived 20 µM of BSO treatment only when doxycycline was included in the cell culture medium. These experiments demonstrated that in the absence of Txnrd1, proliferation and/or survival of transformed cells relied on the GSH-dependent system.

4.2.10 Analysis of members of the GSH-dependent systems at the transcriptional level by qRT-PCR

Since *Txnrd1* knockout cells were highly susceptible to BSO-mediated GSH depletion, the hypothesis was formulated that *Txnrd1* knockout cells extensively relied on the GSH-dependent system. To test this hypothesis, RNA was isolated from the transformed *Txnrd1* knockout cells lines and their respective parental cell lines. 1 µg RNA was used for cDNA synthesis. The expression of different genes of the GSH-dependent system was quantified by qRT-PCR. Data was normalized against *18S* mRNA levels and represented with respect to the parental cell line. As shown in figure 35, the mRNA level of *Gclc, Gclm* and *Gsr* was found to be increased in knockout cell lines as compared to the respective parental cell lines. While *Gclc* was 2.62±0.75- and 3.17±1.5-fold higher in 51MRB3ΔF1 and 53MRC4ΔE3 cell lines respectively, the *Gclm* level was 4- and 7-fold increased in two knockout cell lines. This was in the line of a recently published report of Bondareva et al (Bondareva et al., 2007). The *Gsr* was 1.5- and 2.62-fold up regulated in 51MRB3ΔF1 and 53MRC4ΔE3 cell lines as compared to respective parental cell lines. These results indicated that enzymes of GSH-dependent pathway are invariably up regulated in transformed *Txnrd1* knockout cells.

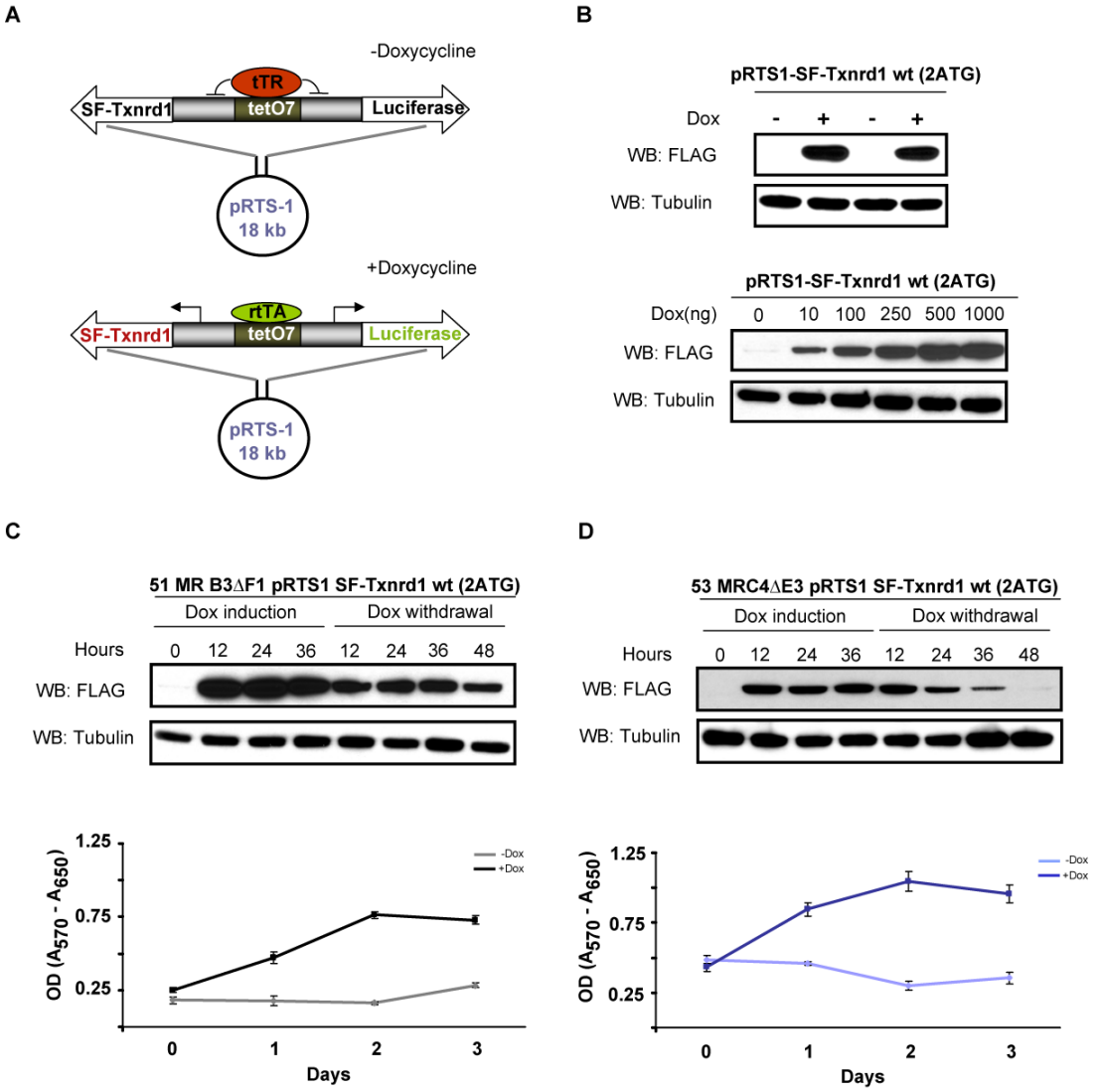

Figure 34. Doxycycline-inducible over-expression of Txnrd1 rescued transformed *Txnrd1*$^{-/-}$ cells from BSO-induced cell death. (A) Schematic representation of the doxycycline-inducible construct. The *Txnrd1* knockout cell lines 51MRB3ΔF1 and 53MRC4ΔE3 were electroporated with the doxycycline-inducible expression vector pRTS1 SF-Txnrd1 wt (2ATG) and selected by hygromycin B. **(B)** SF-Txnrd1 wt (2ATG) expression was confirmed by immunobloting in a doxycycline-inducible manner. **(C)** and **(D)** The rescue experiments were performed in two independently established knockout cell lines after confirming the expression of SF-Txnrd1 wt (2ATG) by Western blot in a time-dependent manner in the presence of doxycycline (upper panels of C and D). The expression of SF-Txnrd1 decreased with the removal of doxycycline which was monitored 48 h of withdrawal. Analysis of proliferation of *Txnrd1* knockout cells after BSO treatment in the presence (1 μg/ml) or absence of doxycycline revealed that the reconstitution of Txnrd1 expression provided rescue against BSO-induced cell death. Cell proliferation was measured by MTT assay over a period of 3 days in the presence or absence of doxycycline (1 μg/ml).

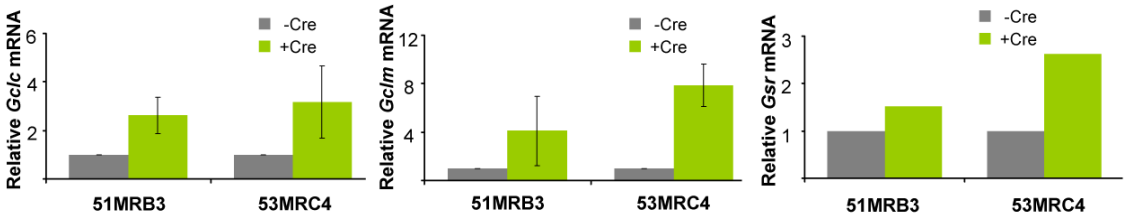

Figure 35. Up regulation of the GSH-dependent pathway in transformed *Txnrd1* knockout cell lines. The quantification of mRNA levels for *Gclc, Gclm* and *Gsr* revealed that there was an approximately more than two-fold up regulation in the respective genes as a compensatory response. Data was normalized against *18S* mRNA levels and represented with respect to the parental cells line taken as 1 (mean±SD).

4.2.11 Quantification of GSH levels in transformed Txnrd1 knockout cells

The results of qRT-PCR were further verified by measuring GSH concentration and GR activity (section 4.2.12) in transformed *Txnrd1* knockout cells. The total GSH (GSH+GSSG), reduced GSH (GSH) and oxidized GSH (GSSG) concentration in *Txnrd1* knockout cells and their respective parental cell lines were determined by the isocratic HPLC method. The concentration of GSH was calculated from the integration of the peak area in the chromatogram. As shown in figure 36A, B and C, GSH concentrations in *Txnrd1* knockout cells were considerably higher than in the parental cell lines. Total GSH and reduced GSH concentration in the transformed *Txnrd1* knockout cell line 53MRC4ΔE3 were both 2.7-fold higher (2.76±0.85) than in the parental cell line 53MRC4 (taken as 1); this difference was less pronounced in the second *Txnrd1* knockout cell line, but total and reduced GSH were still 1.5-fold higher than that of the parental cell line. The GSSG concentration was more than 3-fold higher in the knockout cell lines as compared to the parental cell lines, which indicates the existence of oxidative stress in knockout cells. Our findings were in line with the previously published report in yeast where loss of both trx1 and trx2 results in elevated GSSG, indicating a link between the thioredoxin system and the redox status of GSH in the cell (Grant, 2001; Muller, 1996; Trotter and Grant, 2003).

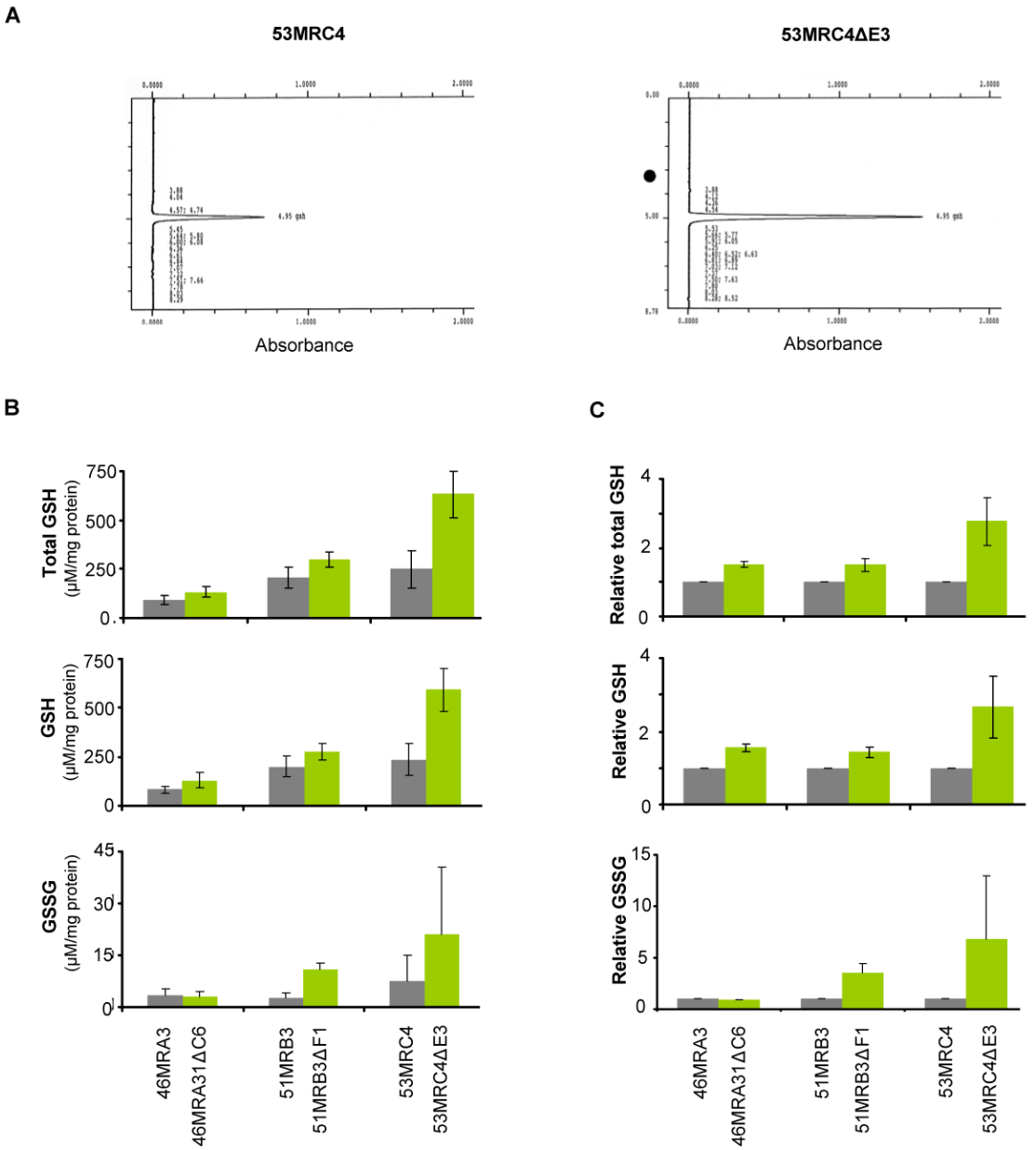

Figure 36. GSH concentrations were higher in transformed *Txnrd1* knockout cells. (A) GSH concentration was determined by HPLC. The chromatogram represented the GSH peak. The concentration of GSH was calculated for the area of peak. **(B)** Total glutathione (GSH+GSSG), GSH (reduced glutathione) and GSSG (oxidized glutathione) concentrations were determined. **(C)** The relative level of total GSH, GSH and GSSG were determined by taking the respective values for the parental cell line as 1. The total GSH level in transformed *Txnrd1* knockout cells was higher than in the parental cell lines. Of note, *Txnrd1* knockout cells showed a more than three-fold higher concentration of GSSG as compared to parental cell lines. Data is pooled from three experiments and represented as mean values±SD.

4.2.12 Transformed Txnrd1 knockout cells showed higher glutathione reductase activity

The data from qRT-PCR showed more than 1.5-fold up regulation of *Gsr* at the transcriptional level which was further verified at the enzyme activity level. GR activity was measured in *Txnrd1* knockout cells. As shown in figure 37A and B, the GR activity was in fact higher in transformed *Txnrd1* knockout cells than in the corresponding parental cell line. Compared to the parental cell lines 51MRB3 (0.612±0.014 U/mg protein) and 53MRC4 (0.87±0.27 U/mg protein), *Txnrd1* knockout cells 51MRB3ΔF1 (1.178±0.41 U/mg protein) and 53MRC4ΔE3 (2.053±0.36 U/mg protein) showed an approximately more than 2-fold higher GR activity. GR activity in the heterozygous control cell line was similar to the parental cell line (0.89±0.22 U/mg protein v/s 0.805±0.26 U/mg protein).

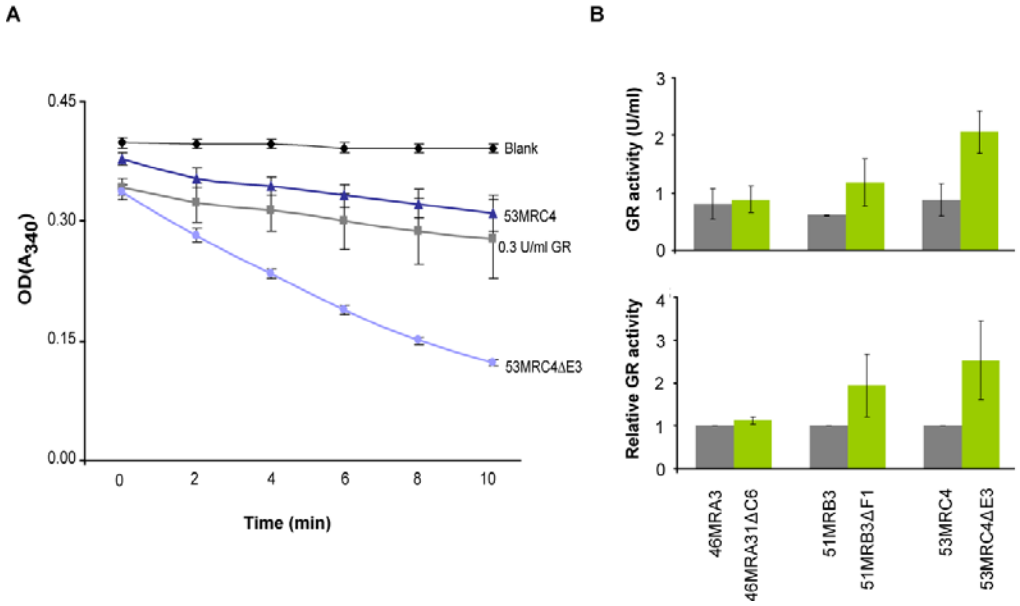

Figure 37. Transformed *Txnrd1* knockout cells displayed higher GR activity. (A) GR activity was measured as the rate of consumption of NADPH/H^+ which is associated with a decrease in OD at 340 nm. Yeast GR was used as positive control. **(B)** GR activity (U/mg protein) and relative GR activity (GR activity of the parental cell line sets as 1) was determined from the standard curve obtained from known concentrations of yeast GR. The transformed *Txnrd1* knockout cells 51MRB3ΔF1 and 53MRC4ΔE3 showed more than a two-fold higher GR activity (1.178±0.415 and 2.053±0.36 U/mg protein, respectively) as compared to the parental cell lines 51MRB3 and 53MRC4 (0.612±0.014 and 0.877±0.27 U/mg protein, respectively). Pooled data from three experiments (mean±SD).

4.2.13 Re-expression of Txnrd1 in Txnrd1 knockout cells reverted GSH levels and GR activity

The augmented GSH concentrations and GR activity of transformed *Txnrd1* knockout cells compared to parental cells suggested that *Txnrd1* knockout cells up-regulated the GSH-dependent pathway as a compensatory mechanism for the loss of Txnrd1 function. If this was the case then the GSH level and GR activity might be reverted to wild-type levels when *Txnrd1* was re-expressed in these cells. To test this hypothesis, SF-Txnrd1 wt (2ATG) was expressed in transformed *Txnrd1* knockout cells from the previously described doxycycline-inducible expression vector (Section 4.2.9). As shown in figure 34A, Txnrd1 expression in the transfected cells was doxycycline-dependent. GSH levels and GR activity in these cells were determined in the presence (1 µg/ml) or absence of doxycycline. As shown in figure 38A and B, the addition of doxycycline indeed caused a decrease in GSH levels and GR activity in a time-dependent manner.

The total GSH concentration in doxycycline-untreated knockout cells (1.48±0.16 mM/mg protein) was 3-fold higher than in *Txnrd1* knockout cells that were maintained on doxycycline (0.547±0.016 mM/mg protein). Transient addition of doxycycline for 36 h led to a drop in GSH level to 1.04±0.09 mM/mg protein. The reverse effect was observed when doxycycline was withdrawn from the long-term treated cells for 36 h (0.67±0.09 mM/mg protein). Also, the levels of GSH changed similarly in these cells. Continuous treatment of the cells with doxycycline led to a 3-fold reduction in GSSG levels (13.0±10 µM/mg protein) as compared to untreated cells (39.4±11.3 µM/mg protein) (Figure 38A). The drop in GSH levels after addition of doxycycline was paralleled by a reduction in GR activity. As compared to untreated cells (2.8±0.3 U/mg protein), transformed *Txnrd1* knockout cells maintained in the presence of doxycycline showed an approximately 50% decrease in GR activity (1.4±0.35 U/mg protein) (Figure 38B).

4.2.14 Loss of Txnrd1 had no effect on clonogenicity and tumorigenicity of transformed cells

In order to determine the effect of loss of *Txnrd1* on the clonogenicity, soft agar assays were performed. 500 cells/well were plated in 0.3% agar in 6-well plates.

After 10-14 days the cells were fixed in methanol, stained with 0.5% crystal violet and the number of visible colonies was counted. As shown in figure 39A, the knockout cell lines were able to form colonies in soft agar, suggesting that the loss of Txnrd1 function apparently had no effect on the clonogenicity of the cells.

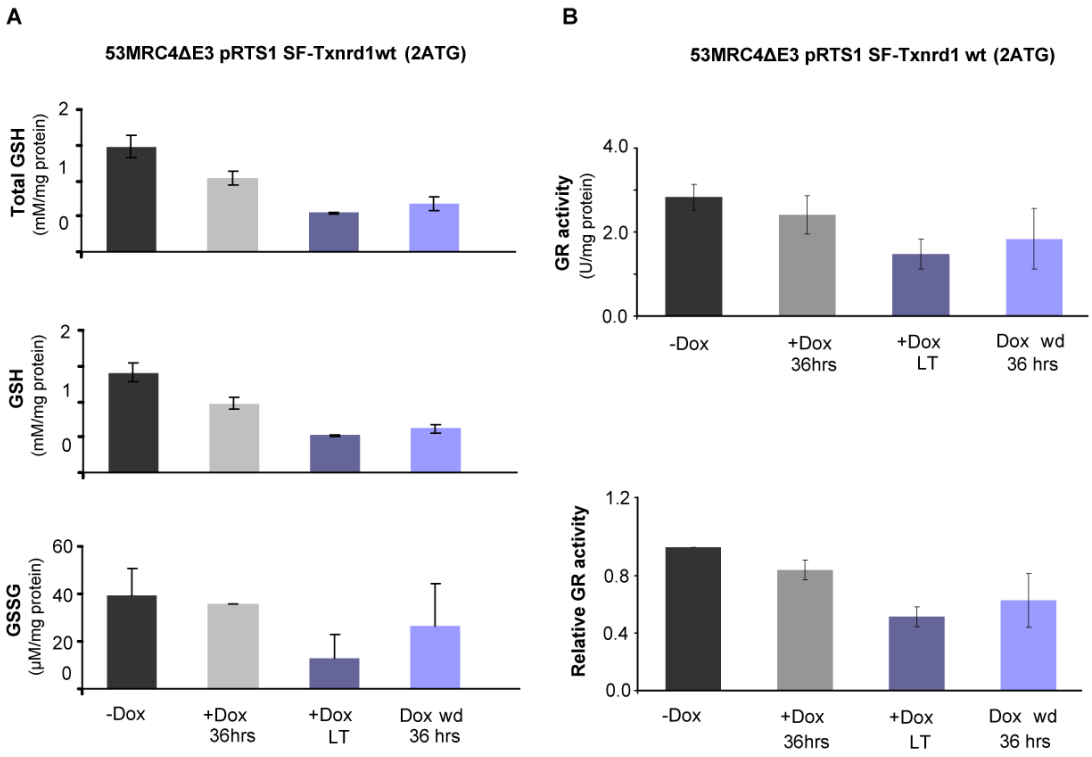

Figure 38. Re-expression of Txnrd1 in an inducible manner decreased GSH concentrations and GR activity in transformed *Txnrd1* knockout cells. (A) GSH concentration was determined by HPLC. **(B)** GR activity was determined by measuring the rate of $NADPH/H^+$ consumption. Transient induction of Txnrd1 expression for 36 h led to a decrease in GSH concentration and GR activity. Long-term maintenance of these cells in the presence of doxycycline (+Dox LT) led to a 3-fold reduction of total GSH, GSH and GSSG levels (1.48±0.16 mM/mg protein to 0.547±0.016 mM/mg protein). Similarly, there was a two-fold reduction in GR activity upon re-expression of Txnrd1 (2.8±0.3 U/mg protein to 1.4±0.35 U/mg protein). An increase in GSH levels and GR activity was observed when Txnrd1 expression was abolished by doxycycline withdrawal (Dox wd).

The tumorigenic potential of transformed *Txnrd1* knockout cells was further assessed by transplanting $1x10^6$ cells into *C57BL/6* mice (*n* = 6 per group). The tumor was allowed to grow for 10 days. As shown in figure 39B, both the knockout cell lines 51MRB3ΔF1 (1.52±0.33 g) and 53MRC4ΔE3 (2.45±0.38 g) formed tumors of size and mass comparable to the respective parental cell lines 51MRB3 (1.42±0.43 g) and 53MRC4 (1.67±0.45 g). These results clearly showed that loss of Txnrd1 had apparently no effect on clonogenicity and tumorigenicity of transformed cells. From these studies Txnrd1 emerges as being dispensable for tumor growth. Since both knockout cell lines showed higher GSH content and GR activity, loss of Txnrd1

function might be compensated for by the GSH-dependent system, at least to some extent. Further experiments need to be conducted to address the overlapping functions between the GSH-dependent and the thioredoxin-dependent pathway.

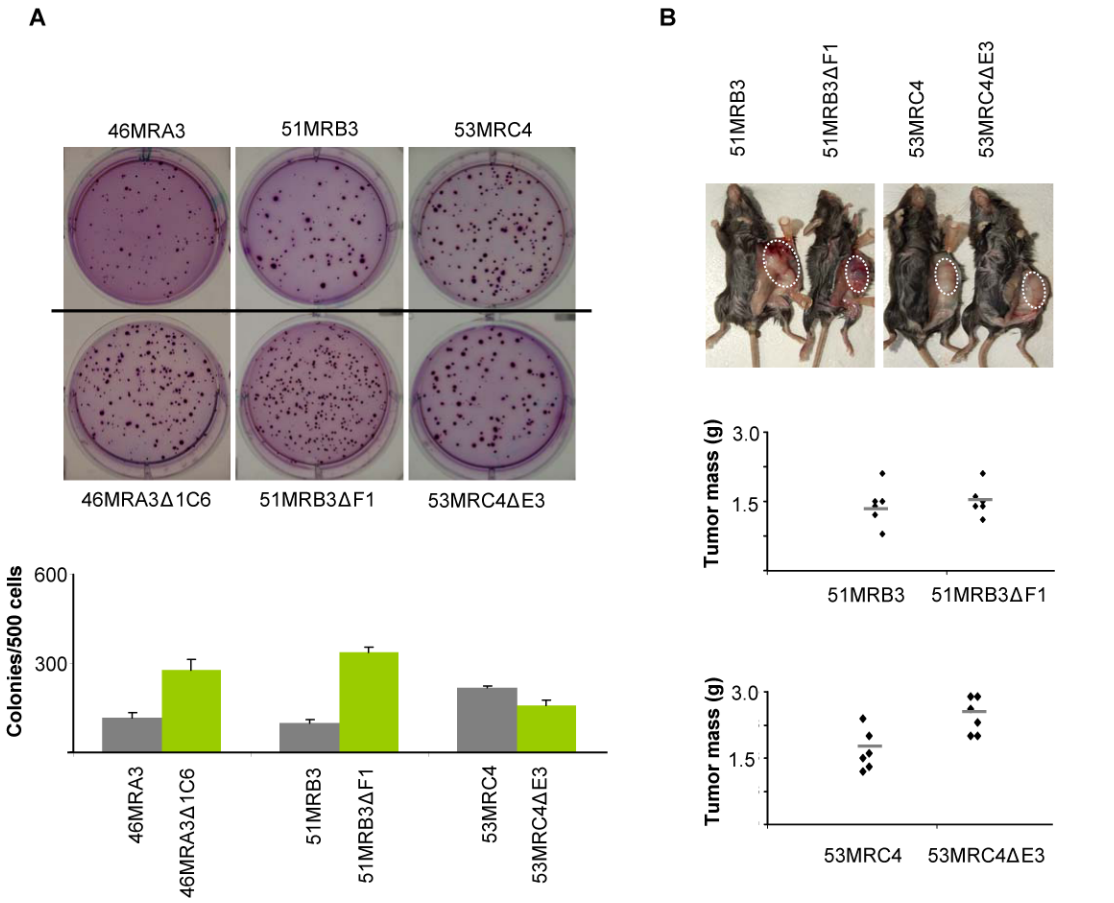

Figure 39. Loss of Txnrd1 had no effect on the clonogenic and tumorigenic potential of transformed MEFs. (A) Soft agar assay. 500 cells/well were seeded in 0.3% soft agar and colonies were allowed to grow for 10-14 days. The colonies were counted after staining with crystal violet. Transformed *Txnrd1* knockout cells formed colonies in soft agar without showing any loss of clonogenic potential. **(B)** Tumor transplantation in *C57BL/6* mice. $1x10^6$ transformed *Txnrd1* knockout cells and the parental cell lines were subcutaneously transplanted into the flanks of *C57BL/6* mice and allowed to grow for 10 days. Animals were sacrificed and tumor mass was determined. The result of the transplantation experiment revealed that there was no loss in tumorigenic potential of *Txnrd1* knockout cells, as both the knockout cell lines 51MRB3ΔF1 and 53MRC4ΔE3 formed tumor mass of comparable size (1.52±0.33 and 2.45±0.38) to that of parental cells lines 51MRB3 and 53MRC4 (1.42±0.43 and 1.67±0.45), respectively.

4.2.15 Txnrd1-deficient tumors were susceptible to pharmacological inhibition of GSH

In vitro experiments had indicated that transformed Txnrd1-deficient cells showed higher GSH content and GR activity and were susceptible to BSO-mediated GSH depletion. This indicated that *Txnrd1* knockout cells relied heavily on the GSH/GSH-

dependent pathway for survival and proliferation which rendered *Txnrd1* dispensable for tumorigenesis. If Txnrd1-deficient tumors solely depended on the GSH/GSH-dependent system then pharmacological intervention of GSH/GSH-dependent pathway might be effectively exploited therapeutically in cancer treatment.

To test this hypothesis, $1x10^5$ transformed *Txnrd1* knockout cells along with parental cell lines were implanted in both the flanks of *C57BL/6* mice (*n = 6* per group). The cells were allowed to establish and they formed small tumors after 3 days. Then the mice were treated with BSO (20 mM) in drinking water for 10 days (Figure 40A). At the end of the experiments, mice were sacrificed, tumors were collected and analyzed. As shown in figure 40B and C, *Txnrd1* knockout tumors were highly susceptible to BSO treatment *in vivo* and formed very small tumors (0.0622±0.051 g) as compared to untreated tumors (0.488±0.429 g).

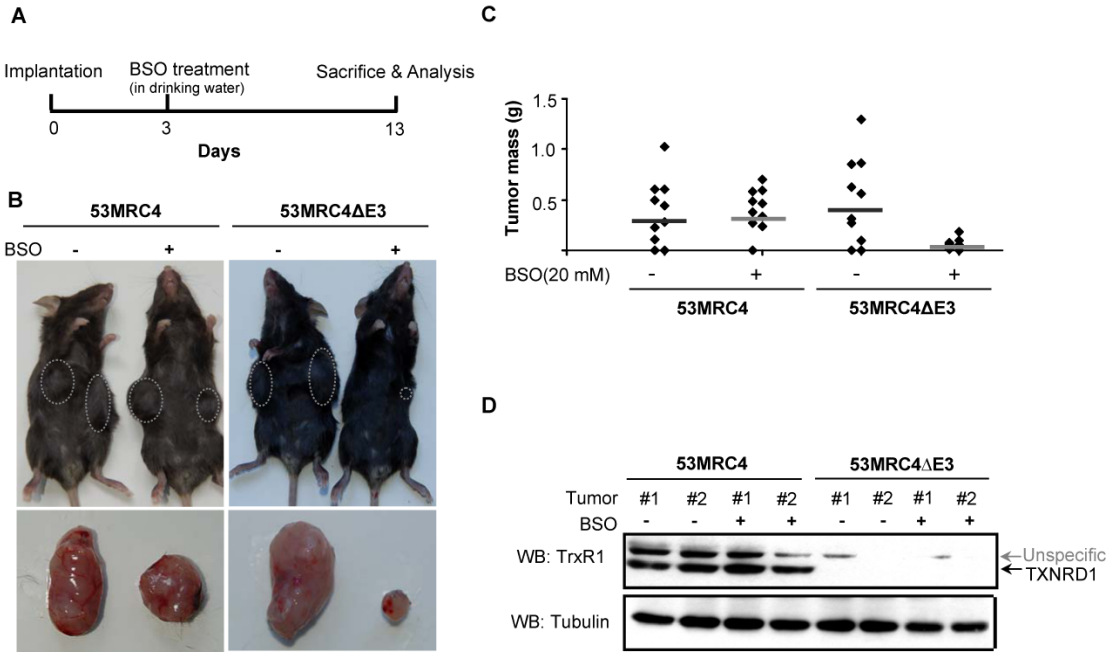

Figure 40. Txnrd1-deficient tumors were highly susceptible to pharmacological inhibition of GSH synthesis. A) Protocol for BSO administration to tumor-bearing mice. **B)** Txnrd1-deficient tumors were highly susceptible to BSO (0.0622±0.051 g) as compared to untreated tumors (0.488±0.429 g). Wild-type tumors were resistant to BSO treatment. **C)** Tumor mass was calculated at the end of the experiment. Txnrd1-deficient tumors showed an 8-fold reduction in tumor mass upon BSO treatment. **D)** Absence of Txnrd1 in these tumors was confirmed by Western blot.

The wild-type tumors were resistant to BSO treatment and formed tumors of comparable masses (0.379±0.322 g) as compared to the untreated group (0.405±0.205 g). The analysis of the long-term effect of BSO treatment on tumor growth and survival of tumor-bearing mice is ongoing. Absence of Txnrd1 in these tumors was confirmed by Western blot (Figure 40D). Thus it was concluded from these experiments that Txnrd1-deficient tumors are highly susceptible to pharmacological inhibition of GSH, which may be utilized as an adjunct to Txnrd1 inhibition in cancer treatment.

5. Discussion

A growing body of evidence accumulated over the past decade has put the redox regulation of cell signaling as pivotal for the regulation of many physiological processes like proliferation, differentiation and cell death through reversible oxidation-reduction of redox-sensitive proteins. Reactive oxygen species are not only detrimental to the cells; at lower concentration they are used as second messengers for signaling. While the basal level of ROS plays important roles in normal cellular physiology, an increase in the ROS burden or the loss of antioxidant functions has detrimental effects on the cells and is reflected in many patho-physiological processes like neurodegeneration and cancer. Although the understanding of ROS signaling and antioxidant defense is still in its juvenile stage, a better understanding of these processes will open new avenues for the treatment of many complex (age-related) degenerative diseases - the progress made over the years is tremendous and showed a promising prospective. The present study sought to address the role of one of the major redox enzymes, cytosolic thioredoxin reductase 1, in antioxidant defense, growth and proliferation, and transformation.

5.1 Thioredoxin reductase 1 function in MEFs

5.1.1 Transgenic mouse models for Txnrd1 and Txnrd2

Txnrd1 has been implicated in proliferation as it is highly expressed in neoplastic tissue and in tumor cell lines. Moreover, it was also reported to be a target gene of the *c-myc* oncogene in human B cell lines (Schuhmacher et al., 2001). Using the Cre-*lox*P technology, a conditional *Txnrd1* knockout mouse line was generated in our laboratory to address the role of *Txnrd1* in proliferation and growth. Exon 15 harboring the C-terminal catalytic centre and SECIS element was flanked by *lox*P sites, which are targeted by Cre recombinase, leading to the disruption of the *Txnrd1* gene and ultimately Txnrd1 functions. Targeted disruption of *Txnrd1* resulted in embryonic lethality as the knockout embryos died at E10.5. *Txnrd1* knockout embryos showed marked growth and developmental retardation and exhibited severe proliferation defects in all tissues except the heart, implicating the role of *Txnrd1* in proliferation and early embryogenesis (Jakupoglu et al., 2005). The phenotype of *Txnrd1* knockout was entirely different from that of the mitochondrial isoform (*Txnrd2*). While *Txnrd1* knockout showed severe proliferation defects and

growth retardation, *Txnrd2* knockout resulted in abnormal hematopoiesis, impaired heart development and increased apoptosis due to mitochondrial dysfunctions (Conrad et al., 2006; Conrad et al., 2004). Thus, it appears that the two isoforms, being located in different sub-cellular compartments and being expressed in different tissues, have widely non-redundant functions. In the meantime, by using Cre/*lox*P technology another group reported the generation of conditional *Txnrd1* knockout mice (Bondareva et al., 2007). They targeted the first two protein-encoding exons with loxP sites to disrupt the entire gene. They reported similar findings of early embryonic lethality at E7.5 confirming our previous published report that thioredoxin reductase 1 is indispensable for proliferation and embryogenesis (Jakupoglu et al., 2005). In the present study, conditional *Txnrd1* knockout mice and MEFs cell line derived from the mice generated by Jakupoglu et al. were used as it was not possible to establish knockout MEFs cell lines directly from knockout embryos (Jakupoglu et al., 2005).

5.1.2 Txnrd1 was dispensable for proliferation of MEFs in culture

To study the *in vitro* effects of *Txnrd1* disruption, conditional *Txnrd1* knockout MEFs cell lines were established. The cell lines were treated with the Tat-Cre protein to achieve the deletion of *Txnrd1*. Contrary to our expectations, *Txnrd1* knockout cell lines could be established and propagated in the cell culture. The diametrically opposed observations - the failure to establish *Txnrd1*-deficient cell lines directly from knockout embryos and the successful establishment of *Txnrd1* knockout cell lines from culture-adapted cells - were indicative of the fact that after adaptation, the cells can compensate for the loss of *Txnrd1* by up-regulating a yet unrecognized pathway. In line of the above observation, Yoo et al. had reported that thioredoxin reductase 1 is not required in culture as siRNA-mediated knock-down of *Txnrd1* had no impact on the cell proliferation in culture, although they loose their metastatic or tumorigenic potential (Yoo et al., 2006). But their report did not provide any explanation for a putative compensatory mechanism that render Txnrd1 dispensable for proliferation. Subsequently, the same group has published another report that *Txnrd1* is required for proliferation and DNA polymerase activity under serum-deprived conditions (Yoo et al., 2007). Thus, it is very likely that a complex regulation of the cellular redox network must exist in cells, and depending on the cell/tissue types, their proliferation rate and differentiation status, loss of Txnrd1 may have

different outcomes on cell survival and cell proliferation. In line of this notion, Txnrd1 was shown to be dispensable for heart development (Jakupoglu et al., 2005), while it plays an essential role in cerebellar development (Soerensen et al., 2008). It will be interesting to dissect the mechanism which may compensate for the loss of *Txnrd1* functions.

5.1.3 Txnrd1 knockout cells were susceptible to GSH depletion

Previous work from our laboratory had shown that *Txnrd2* knockout cells were highly sensitive to GSH depletion and rapidly died, which could be prevented by NAC treatment (Conrad et al., 2004). The above observation led to the hypothesis that *Txnrd1* knockout cells might also be susceptible to GSH depletion. Similar to *Txnrd2* knockout cells, *Txnrd1* knockout cells, when challenged with the GSH depleting agent BSO, died at a much lower concentration of BSO (5 µM) as compared to wild-type cells (20 µM or more). Thus the above observation indicated that in the absence of *Txnrd1*, GSH depletion has a detrimental effect on cell survival. To further reconfirm that this phenotype was due to loss of *Txnrd1*, Txnrd1 was reconstituted in *Txnrd1* knockout cells by over-expressing Strep-FLAG tagged Txnrd1 (SF-Txnrd1 wt (2ATG)). The add-back of SF-Txnrd1 wt (2ATG) provided resistance to BSO treatment. The rescue of *Txnrd1* knockout cells against BSO treatment by SF-Txnrd1 over-expression was approximately 40%, which could be due to the limited amounts of selenium present in normal cell culture medium. Further experimentation is needed to study the effects of selenium supplementation. It would not be surprising if selenium supplementation would increase the rescue efficiency after re-introducing the wild-type *Txnrd1* gene into *Txnrd1* knockout cells. Site-directed mutagenesis was used to alter 4 amino acids previously reported to be involved in catalysis of thioredoxin reductase 1. The N-terminal cysteine mutants (C59S, C64S) provided rescue comparable to wild-type under normal cell culture conditions. In contrast, the C-terminal mutants were enzymatically less efficient in restoring the loss of Txnrd1 function, highlighting the importance of the C-terminal catalytic centre in catalysis as the electrons are finally transferred to the substrate by this redox centre. Although the selenocysteine to cysteine mutant showed a partial effect in rescuing the phenotype, this indicates that the lack of selenocysteine impairs the enzyme function to some extent; but the absence of selenocysteine or cysteine leads to a drastic loss of enzyme function (approximately 25% with respect to wild-type and 50% loss in

functionality with respect to U498C mutants), which is in line with previous reports. As described earlier, the mutation of selenocysteine to cysteine leads to more than 90 % loss of catalytic function of Txnrd1 (Lee et al., 2000; Zhong and Holmgren, 2000) highlighting the critical involvement of Sec during the catalytic cycle. Although Sec is critical for the catalytic function, our findings indicate that Cys497 is the most important amino acid involved in catalysis as it provides electrons for the reduction of thioselenide. Additionally, the orthologous cysteine variants of Txnrd1 were reported to exist in *Drosophila* which exhibit similar catalytic activity as the selenocysteine-containing Txnrd1 form in mice and humans (Bauer et al., 2003; Gromer et al., 2003). The occurrance of selenocysteine in the mammalian thioredoxin reductase presumably provides a selective advantage through broadening the substrate specificity and activity in diverse microenvironments (Gromer et al., 2003).

The localization of these mutants was examined by immunocytochemistry and confocal microscopy using an anti-FLAG antibody. Thioredoxin reductase 1 has been reported being mainly localised in the cytosol. Although in the case of wt (2ATG) Txnrd1 the cellular localisation was predominantly cytosolic, it was also detected in nucleus. This showed that *Txnrd1* can translocate to the nucleus and may exert different functions in the nucleus and in the cytosol. The U498STOP mutant and C497S mutant (to a lesser extent) were also detected in the nucleus. The other mutant forms of Txnrd1 were located in cytosol. The staining pattern for C64S and C497S exhibited granularity, thus localization to other sub-cellular compartments can not be ruled out at the moment. Further studies are needed to describe in more detail the unusual localization and staining pattern of these mutants and their physiological significance.

5.1.4 Antioxidants failed to rescue Txnrd1 knockout cells from cell death triggered by GSH depletion

Since antioxidants were reported to antagonize the GSH depletion-induced cell death in various cell types, including γ-*GCS*$^{-/-}$ (Shi et al., 2000) and *Txnrd2*$^{-/-}$ cells (Conrad et al., 2004), three different antioxidants (NAC, Trolox and 2-ME) were tested on *Txnrd1* knockout cells treated with BSO. When the *Txnrd1* knockout cells were cultured in the presence of antioxidants to prevent BSO-mediated cell death, all tested antioxidants (NAC, Trolox and 2-ME) invariably failed to rescue the cells from

cell death, which was unprecedented. The failure of antioxidants to rescue *Txnrd1* knockout cells was further confirmed by Annexin-PI staining showing comparable rate of cell death in antioxidant-treated and untreated samples. In the heterozygous control cell line, all the tested antioxidants protected the cells against BSO-induced cell death. GSH constitutes the major cellular redox buffer, being present in millimolar concentration (1-10 mM). Its importance had been demonstrated *in vivo* and *ex vivo*, since mice specifically lacking GSH synthesis die at E7.5. Likewise, *γ-GCS* knockout cells also die rapidly in cell culture (Shi et al., 2000), which, somehow surprisingly, could be prevented by culturing these cells in the presence of thiol-containing antioxidants (Shi et al., 2000). Similarly, *Txnrd2* knockout cells can be rescued from GSH depletion-mediated cell death by NAC (Conrad et al., 2004). Moreover, *xCT* knockout cells die within 24 hours after withdrawal of the antioxidant 2-ME and NAC due to severe oxidative stress in cell culture (Sato et al., 2005). In this context it is noteworthy, however, that *xCT* knockout mice are fully viable! Taken together, the requirement for GSH can be bypassed by thiol-containing antioxidants. The results of the present study that *Txnrd1* knockout cells can not be rescued from BSO-mediated cell death by antioxidants led to the conclusion that Txnrd1 is required for antioxidant activity to bypass the GSH requirement and therefore, antioxidants were ineffective in rescuing the *Txnrd1* knockout cells.

5.1.5 xCT over-expression in Txnrd1 knockout cells aggravated the detrimental effects of GSH depletion

Previous work in our laboratory had shown that xCT, the substrate specific subunit of system $\mathbf{X_c^-}$ provides resistance to Burkitt's lymphoma cells against oxidative stress and BSO-induced cell death (Banjac et al., 2008). The mechanism was shown to be augmented cystine uptake, thus increasing the intracellular and extracellular cysteine level without any impact on GSH synthesis or on the expression of anti-apoptotic genes. The work of Ana Banjac had suggested that the Cys_2/Cys redox couple operated independently of GSH, thus delineating the xCT-driven Cys_2/Cys cycle as an independent powerful redox cycle that protects the cells from cell death under GSH limiting conditions by maintaining the intracellular and extracellular redox balance. In the same line of observation, unpublished work of Seiler A. (Seiler, 2008) showed that xCT over-expression in *γ-GCS* knockout cells, which lack endogenous GSH synthesis, can successfully bypass their GSH/thiol requirement. This

observation was an extension of the published report by Shi et al. which showed that the *γ-GCS* knockout cells can be rescued by exogenously added thiol-containing compounds, such as GSH and NAC (Shi et al., 2000). The basic mechanism remains the same: antioxidant supplementation, thiol-containing compounds or cystine transporter that facilitates the delivery of cystine to sustain the pool of non-GSH reducing equivalents to the cells can bypass the requirement for GSH. The question of how the antioxidants achieve this and what is the driving force for the reduction of cystine to cysteine inside the cell under GSH depletion, however, remained unanswered in previous studies. The mechanistic answer to this question was revealed in the present study when the over-expression of xCT failed to rescue the *Txnrd1* knockout cells from GSH depletion-induced cell death. Unlike in γ-GCS knockout cells, Burkitt's lymphoma cells, and *Txnrd2* knockout cells, where xCT was found to be highly protective, xCT over-expression in *Txnrd1* null cells appeared to be detrimental to the cells under GSH deprivation and even sparked the rapid onset of cell death. Although ROS levels in xCT over-expressing *Txnrd1* knockout cells were comparable to mock transfected cells, there was, within the time frame of the experiment, four times more dead cells in xCT over-expressing *Txnrd1* knockout cells as compared to mock-transfected cells. The rapid induction of cell death in xCT over-expressing *Txnrd1* knockout cells can be attributed to the concomitant loss of GSH and overloading of the cells with cystine which could aggravate oxidative stress due to "disulfide-overload". The assumption that more accumulation of cystine in xCT over-expressing cells could lead to toxicity upon GSH depletion by itself, can be argued against with the fact that over-expression of SF-Txnrd1 wt (2ATG) fully rescued these cells from GSH depletion. Moreover, these xCT-over expressing *Txnrd1* knockout cells with restored SF-Txnrd1 expression tolerated higher doses of BSO as compared to SF-Txnrd1 wt (2ATG)-transduced eGFP control cells (that did not express xCT) under GSH depletion and mock-transduced xCT-over expressing *Txnrd1* knockout cells which were extremely sensitive to GSH depletion.

The failure of xCT over-expression in rescuing the *Txnrd1* knockout cells upon GSH depletion led to the conclusion that *Txnrd1* knockout cells lack the essential enzymatic make-up to reduce the imported cystine. xCT over-expression has been shown to provide a feeder-like effect to Burkitt´s lymphoma cells (Banjac et al., 2008) and to rescue the mock-transfected *γ-GCS* knockout control cells (Seiler, 2008) by secreting cysteine into the medium and maintaining the extracellular environment

reducing. Although xCT over-expression failed to rescue the *Txnrd1* knockout cells form GSH depletion-mediated cell death, it was hypothesized that *Txnrd1* knockout cells may be rescued from GSH depletion if grown in reducing extracellular milieu by co-culturing these cells with xCT over-expressing cells with intact *Txnrd1*. Even in co-culture experiments *Txnrd1* knockout cells could not be rescued, indicating that they have a severe impairment in the utilization of cysteine. Taken together, it can be concluded that *Txnrd1* knockout cells are extremely susceptible to GSH depletion, which can not be antagonized by antioxidant supplementation, xCT over-expression or by culturing them in a reducing extracellular environment. Studies in lower organisms had shown that a simultaneous block of both disulfide-reducing pathways (thioredoxin and GSH-dependent pathways) is incompatible with growth and survival under aerobic conditions (Grant, 2001; Muller, 1996; Prinz et al., 1997), but limited growth of these mutants can be restored using anaerobic conditions, indicating that oxidative stress may play a crucial role in cell death progression. The redundancies between the two pathways are apparent by the fact that in the absence of only one of the pathways, bacterial and yeast strains can survive and grow reasonably well. But in mammals, disruption of GSH synthesis alone is sufficient to cause embryonic lethality (Shi et al., 2000), even in the presence of an intact thioredoxin-system which is an alternative pathway involved in the maintenance of the dNTP pool suggesting that it is the redox balance which is severely compromised in these cells. This is further supported by the finding that the viability of these cells can be restored by antioxidant supplementation (Shi et al., 2000), and depletion of GSH has no effect on the dNTP pool and DNA synthesis (Spyrou and Holmgren, 1996). The essential requirement of ribonucleotide reductase for the maintenance of the cellular dNTP pool and DNA synthesis had led to the speculation on the existence of an additional hydrogen donor for ribonucleotide reductases apart from the thioredoxin and GSH-dependent system in mammals (Spyrou and Holmgren, 1996). In *E.coli*, a third hydrogen donor system for ribonucleotide reductase has already being identified in double mutants lacking thioredoxin and glutaredoxin (Aslund et al., 1994; Miranda-Vizuete et al., 1994). Moreover, a thioredoxin/thioredoxin reductase mutant of *Bacteroides fragilis*, which is a facultative anaerobic organism and lacks the glutathione/glutaredoxin system, can be grown in culture with the addition of reductants (Rocha et al., 2007). Furthermore, in mammals, the disruption of either thioredoxin 1 or thioredoxin 2 is incompatible with murine viability (Matsui et al., 1996; Nonn et al., 2003b) despite the presence of an intact GSH-dependent system,

again indicating that compromised viability is due to impaired redox balance rather than interference with DNA synthesis. Although disruption of both thioredoxin reductase 1 and 2 was associated with embryonic lethality in mice (Conrad et al., 2004; Jakupoglu et al., 2005), MEFs deficient in thioredoxin reductases can be grown in culture (present study and (Conrad et al., 2004). Both *Txnrd2* and *Txnrd1* deficient MEFs are highly susceptible to GSH depletion indicating an overlapping link between the two disulfide reducing systems. But the contrasting observations that antioxidant supplementation rescues *Txnrd2* knockout cells, but not *Txnrd1* knockout cells from GSH depletion, support the fact that Txnrd1 is required for the utilization and/or recycling of antioxidants. Several *in vitro* studies had shown that thioredoxin reductase 1 is involved in the recycling of ascorbate (May, 2002; May et al., 1998), vitamin E, L-cysteine (Luthman and Holmgren, 1982) and other small metabolites or compounds known to harbor antioxidant property (Nordberg and Arner, 2001). Of particular importance is the reduction of L-cystine. While characterizing the rat liver thioredoxin reductase, Holmgren´s group had shown that L-cystine is efficiently reduced *in vitro* by thioredoxin reductase (Luthman and Holmgren, 1982). Thus, the outcome of the present study lends support to the previous *in vitro* studies and this is the first *in vivo* result that shows that antioxidants are unable to antagonize the GSH-depletion-mediated cell death of *Txnrd1* knockout cells. This could explain the observation that rapid onset of cell death in xCT over-expressing *Txnrd1* knockout cells is due to “disulfide-stress” resulting from cystine overload. This was evident from the preferential activation of the stress-activated SAPK/JNK pathway in xCT over-expressing *Txnrd1* knockout cells upon GSH depletion, although ROS accumulation in these cells was comparable to that of mock cells. That disulfide overload triggers oxidative stress has long been speculated and the experimental evidence is now provided by this study (Aslund and Beckwith, 1999). Thus, based on our findings and existing information, we speculate that thioredoxin reductase 1 is essential for the utilization and recycling of small thiol-containing compounds and is the main driving force for the maintenance of the non-GSH reducing pool. This can be explained by the following model being operative in the cells (Figure 41).

The GSH is the main reducing equivalent in the cell being present in millimolar concentration. It has been speculated since long that GSH is the main driving force for intracellular reduction of cystine (Figure 41A). But the essential requirement of GSH can be bypassed by antioxidant supplementation or xCT over-expression that

provides cystine. In the absence of GSH, xCT over-expression bypasses the requirement for GSH by increasing the cellular uptake of cystine, boosting the intracellular and extracellular cysteine concentrations (Seiler, 2008). Thus, it acts as a powerful redox cycle across membrane (Figure 41B).

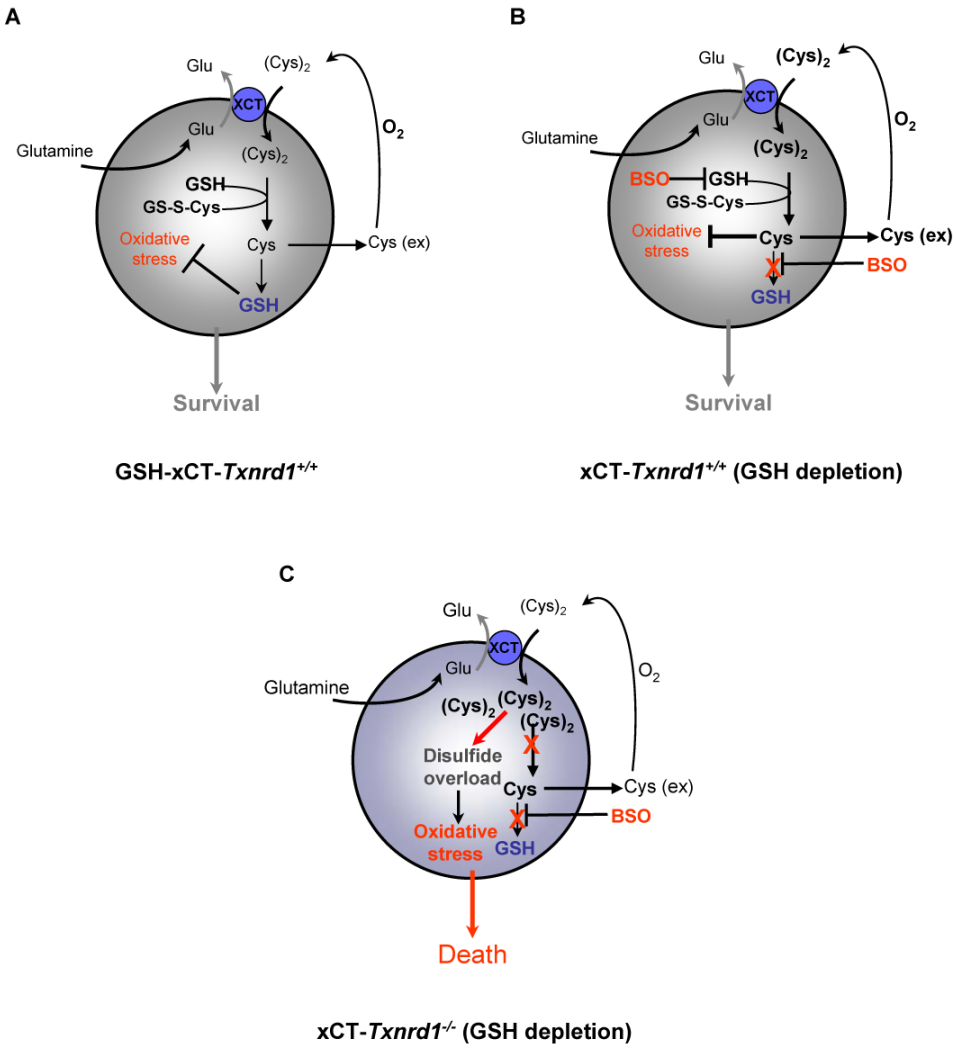

Figure 41. Molecular model depicting the essential requirement of Txnrd1 for intracellular reduction of cystine under GSH depletion. (A) GSH is the predominant reducing equivalent inside the cells counteracting the oxidative stress along with the thioredoxin-dependent system. It is believed to be the main driving force for the reduction of cystine inside the cells. **(B)** Under GSH deficiency xCT over-expression can bypass the essential requirement of GSH. **(C)** The failure of xCT-overexpression in rescuing the *Txnrd1*$^{-/-}$ cells of GSH depletion-induced cell death prompted us to hypothesize that Txnrd1 is the main driving force for intracellular reduction of cystine.

But the observations that in the absence of GSH and simultaneous over-expression of xCT there was effective intracellular reduction of cystine and failure of antioxidant supplementation or xCT over-expression to rescue the *Txnrd1*$^{-/-}$ cells led us to

hypothesize that Txnrd1 is the main driving force for the utilization/recycling of antioxidants and intracellular reduction of cystine to cysteine as depicted in figure 41C. The rapid onset of cell death in xCT-over-expressing *Txnrd1* knockout cells upon GSH depletion can be explained by the fact that *Txnrd1* knockout cells not only failed to reduce the cystine, but accumulation of imported cystine inside the cells leads to “disulfide overload”-mediated oxidative stress. Experimental validation of the proposed model is currently being performed.

5.2 Thioredoxin reductase 1 functions in oncogene-transformed cell lines

5.2.1 Thioredoxin reductase1 was dispensable for c-myc and Ha-ras^{V12} transformed cells

Thioredoxin reductase 1 has multiple functions in cellular growth, proliferation, and defense against oxidative stress. The Trx system is crucially involved in the reduction of ribonucleotides to yield deoxyribonucleotides and is indispensable for embryogenesis. The mammalian thioredoxin reductases have been implicated in the selenium metabolism (Kumar et al., 1992) and thus are in part responsible for a putative chemopreventive effect of selenium against cancer. Thioredoxin reductase 1 is reported to be augmented in many cancers and is positively correlated with invasiveness, metastasis and poor survival rate. Hence it might offer an Achilles heal for cancer treatment. Previous work in the lab had identified human thioredoxin reductase 1 as a target gene of *c-myc* (Schuhmacher et al., 2001). Therefore, the *c-myc* driven tumor model was chosen to dissect the role of *Txnrd1* in tumorigenesis by genetic means. Conditional *Txnrd1* knockout MEFs were transformed by co-transducing them with *c-myc* and *Ha-ras^{V12}* expressing lentiviruses. The targeted disruption of *Txnrd1* was achieved by exploiting the Cre-loxP technology.

Contrary to previous reports, which demonstrated that thioredoxin reductase 1 is indispensable for proliferation and tumorigenesis (Lu et al., 2007; Yoo et al., 2006; Yoo et al., 2007), *c-myc* and *Ha-ras^{V12}* transformed cell lines deficient in thioredoxin reductase 1 could be successfully established and maintained in culture. Apparently there was no difference in the proliferative capacity and cell cycle distribution of

knockout cells with respect to parental cell lines, indicating that the loss of *Txnrd1* had little if any impact on the growth-behavior of tumor cells. In their first report, Yoo et al. had reported that loss of *Txnrd1* functions by siRNA knock-down led to dramatic loss in tumorigenicity and metastatic properties of the Lewis Lung Cancer cell line (LLC1) manifested as a reversal in phenotype similar to those of normal cells (Yoo et al., 2006). Later they reported that under normal culture conditions, knockdown of *Txnrd1* has essentially no effect on cell growth, although they lost their ability to form colonies in soft agar. But when cultivated under serum-deprived conditions, *Txnrd1* knockdown led to defective progression through S-phase and decreased expression of DNA polymerase α, suggesting that *Txnrd1* may act as a pro-cancer protein (Yoo et al., 2007) and is required for proliferation. In our system, loss of *Txnrd1* had no apparent phenotype under normal culture condition, which is in line with the previously published report. The effect of low serum on proliferation of knockout cells has not been addressed yet. But interestingly, there was no effect on the colonigenicity or tumorigenicity of knockout cells suggestive of a yet-unrecognized compensatory mechanism replacing Txnrd1 (discussed later).

Numerous reports indicated that TrxR1 has opposing effects on tumor development. On the one hand it is reported to have a role in cancer prevention as it supports p53 functions and may induce apoptosis in certain tumors, while the up-regulation of *Txnrd1* in various cancers is suggestive of a cancer promoting role and is linked to the resistance to chemotherapy, metastasis, invasiveness and poor prognosis (Arner and Holmgren, 2006). The ambiguous nature of published reports could be due to the different tumor cell lines and chemical agents used and the lack of a proper genetic model to study the effect of loss of Txnrd1 in tumorigenesis. Another inherent problem while addressing the role of Txnrd1 in tumorigenesis is to dissect the thioredoxin-dependent role from that of the thioredoxin-independent role of thioredoxin reductase 1. As both Trx and TrxR are upregulated in multiple tumors, it is hard to distinguish the individual contributions of the two components of the Trx system. Although Trx expression is increased in a variety of human malignancies including lung, colorectal, cervical, hepatic and pancreatic cancers, the relationship between TrxR activity and tumor growth is less clear at present (Arner and Holmgren, 2006). It may be possible that tumor cells may need not to increase TrxR1 protein levels *per se*; on the other hand augmented, catalytic activity may be sufficient to drive TrxR1-dependent functions. It has also been shown that in human

B cell lines and leukemic cell lines derived from B cells, TrxR1 levels remained unaltered after selenium supplementation. So it is probable that some cancers rely on the Trx system to a greater extent than others. Therefore in some cases it might be essential, while in others loss of TrxR1 seems to have no effect on tumor growth behavior as they can easily compensate the loss of TrxR1 functions (as discussed in following section).

5.2.2 Response of transformed Txnrd1 knockout cells to different stress-inducing agents

Since thioredoxin reductase 1 plays an important role in the maintenance of cellular redox balance and defense against oxidative stress, we hypothesized that *Txnrd1* knockout cells would be more susceptible to different stress-inducing agents. Surprisingly, when challenged with hydrogen peroxide and alkyl hydroperoxide (t-butyl hydroperoxide) there was no difference in viability between knockout and wild-type cells over the tested concentrations. This was unexpected since thioredoxin reductase 1 has been linked to the scavenging of lipid hydroperoxide (Bjornstedt et al., 1995; May et al., 2002). Also thioredoxin reductase 1 is involved in the reduction of different peroxiredoxins, which are crucial for the scavenging of hydrogen peroxide, in a thioredoxin-dependent manner. The above observation is suggestive of the fact that, as long as thioredoxin 1 is maintained in its reduced state, cells deficient in Txnrd1 do not suffer from severe oxidative stress inflicted by H_2O_2 and t-BOOH. In the same line of observation, it was reported that thioredoxin 1 is maintained in a reduced state in *Txnrd1* knockdown cells by an unknown mechanism (Watson et al., 2008). This could be done by thioredoxin reductase 2, as one of the spliced forms is reported to be localized in the cytosol. In this respect *Txnrd1* knockout cells will be a valuable tool to explore the unidentified reductase responsible for the reduction of thioredoxin 1 as so far only thioredoxin reductase 1 is the known enzyme responsible for reducing thioredoxin 1. The generation of cell lines deficient in both thioredoxin reductases is needed to address this question. It has been reported that thioredoxin glutaredoxin reductase (TGR) has specificity for both thioredoxin and glutaredoxin and could be the common reductase for both pathways (Sun et al., 2001a).

Heavy metal compounds like arsenic (III) oxide, platinum, gold and organotellurium compounds are known inhibitors of thioredoxin reductase 1. The anti-cancer effect of arsenic (III) oxide and cisplatin is due to the inhibition of thioredoxin reductase 1 (Lu et al., 2007; Witte et al., 2005). Accordingly, if the cytotoxic effects of these agents are due to specific inhibition of thioredoxin reductase 1, then *Txnrd1* knockout cells should be more resistant to these compounds. Three compounds, arsenic (III) oxide, TEPAu and cisplatin, were applied to transformed *Txnrd1* knockout cells. Transformed *Txnrd1* knockout cells were moderately resistant to the three agents tested; confirming previously published reports that therapeutic efficacy of these agents is partially due to inhibition of thioredoxin reductase 1. *Txnrd1* knockout cells were found to be moderately resistant to arsenic (III) oxide and TEP Au at lower concentration, but at higher concentration these cells were equally susceptible which showed that at higher concentration inhibition of cellular enzymes other than thioredoxin reductase 1 is responsible for cell death. The data obtained in the present study rule out a high specificity of arsenic (III) oxide towards Txnrd1 as claimed by Holmgren's group (Lu et al.; 2007) who reported that chemotherapeutic efficacy of arsenic (III) oxide is due to inhibition of thioredoxin reductase 1. In particular, resistance to cisplatin was an interesting phenotype. In the present study, it was found that *Txnrd1* knockout cells were only moderately resistant to cisplatin suggesting thioredoxin reductase 1 as one amongst other targets of cisplatin. This was in line of a published report that cisplatin inhibits thioredoxin reductase 1 but not glutathione reductase (Witte et al., 2005). However, the report of Sasada et al. that thioredoxin reductase 1 confers resistance towards cisplatin therapy as knockdown of thioredoxin reductase 1 sensitizes tumor cells towards cisplatin is contradictory to our observation (Sasada et al., 1999).

In response to the DNA-damaging agent doxorubicin, it was found that *Txnrd1* knockout cells were equally sensitive like the parental cell lines. Doxorubicin does not inhibit TrxR1 function as it is a poor substrate of TrxR1 (Witte et al., 2005). Accordingly, there was no difference in the dose-response between wild-type and knockout cells towards doxorubicin.

5.2.3 Loss of thioredoxin reductase 1 had little impact on clonogenicity and tumorigenicity

Thioredoxin reductase 1 has been frequently linked to cellular proliferation. However, there are some reports showing that over-expression of thioredoxin reductase 1 in HEK 293 cells resulted in decreased proliferation (Nalvarte et al., 2004). The odd observation that loss of Txnrd1 functions had no impact on the proliferative capacity and cell cycle distribution of knockout cells prompted us to identify a putative compensatory mechanism operating in the cells. This observation was in line of published findings of Yoo et al. that under normal growth condition knock-down of thioredoxin reductase 1 has little effect on tumor cell proliferation, although under serum deprivation deficiency of Txnrd1 leads to deregulated S-phase transition. But the loss of Txnrd1 function, either by chemical inhibition or siRNA-mediated knockdown, invariably resulted in loss of clonogenicity and tumorigenicity (Lu et al., 2007; Wang et al., 2008; Yoo et al., 2006; Yoo et al., 2007). Contradictory to all the published reports, *Txnrd1* knockout cell lines were able to form colonies in soft agar, suggesting that the loss of Txnrd1 function had no effect on the clonogenicity of the cells. Most strikingly, the knockout cell lines formed aggressive tumors comparable in size to those of parental cell lines when implanted into mice, which further corroborated the findings obtained from *in vitro* soft agar assays.

5.2.4 Up-regulation of the GSH-dependent pathway compensated for the loss of Txnrd1

5.2.4.1 Transformed *Txnrd1* knockout cells were highly susceptible to GSH

Because *Txnrd1* knockout cells were highly susceptible to GSH depletion by BSO, which could not be rescued by antioxidant supplementation or xCT over-expression, it indicated that *Txnrd1* knockout cells may adopt components of the GSH-dependent pathway as salvage for survival. As both, the thioredoxin and the glutaredoxin system donate electrons to ribonucleotide reductase thus maintaining the dNTP pool and DNA synthesis, loss of one system may be compensated by the up-regulation of the other. In all possibilities, tumor cells may exploit the same mechanism, i.e. up-regulation of components of the GSH-dependent system to sustain the loss of Txnrd1. When GSH was depleted from the transformed *Txnrd1* knockout cells, the knockout cells displayed high sensitvity towards GSH depletion.

Thus, like untransformed cells, transformed *Txnrd1* knockout cells were also susceptible to GSH depletion, which indicated that irrespective of cell growth characteristics (untransformed versus transformed), cell survival and proliferation in the absence of Txnrd1 relies on the GSH-dependent pathway.

When two other compounds, cadmium chloride and PEITC, which are known to inhibit components of the GSH-dependent pathway, were tested, *Txnrd1* knockout cells exhibited only marginal resistance towards these compounds, which was an unexpected finding. The obscure nature and undefined mechanism of action of these compounds pose problems in drawing some concrete inference from the existing sets of data. But the specific nature of BSO as a GSH-depleting agent led to the conclusion that *Txnrd1* knockout cells heavily depend on the GSH-dependent pathway.

The above notion was further confirmed by reconstitution experiments. SF-Txnrd1 was over-expressed in a doxycycline-inducible manner (Bornkamm et al., 2005). Expression slowly declined after doxycycline withdrawal and was still detectable, although at lower level, 48 hours after withdrawal of the drug. In the presence of doxycycline, SF-Txnrd1 over-expressing *Txnrd1* knockout cells displayed strong resistance towards GSH-depletion as compared to the same cells in the absence of doxycycline. This provided the final proof that, in the absence of *Txnrd1*, GSH and/or a GSH-dependent pathway become crucial for survival of these cells. Therefore, components of the GSH-dependent pathway were examined in detail to identify the compensatory mechanism both at the transcriptional and enzyme activity level and by GSH/GSSG measurements.

5.2.4.2 Higher GSH concentration and glutathione reductase activity compensated the loss of Txnrd1 functions in transformed *Txnrd1* knockout cells

Analysis of the components of GSH-dependent pathway in transformed Txnrd1 knockout cells at the transcriptional level showed that *Gclc*, *Gclm* and *Gsr* were more than two-fold higher in knockout cells as compared to parental cell lines. To verify the results of qRT-PCR, GSH concentration and GR activity were measured in these

cells. GSH concentration was determined by HPLC, which revealed that total GSH concentration was considerably higher in transformed *Txnrd1* knockout cells. While total GSH (GSH+GSSG) and GSH concentration was 1.5- to 3-fold higher in *Txnrd1* knockout cells, a more than 3-fold increase in GSSG concentration was found in *Txnrd1* null cells. Although cells compensate for the loss of Txnrd1 by increasing total GSH concentration, the higher GSSG concentration in these cells is suggestive of sustained oxidative stress and increased pressure on the GSH-dependent system to compensate for the loss of Txnrd1. Yeast strains lacking both trx1 and trx2 showed elevated levels of GSSG (Muller, 1996), indicating a direct link between the thioredoxin system and the redox status of GSH in the cell. Thus, the compensatory up-regulation of either of the disulfide-reducing pathways in the absence of the other is evolutionary conserved, and the thioredoxin and GSH/glutaredoxin systems are functionally coupled.

Similarly, GR activity was up-regulated in these cells. *Txnrd1* knockout cells showed more than a 2-fold increase in GR activity as compared to the respective parental cell lines. The increase in GSH and GR activity was quantitatively variable when two knockout cell lines were compared. One knockout cell line (53MRC4ΔE3) showed a more than 2.5-fold increase in GSH and GR activity, while in the second knockout cell line (51MRB3ΔF1) a 1.5-fold increase in GSH and an approximately 2-fold increase in GR activity was observed. Therefore, one may conclude that the adaptation to Txnrd1-deficiency is more complex and involves at least two mechanisms, altered GSH synthesis and augmented GR activity. Needless to say, this does not rule out that other enzymes of the GSH-dependent sytems may additionally contribute to the salvage pathway. Nonetheless, these findings clearly indicate that the GSH-dependent system is the major back-up system for loss of Txnrd1. There are at least two published reports which support the findings of the present study. It is noteworthy, that in *Arabidopsis thaliana* and in *Drosophila melanogaster* there is a complex cross-talk between the Txn and GSH system (Reichheld et al., 2007). Accordingly, Txnrd1-deficiency could be bypassed by the GSH-dependent pathway. So to say, there is a common evolutionary signature with regard to the utilization of the GSH and thioredoxin systems. The other compensatory mechanism suggested by Bondereva et al. is the up regulation of sulfiredoxin (Bondareva et al., 2007).

5.2.4.3 Add-back of Txnrd1 caused reduction in GSH and GR activity

To rule out any clonal effect that *Txnrd1* knockout cells may exhibit, Txnrd1 was over-expressed in these cells in a doxycycline-inducible manner. If the increase in GSH and GR was a compensatory response, then upon re-introduction of Txnrd1, there should be a decrease in GSH and GR level. When Txnrd1 was reconstituted in the knockout cells, the GSH level and GR activity were indeed decreased in a time-dependent manner. The total GSH concentration in doxycycline-treated cells decreased to one third of that of untreated cells. The decrease in GSH levels after addition of doxycycline was paralleled by a reduction in GR activity. Re-expression of Txnrd1 led to a decrease in GR activity by approximately 50%. The re-constitution experiment finally proved that loss of *Txnrd1* could lead to up-regulation of the GSH-dependent pathway, which could be reverted by re-expression of Txnrd1 in a time-dependent manner. Thus, the GSH-dependent system can compensate for the loss of Txnrd1 rendering Txnrd1 dispensable for tumorigenesis.

5.2.5 Txnrd1-deficient tumors were highly susceptible to pharmacological inhibition of GSH

After proving that the loss of Txnrd1 has no effect on clonogenicity and tumorigenicity of transformed cells due to compensatory up-regulation of the GSH-dependent pathway, we asked the question if it is possible to exploit this mechanism as a therapeutic intervention to treat Txnrd1-deficient tumors. Pharmacological inhibition of GSH led to approximately 8-fold reduction in tumor mass, which successfully recapitulated the *in vitro* findings. Thus, these results showed that inhibition of one disulfide reducing pathway is not sufficient to combat tumor growth as they can shift to the other pathway for survival and proliferation. Long-term studies on the potential of GSH inhibition as a therapeutic stratergy for the cure of Txnrd1-deficient tumors are ongoing in mice. As the ROS burden is increased in tumor cells due to replicative stress, inhibition of both pathways may eventually provide a therapeutic window for the treatment of cancer, leaving normal cells unaffected. Drugs targeting both pathways like motexafin gadolinium are in clinical trial phase with promising results. Motexafin gadolinium not only inhibits thioredoxin reductases but also elevates the level of ROS generation by depleting the intracellular reducing metabolites like ascorbate, glutathione, and NADPH. It induces cell death by elevating the

intracellular zinc concentration and by releasing of mitochondrial caspases (Chen et al., 2005; Evens et al., 2005a; Evens et al., 2005b; Hashemy et al., 2006; Lecane et al., 2005; Richards and Mehta, 2007; William et al., 2007) .

5.3 Future prospects

Recent advancement in the field of redox regulation and antioxidant research had shown that ROS and antioxidant systems play an important role in tumorigenesis. As the basal ROS production is increased in tumor cells as compared to normal cells, agents that increase the ROS production or deplete the antioxidant system are emerging as novel therapeutics for chemotherapy. Redox modifiers including buthionine sulfoximine, ascorbic acid, arsenic trioxide, imexon, PEITC and motexafin gadolinium are in pre-clinical or clinical trials as single-agents or in combination, and a better understanding of ROS-induced cell death and senescence is prerequisite for the development of a rationale chemotherapy against cancer using redox modulators (Engel and Evens, 2006). The outcome of the present study indicates that inhibition of one component of an antioxidant defense system is not sufficient to combat the cancer as tumors can exploit the other pathway for the survival. The future therapeutic approaches should target both the thioredoxin and the GSH-dependent system, for effective outcome without doing too much harm to the normal tissue.

6. Summary

The thioredoxin dependent system consists of thioredoxin reductases, thioredoxins and thioredoxin-dependent peroxidases. Along with the glutathione (GSH)-dependent system, it is critically involved in the maintenance of the intracellular redox balance. In particular, cytosolic thioredoxin reductase (Txnrd1) substantially contributes to proliferation, growth and development as *Txnrd1* disruption leads to growth arrest and embryonic lethality in mice. Being up-regulated in various tumors, Txnrd1 and its major substrate thioredoxin 1 have been considered as promising drug targets for cancer therapy. Although various reports implicated that Txnrd1 is indispensable for proliferation and tumorigenesis, in this work both untransformed and transformed *Txnrd1*-deficient cell lines could be established that contrary to our expectations did not show any proliferation defects or altered cell cycle distribution. Like *mitochondrial thioredoxin reductase* (*Txnrd2*) null cells they were highly susceptible to experimental GSH depletion.

The GSH-depletion in immortalized, untransformed *Txnrd1* knockout cells triggered rapid cell death, which could not be prevented by antioxidants, by xCT over-expression or by co-culturing these cells with cells that provide a reducing extracellular milieu. This was a unique feature as cells with genetic defects in other redox-regulating enzymes like γ-*GCS* and *Txnrd2* and *xCT* cells could be readily protected from GSH depletion-induced cell death by antioxidants or xCT overexpression. The present study shows that Txnrd1 is required for the utilization and recycling of thiol-containing antioxidants. Reconstitution of Txnrd1 expression in *Txnrd1*$^{-/-}$ cells reversed the aforementioned effects and confirms that the effects were solely due to Txnrd1 depletion and not caused by other possible side effects.

The present study thus reveals that Txnrd1 is dispensable for tumor growth as loss of Txnrd1 function had little impact on proliferation, clonogenicity, and tumorigenicity of transformed cells. Detailed molecular and biochemical analysis of transformed *Txnrd1*$^{-/-}$ cells provided evidence that increased GSH synthesis and augmented glutathione reductase activity act as compensatory mechanisms that render Txnrd1 dispensable for tumor growth. This was evident from the fact that transformed *Txnrd1*$^{-/-}$ cells were highly susceptible to GSH depletion. The fact was further corroborated by *in vivo* studies, demonstrating an 8-fold reduction in the tumor mass of *Txnrd1*$^{-/-}$ tumors compared to control tumor treated with BSO. Thus, it was concluded that growth and proliferation of *Txnrd1*$^{-/-}$ tumors rely on the GSH-dependent system, which makes them highly susceptible to pharmacological depletion of intracellular GSH levels.

7. Zusammenfassung

Das Thioredoxin-abhängige System bestehend aus den Thioredoxin-Reduktasen, Thioredoxinen und Thioredoxin-abhängigen Peroxidasen bestimmt zusammen mit dem Glutathion (GSH) -abhängigen System maßgeblich die zelluläre Redox-Balance. Eine zentrale Rolle in der Regulation von Proliferation, Wachstum und Entwicklung spielt v.a. die zytosolische Thioredoxin-Reduktase (Txnrd1). Die gezielte Inaktivierung der Txnrd1 führt zu Wachstumsarrest und früher embryonaler Letalität in Mäusen. Da zytosolisches Thioredoxin und Txnrd1 häufig in Tumoren überexprimiert sind, wurden sie als ideale Zielmoleküle für die Tumortherapie erachtet. Obwohl einige frühere Arbeiten aus anderen Labors einschließlich unserem Labor implizierten, dass die Txnrd1 essenziell für die Zellproliferation und Tumorentwicklung sei, konnten in dieser Arbeit immortale und transformierte Txnrd1-knockout Zelllinien etabliert werden. Entgegen unserer Erwartungen weisen diese Zellen keine offensichtlichen Wachstumsdefekte, noch eine veränderte Zellzyklusverteilung auf. Allerdings reagieren diese Zellen, ähnlich wie mitochondriale *Thioredoxin-Reduktase* (*Txnrd2*)-knockout Zellen, sehr sensitiv auf pharmakologische GSH-Depletion.

Die GSH-Depletion löste sowohl in immortalisierten, als auch in transformierten Txnrd1-defizienten Zellen sehr schnell Zelltod aus, der weder durch Antioxidantien, noch durch die xCT-Überexpression oder durch Ko-Kulturen mit Zellen, die ein reduzierendes extrazelluläres Milieu verschaffen, verhindert werden konnte. Dies war ein bislang noch nicht beobachtetes Phänomen. Frühere Studien mit Zellen, denen Redox-regulierende Enzyme wie z.B. γ-*GCS*, *Txnrd2* und *xCT* fehlen, ergaben, dass Antioxidantien oder die Überexpression von xCT die Zellen vor GSH-Depletion-induziertem Zelltod schützen. Deshalb kann behauptet werden, dass die Txnrd1 zusätzlich wichtig für die Nutzung und das Recycling von Antioxidantien ist. Die Rekonstitution der Txnrd1-Expression in *Txnrd1*$^{-/-}$ Zellen reversierte alle oben genannten Phänotypen, was dafür spricht, dass alle Effekte durch die gezielte Inaktivierung der Txnrd1 hervorgerufen wurden und nicht durch mögliche Nebeneffekte.

Diese Studie zeigt zum ersten Mal, dass die Txnrd1 nicht essenziell ist für das Tumorwachstum, da der Verlust der Txnrd1-Expression kaum Einfluss auf die Proliferation, Klonogenität und Tumorigenese von transformierten Zellen hat. Weitere molekulare und biochemische Analysen ergaben, dass die gesteigerte GSH-Synthese und die erhöhte GSH-Reduktase den Verlust der Txnrd1 kompensieren. Deshalb reagierten die Zellen auch sehr empfindlich auf GSH-Depletion. Diese Eigenschaft konnte auch *in vivo* ausgenutzt werden, da die BSO-Behandlung von Mäusen mit implantierten *Txnrd1*$^{-/-}$ Tumorzellen eine 8-fache Reduktion des Tumorwachstums im Vergleich zu Kontrolltumoren aufwiesen. Aus diesen Daten kann geschlossen werden, dass das Wachstum und die Proliferation von *Txnrd1*$^{-/-}$ Tumoren von einem funktionellen GSH-abhängigen System abhängt, was sie sehr empfindlich gegenüber pharmakologischer GSH-Depletion macht.

8. References

Adachi, T., Pimentel, D. R., Heibeck, T., Hou, X., Lee, Y. J., Jiang, B., Ido, Y., and Cohen, R. A. (2004). S-glutathiolation of Ras mediates redox-sensitive signaling by angiotensin II in vascular smooth muscle cells. J Biol Chem *279*, 29857-29862.

Aghib, D. F., Bishop, J. M., Ottolenghi, S., Guerrasio, A., Serra, A., and Saglio, G. (1990). A 3' truncation of MYC caused by chromosomal translocation in a human T-cell leukemia increases mRNA stability. Oncogene *5*, 707-711.

Andersson, M., Holmgren, A., and Spyrou, G. (1996). NK-lysin, a disulfide-containing effector peptide of T-lymphocytes, is reduced and inactivated by human thioredoxin reductase. Implication for a protective mechanism against NK-lysin cytotoxicity. J Biol Chem *271*, 10116-10120.

Andresen, M., Regueira, T., Bruhn, A., Perez, D., Strobel, P., Dougnac, A., Marshall, G., and Leighton, F. (2008). Lipoperoxidation and protein oxidative damage exhibit different kinetics during septic shock. Mediators Inflamm *2008*, 168652.

Arner, E. S., and Holmgren, A. (2006). The thioredoxin system in cancer. Semin Cancer Biol *16*, 420-426.

Arner, E. S., Nakamura, H., Sasada, T., Yodoi, J., Holmgren, A., and Spyrou, G. (2001). Analysis of the inhibition of mammalian thioredoxin, thioredoxin reductase, and glutaredoxin by cis-diamminedichloroplatinum (II) and its major metabolite, the glutathione-platinum complex. Free Radic Biol Med *31*, 1170-1178.

Arner, E. S., Nordberg, J., and Holmgren, A. (1996). Efficient reduction of lipoamide and lipoic acid by mammalian thioredoxin reductase. Biochem Biophys Res Commun *225*, 268-274.

Arnold, N. B., Ketterer, K., Kleeff, J., Friess, H., Buchler, M. W., and Korc, M. (2004). Thioredoxin is downstream of Smad7 in a pathway that promotes growth and suppresses cisplatin-induced apoptosis in pancreatic cancer. Cancer Res *64*, 3599-3606.

Aslund, F., and Beckwith, J. (1999). Bridge over troubled waters: sensing stress by disulfide bond formation. Cell *96*, 751-753.

Aslund, F., Berndt, K. D., and Holmgren, A. (1997). Redox potentials of glutaredoxins and other thiol-disulfide oxidoreductases of the thioredoxin superfamily determined by direct protein-protein redox equilibria. J Biol Chem *272*, 30780-30786.

Aslund, F., Ehn, B., Miranda-Vizuete, A., Pueyo, C., and Holmgren, A. (1994). Two additional glutaredoxins exist in Escherichia coli: glutaredoxin 3 is a hydrogen donor for ribonucleotide reductase in a thioredoxin/glutaredoxin 1 double mutant. Proc Natl Acad Sci U S A *91*, 9813-9817.

Bae, Y. S., Kang, S. W., Seo, M. S., Baines, I. C., Tekle, E., Chock, P. B., and Rhee, S. G. (1997). Epidermal growth factor (EGF)-induced generation of hydrogen peroxide. Role in EGF receptor-mediated tyrosine phosphorylation. J Biol Chem *272*, 217-221.

Banjac, A., Perisic, T., Sato, H., Seiler, A., Bannai, S., Weiss, N., Kolle, P., Tschoep, K., Issels, R. D., Daniel, P. T.*, et al.* (2008). The cystine/cysteine cycle: a redox cycle regulating susceptibility versus resistance to cell death. Oncogene *27*, 1618-1628.

Barral, A. M., Kallstrom, R., Sander, B., and Rosen, A. (2000). Thioredoxin, thioredoxin reductase and tumour necrosis factor-alpha expression in melanoma cells: correlation to resistance against cytotoxic attack. Melanoma Res *10*, 331-343.

Barrett, W. C., DeGnore, J. P., Keng, Y. F., Zhang, Z. Y., Yim, M. B., and Chock, P. B. (1999). Roles of superoxide radical anion in signal transduction mediated by reversible regulation of protein-tyrosine phosphatase 1B. J Biol Chem *274*, 34543-34546.

Bauer, H., Massey, V., Arscott, L. D., Schirmer, R. H., Ballou, D. P., and Williams, C. H., Jr. (2003). The mechanism of high Mr thioredoxin reductase from Drosophila melanogaster. J Biol Chem *278*, 33020-33028.

Berggren, M., Gallegos, A., Gasdaska, J. R., Gasdaska, P. Y., Warneke, J., and Powis, G. (1996). Thioredoxin and thioredoxin reductase gene expression in human tumors and cell lines, and the effects of serum stimulation and hypoxia. Anticancer Res *16*, 3459-3466.

Bjornstedt, M., Hamberg, M., Kumar, S., Xue, J., and Holmgren, A. (1995). Human thioredoxin reductase directly reduces lipid hydroperoxides by NADPH and selenocystine strongly stimulates the reaction via catalytically generated selenols. J Biol Chem *270*, 11761-11764.

Bondareva, A. A., Capecchi, M. R., Iverson, S. V., Li, Y., Lopez, N. I., Lucas, O., Merrill, G. F., Prigge, J. R., Siders, A. M., Wakamiya, M.*, et al.* (2007). Effects of thioredoxin reductase-1 deletion on embryogenesis and transcriptome. Free Radic Biol Med *43*, 911-923.

Bornkamm, G. W., Berens, C., Kuklik-Roos, C., Bechet, J. M., Laux, G., Bachl, J., Korndoerfer, M., Schlee, M., Holzel, M., Malamoussi, A.*, et al.* (2005). Stringent doxycycline-dependent control of gene activities using an episomal one-vector system. Nucleic Acids Res *33*, e137.

Bosl, M. R., Takaku, K., Oshima, M., Nishimura, S., and Taketo, M. M. (1997). Early embryonic lethality caused by targeted disruption of the mouse selenocysteine tRNA gene (Trsp). Proc Natl Acad Sci U S A *94*, 5531-5534.

Butler, L. M., Zhou, X., Xu, W. S., Scher, H. I., Rifkind, R. A., Marks, P. A., and Richon, V. M. (2002). The histone deacetylase inhibitor SAHA arrests cancer cell growth, up-regulates thioredoxin-binding protein-2, and down-regulates thioredoxin. Proc Natl Acad Sci U S A *99*, 11700-11705.

Camier, S., Ma, E., Leroy, C., Pruvost, A., Toledano, M., and Marsolier-Kergoat, M. C. (2007). Visualization of ribonucleotide reductase catalytic oxidation establishes thioredoxins as its major reductants in yeast. Free Radic Biol Med *42*, 1008-1016.

Chen, C. Y., and Shyu, A. B. (1995). AU-rich elements: characterization and importance in mRNA degradation. Trends Biochem Sci *20*, 465-470.

Chen, J., Ramos, J., Sirisawad, M., Miller, R., and Naumovski, L. (2005). Motexafin gadolinium induces mitochondrially-mediated caspase-dependent apoptosis. Apoptosis *10*, 1131-1142.

Cheng, Q., Sandalova, T., Lindqvist, Y., and Arner, E. S. (2009). Crystal structure and catalysis of the selenoprotein thioredoxin reductase 1. J Biol Chem *284*, 3998-4008.

Chinta, S. J., and Andersen, J. K. (2008). Redox imbalance in Parkinson's disease. Biochim Biophys Acta *1780*, 1362-1367.

Chrestensen, C. A., Starke, D. W., and Mieyal, J. J. (2000). Acute cadmium exposure inactivates thioltransferase (Glutaredoxin), inhibits intracellular reduction of protein-glutathionyl-mixed disulfides, and initiates apoptosis. J Biol Chem *275*, 26556-26565.

Chung, Y. M., Yoo, Y. D., Park, J. K., Kim, Y. T., and Kim, H. J. (2001). Increased expression of peroxiredoxin II confers resistance to cisplatin. Anticancer Res *21*, 1129-1133.

Conrad, M., Brielmeier, M., and Bornkamm, G. W. (2006). Mitochondrial and Cytosolic Thioredoxin Reductase Knockout Mice. Selenium : Its Molecular Biology and Role in Human Health: Springer, New York.).

Conrad, M., Jakupoglu, C., Moreno, S. G., Lippl, S., Banjac, A., Schneider, M., Beck, H., Hatzopoulos, A. K., Just, U., Sinowatz, F.*, et al.* (2004). Essential role for mitochondrial thioredoxin reductase in hematopoiesis, heart development, and heart function. Mol Cell Biol *24*, 9414-9423.

Cunnick, J. M., Dorsey, J. F., Standley, T., Turkson, J., Kraker, A. J., Fry, D. W., Jove, R., and Wu, J. (1998). Role of Tyrosine Kinase Activity of Epidermal Growth Factor Receptor in the Lysophosphatidic Acid-stimulated Mitogen-activated Protein Kinase Pathway. J Biol Chem *273*, 14468-14475.

D'Autreaux, B., and Toledano, M. B. (2007). ROS as signalling molecules: mechanisms that generate specificity in ROS homeostasis. Nat Rev Mol Cell Biol *8*, 813-824.

Engel, R. H., and Evens, A. M. (2006). Oxidative stress and apoptosis: a new treatment paradigm in cancer. Front Biosci *11*, 300-312.

Engman, L., Al-Maharik, N., McNaughton, M., Birmingham, A., and Powis, G. (2003). Thioredoxin reductase and cancer cell growth inhibition by organotellurium antioxidants. Anticancer Drugs *14*, 153-161.

Engman, L., McNaughton, M., Gajewska, M., Kumar, S., Birmingham, A., and Powis, G. (2006). Thioredoxin reductase and cancer cell growth inhibition by organogold(III) compounds. Anticancer Drugs *17*, 539-544.

Evens, A. M., Balasubramanian, L., and Gordon, L. I. (2005a). Motexafin gadolinium induces oxidative stress and apoptosis in hematologic malignancies. Curr Treat Options Oncol *6*, 289-296.

Evens, A. M., Lecane, P., Magda, D., Prachand, S., Singhal, S., Nelson, J., Miller, R. A., Gartenhaus, R. B., and Gordon, L. I. (2005b). Motexafin gadolinium generates reactive oxygen species and induces apoptosis in sensitive and highly resistant multiple myeloma cells. Blood *105*, 1265-1273.

Farina, A. R., Tacconelli, A., Cappabianca, L., Masciulli, M. P., Holmgren, A., Beckett, G. J., Gulino, A., and Mackay, A. R. (2001). Thioredoxin alters the matrix

metalloproteinase/tissue inhibitors of metalloproteinase balance and stimulates human SK-N-SH neuroblastoma cell invasion. Eur J Biochem *268*, 405-413.

Fernandes, A. P., and Holmgren, A. (2004). Glutaredoxins: glutathione-dependent redox enzymes with functions far beyond a simple thioredoxin backup system. Antioxid Redox Signal *6*, 63-74.

Feussner, A., Rolinski, B., Weiss, N., Deufel, T., Wolfram, G., and Roscher, A. A. (1997). Determination of total homocysteine in human plasma by isocratic high-performance liquid chromatography. Eur J Clin Chem Clin Biochem *35*, 687-691.

Gallegos, A., Berggren, M., Gasdaska, J. R., and Powis, G. (1997). Mechanisms of the regulation of thioredoxin reductase activity in cancer cells by the chemopreventive agent selenium. Cancer Res *57*, 4965-4970.

Gallegos, A., Gasdaska, J. R., Taylor, C. W., Paine-Murrieta, G. D., Goodman, D., Gasdaska, P. Y., Berggren, M., Briehl, M. M., and Powis, G. (1996). Transfection with human thioredoxin increases cell proliferation and a dominant-negative mutant thioredoxin reverses the transformed phenotype of human breast cancer cells. Cancer Res *56*, 5765-5770.

Gallogly, M. M., and Mieyal, J. J. (2007). Mechanisms of reversible protein glutathionylation in redox signaling and oxidative stress. Curr Opin Pharmacol *7*, 381-391.

Gan, L., Yang, X. L., Liu, Q., and Xu, H. B. (2005). Inhibitory effects of thioredoxin reductase antisense RNA on the growth of human hepatocellular carcinoma cells. J Cell Biochem *96*, 653-664.

Garry, M. R., Kavanagh, T. J., Faustman, E. M., Sidhu, J. S., Liao, R., Ware, C., Vliet, P. A., and Deeb, S. S. (2008). Sensitivity of mouse lung fibroblasts heterozygous for GPx4 to oxidative stress. Free Radic Biol Med *44*, 1075-1087.

Gasdaska, J. R., Gasdaska, P. Y., Gallegos, A., and Powis, G. (1996). Human thioredoxin reductase gene localization to chromosomal position 12q23-q24.1 and mRNA distribution in human tissue. Genomics *37*, 257-259.

Gasdaska, J. R., Harney, J. W., Gasdaska, P. Y., Powis, G., and Berry, M. J. (1999). Regulation of human thioredoxin reductase expression and activity by 3'-untranslated region selenocysteine insertion sequence and mRNA instability elements. J Biol Chem *274*, 25379-25385.

Ghezzi, P. (2005). Regulation of protein function by glutathionylation. Free Radic Res *39*, 573-580.

Gladyshev, V. N., Jeang, K. T., and Stadtman, T. C. (1996). Selenocysteine, identified as the penultimate C-terminal residue in human T-cell thioredoxin reductase, corresponds to TGA in the human placental gene. Proc Natl Acad Sci U S A *93*, 6146-6151.

Gon, S., Faulkner, M. J., and Beckwith, J. (2006). In vivo requirement for glutaredoxins and thioredoxins in the reduction of the ribonucleotide reductases of Escherichia coli. Antioxid Redox Signal *8*, 735-742.

Grant, C. M. (2001). Role of the glutathione/glutaredoxin and thioredoxin systems in yeast growth and response to stress conditions. Mol Microbiol *39*, 533-541.

Greene, E. L., Houghton, O., Collinsworth, G., Garnovskaya, M. N., Nagai, T., Sajjad, T., Bheemanathini, V., Grewal, J. S., Paul, R. V., and Raymond, J. R. (2000). 5-HT(2A) receptors stimulate mitogen-activated protein kinase via H(2)O(2) generation in rat renal mesangial cells. Am J Physiol Renal Physiol *278*, F650-658.

Grogan, T. M., Fenoglio-Prieser, C., Zeheb, R., Bellamy, W., Frutiger, Y., Vela, E., Stemmerman, G., Macdonald, J., Richter, L., Gallegos, A., and Powis, G. (2000). Thioredoxin, a putative oncogene product, is overexpressed in gastric carcinoma and associated with increased proliferation and increased cell survival. Hum Pathol *31*, 475-481.

Gromer, S., Johansson, L., Bauer, H., Arscott, L. D., Rauch, S., Ballou, D. P., Williams, C. H., Jr., Schirmer, R. H., and Arner, E. S. (2003). Active sites of thioredoxin reductases: why selenoproteins? Proc Natl Acad Sci U S A *100*, 12618-12623.

Gromer, S., Urig, S., and Becker, K. (2004). The thioredoxin system--from science to clinic. Med Res Rev *24*, 40-89.

Gromer, S., Wissing, J., Behne, D., Ashman, K., Schirmer, R. H., Flohe, L., and Becker, K. (1998). A hypothesis on the catalytic mechanism of the selenoenzyme thioredoxin reductase. Biochem J *332 (Pt 2)*, 591-592.

Halliwell, B. a. G., J.M.C (1989). Free radicals in biology and medicine.: Oxford University Press, Oxford).

Han, H., Bearss, D. J., Browne, L. W., Calaluce, R., Nagle, R. B., and Von Hoff, D. D. (2002). Identification of differentially expressed genes in pancreatic cancer cells using cDNA microarray. Cancer Res *62*, 2890-2896.

Hanahan, D., and Weinberg, R. A. (2000). The hallmarks of cancer. Cell *100*, 57-70.

Hashemy, S. I., Ungerstedt, J. S., Zahedi Avval, F., and Holmgren, A. (2006). Motexafin gadolinium, a tumor-selective drug targeting thioredoxin reductase and ribonucleotide reductase. J Biol Chem *281*, 10691-10697.

Hedley, D., Pintilie, M., Woo, J., Nicklee, T., Morrison, A., Birle, D., Fyles, A., Milosevic, M., and Hill, R. (2004). Up-regulation of the redox mediators thioredoxin and apurinic/apyrimidinic excision (APE)/Ref-1 in hypoxic microregions of invasive cervical carcinomas, mapped using multispectral, wide-field fluorescence image analysis. Am J Pathol *164*, 557-565.

Hirota, K., Nakamura, H., Masutani, H., and Yodoi, J. (2002). Thioredoxin superfamily and thioredoxin-inducing agents. Ann N Y Acad Sci *957*, 189-199.

Hirt, R. P., Muller, S., Embley, T. M., and Coombs, G. H. (2002). The diversity and evolution of thioredoxin reductase: new perspectives. Trends Parasitol *18*, 302-308.

Ho, Y. S., Xiong, Y., Ho, D. S., Gao, J., Chua, B. H., Pai, H., and Mieyal, J. J. (2007). Targeted disruption of the glutaredoxin 1 gene does not sensitize adult mice to tissue injury induced by ischemia/reperfusion and hyperoxia. Free Radic Biol Med *43*, 1299-1312.

Holmgren, A. (1985). Thioredoxin. Annu Rev Biochem *54*, 237-271.

Hu, Y., Rosen, D. G., Zhou, Y., Feng, L., Yang, G., Liu, J., and Huang, P. (2005). Mitochondrial Manganese-Superoxide Dismutase Expression in Ovarian Cancer:

ROLE IN CELL PROLIFERATION AND RESPONSE TO OXIDATIVE STRESS. J Biol Chem *280*, 39485-39492.

Imai, H., and Nakagawa, Y. (2003). Biological significance of phospholipid hydroperoxide glutathione peroxidase (PHGPx, GPx4) in mammalian cells. Free Radic Biol Med *34*, 145-169.

Imlay, J. A. (2008). Cellular Defenses against Superoxide and Hydrogen Peroxide. Annu Rev Biochem *77*, 755-776.

Iwao-Koizumi, K., Matoba, R., Ueno, N., Kim, S. J., Ando, A., Miyoshi, Y., Maeda, E., Noguchi, S., and Kato, K. (2005). Prediction of docetaxel response in human breast cancer by gene expression profiling. J Clin Oncol *23*, 422-431.

Jakupoglu, C., Przemeck, G. K., Schneider, M., Moreno, S. G., Mayr, N., Hatzopoulos, A. K., de Angelis, M. H., Wurst, W., Bornkamm, G. W., Brielmeier, M., and Conrad, M. (2005). Cytoplasmic thioredoxin reductase is essential for embryogenesis but dispensable for cardiac development. Mol Cell Biol *25*, 1980-1988.

Jurado, J., Prieto-Alamo, M. J., Madrid-Risquez, J., and Pueyo, C. (2003). Absolute gene expression patterns of thioredoxin and glutaredoxin redox systems in mouse. J Biol Chem *278*, 45546-45554.

Kahlos, K., Soini, Y., Saily, M., Koistinen, P., Kakko, S., Paakko, P., Holmgren, A., and Kinnula, V. L. (2001). Up-regulation of thioredoxin and thioredoxin reductase in human malignant pleural mesothelioma. Int J Cancer *95*, 198-204.

Kakolyris, S., Giatromanolaki, A., Koukourakis, M., Powis, G., Souglakos, J., Sivridis, E., Georgoulias, V., Gatter, K. C., and Harris, A. L. (2001). Thioredoxin expression is associated with lymph node status and prognosis in early operable non-small cell lung cancer. Clin Cancer Res *7*, 3087-3091.

Kanda, M., Ihara, Y., Murata, H., Urata, Y., Kono, T., Yodoi, J., Seto, S., Yano, K., and Kondo, T. (2006). Glutaredoxin modulates platelet-derived growth factor-dependent cell signaling by regulating the redox status of low molecular weight protein-tyrosine phosphatase. J Biol Chem *281*, 28518-28528.

Kawahara, N., Tanaka, T., Yokomizo, A., Nanri, H., Ono, M., Wada, M., Kohno, K., Takenaka, K., Sugimachi, K., and Kuwano, M. (1996). Enhanced coexpression of thioredoxin and high mobility group protein 1 genes in human hepatocellular carcinoma and the possible association with decreased sensitivity to cisplatin. Cancer Res *56*, 5330-5333.

Kawai, H., Ota, T., Suzuki, F., and Tatsuka, M. (2000). Molecular cloning of mouse thioredoxin reductases. Gene *242*, 321-330.

Kim, H. J., Chae, H. Z., Kim, Y. J., Kim, Y. H., Hwangs, T. S., Park, E. M., and Park, Y. M. (2003). Preferential elevation of Prx I and Trx expression in lung cancer cells following hypoxia and in human lung cancer tissues. Cell Biol Toxicol *19*, 285-298.

Kishimoto, C., Shioji, K., Nakamura, H., Nakayama, Y., Yodoi, J., and Sasayama, S. (2001). Serum thioredoxin (TRX) levels in patients with heart failure. Jpn Circ J *65*, 491-494.

Klatt, P., Molina, E. P., De Lacoba, M. G., Padilla, C. A., Martinez-Galesteo, E., Barcena, J. A., and Lamas, S. (1999). Redox regulation of c-Jun DNA binding by reversible S-glutathiolation. Faseb J *13*, 1481-1490.

Kopnin, B. P. (2007). [Genome instability and oncogenesis]. Mol Biol (Mosk) *41*, 369-380.

Krieger-Brauer, H. I., and Kather, H. (1995). The stimulus-sensitive H2O2-generating system present in human fat-cell plasma membranes is multireceptor-linked and under antagonistic control by hormones and cytokines. Biochem J *307 (Pt 2)*, 543-548.

Kumar, S., Bjornstedt, M., and Holmgren, A. (1992). Selenite is a substrate for calf thymus thioredoxin reductase and thioredoxin and elicits a large non-stoichiometric oxidation of NADPH in the presence of oxygen. Eur J Biochem *207*, 435-439.

Land, H., Parada, L. F., and Weinberg, R. A. (1983). Tumorigenic conversion of primary embryo fibroblasts requires at least two cooperating oncogenes. Nature *304*, 596-602.

Laurent, T. C., Moore, E. C., and Reichard, P. (1964). Enzymatic Synthesis of Deoxyribonucleotides. Iv. Isolation and Characterization of Thioredoxin, the Hydrogen Donor from Escherichia Coli B. J Biol Chem *239*, 3436-3444.

Lecane, P. S., Karaman, M. W., Sirisawad, M., Naumovski, L., Miller, R. A., Hacia, J. G., and Magda, D. (2005). Motexafin gadolinium and zinc induce oxidative stress responses and apoptosis in B-cell lymphoma lines. Cancer Res *65*, 11676-11688.

Lee, S. R., Bar-Noy, S., Kwon, J., Levine, R. L., Stadtman, T. C., and Rhee, S. G. (2000). Mammalian thioredoxin reductase: oxidation of the C-terminal cysteine/selenocysteine active site forms a thioselenide, and replacement of selenium with sulfur markedly reduces catalytic activity. Proc Natl Acad Sci U S A *97*, 2521-2526.

Lee, S. R., Kwon, K. S., Kim, S. R., and Rhee, S. G. (1998). Reversible inactivation of protein-tyrosine phosphatase 1B in A431 cells stimulated with epidermal growth factor. J Biol Chem *273*, 15366-15372.

Lewin, M. H., Arthur, J. R., Riemersma, R. A., Nicol, F., Walker, S. W., Millar, E. M., Howie, A. F., and Beckett, G. J. (2002). Selenium supplementation acting through the induction of thioredoxin reductase and glutathione peroxidase protects the human endothelial cell line EAhy926 from damage by lipid hydroperoxides. Biochim Biophys Acta *1593*, 85-92.

Lillig, C. H., Berndt, C., and Holmgren, A. (2008). Glutaredoxin systems. Biochim Biophys Acta *1780*, 1304-1317.

Lillig, C. H., Berndt, C., Vergnolle, O., Lonn, M. E., Hudemann, C., Bill, E., and Holmgren, A. (2005). Characterization of human glutaredoxin 2 as iron-sulfur protein: a possible role as redox sensor. Proc Natl Acad Sci U S A *102*, 8168-8173.

Lin, S., Del Razo, L. M., Styblo, M., Wang, C., Cullen, W. R., and Thomas, D. J. (2001). Arsenicals inhibit thioredoxin reductase in cultured rat hepatocytes. Chem Res Toxicol *14*, 305-311.

Lincoln, D. T., Ali Emadi, E. M., Tonissen, K. F., and Clarke, F. M. (2003). The thioredoxin-thioredoxin reductase system: over-expression in human cancer. Anticancer Res *23*, 2425-2433.

Liu, J., Qu, W., and Kadiiska, M. B. (2009). Role of oxidative stress in cadmium toxicity and carcinogenesis. Toxicol Appl Pharmacol.

Lo, Y. Y., and Cruz, T. F. (1995). Involvement of reactive oxygen species in cytokine and growth factor induction of c-fos expression in chondrocytes. J Biol Chem *270*, 11727-11730.

Lopez-Mirabal, H. R., and Winther, J. R. (2008). Redox characteristics of the eukaryotic cytosol. Biochim Biophys Acta *1783*, 629-640.

Lu, J., Chew, E. H., and Holmgren, A. (2007). Targeting thioredoxin reductase is a basis for cancer therapy by arsenic trioxide. Proc Natl Acad Sci U S A *104*, 12288-12293.

Luthman, M., and Holmgren, A. (1982). Rat liver thioredoxin and thioredoxin reductase: purification and characterization. Biochemistry *21*, 6628-6633.

Martin, J. L. (1995). Thioredoxin--a fold for all reasons. Structure *3*, 245-250.

Marzano, C., Gandin, V., Folda, A., Scutari, G., Bindoli, A., and Rigobello, M. P. (2007). Inhibition of thioredoxin reductase by auranofin induces apoptosis in cisplatin-resistant human ovarian cancer cells. Free Radic Biol Med *42*, 872-881.

Matsui, M., Oshima, M., Oshima, H., Takaku, K., Maruyama, T., Yodoi, J., and Taketo, M. M. (1996). Early embryonic lethality caused by targeted disruption of the mouse thioredoxin gene. Dev Biol *178*, 179-185.

Matsutani, Y., Yamauchi, A., Takahashi, R., Ueno, M., Yoshikawa, K., Honda, K., Nakamura, H., Kato, H., Kodama, H., Inamoto, T.*, et al.* (2001). Inverse correlation of thioredoxin expression with estrogen receptor- and p53-dependent tumor growth in breast cancer tissues. Clin Cancer Res *7*, 3430-3436.

May, J. M. (2002). Recycling of vitamin C by mammalian thioredoxin reductase. Methods Enzymol *347*, 327-332.

May, J. M., Cobb, C. E., Mendiratta, S., Hill, K. E., and Burk, R. F. (1998). Reduction of the ascorbyl free radical to ascorbate by thioredoxin reductase. J Biol Chem *273*, 23039-23045.

May, J. M., and de Haen, C. (1979). Insulin-stimulated intracellular hydrogen peroxide production in rat epididymal fat cells. J Biol Chem *254*, 2214-2220.

May, J. M., Morrow, J. D., and Burk, R. F. (2002). Thioredoxin reductase reduces lipid hydroperoxides and spares alpha-tocopherol. Biochem Biophys Res Commun *292*, 45-49.

Meister, A. (1994). Glutathione-ascorbic acid antioxidant system in animals. J Biol Chem *269*, 9397-9400.

Meister, A., and Anderson, M. E. (1983). Glutathione. Annu Rev Biochem *52*, 711-760.

Miranda-Vizuete, A., Martinez-Galisteo, E., Aslund, F., Lopez-Barea, J., Pueyo, C., and Holmgren, A. (1994). Null thioredoxin and glutaredoxin Escherichia coli K-12 mutants have no enhanced sensitivity to mutagens due to a new GSH-dependent hydrogen donor and high increases in ribonucleotide reductase activity. J Biol Chem *269*, 16631-16637.

Mitsui, A., Hamuro, J., Nakamura, H., Kondo, N., Hirabayashi, Y., Ishizaki-Koizumi, S., Hirakawa, T., Inoue, T., and Yodoi, J. (2002). Overexpression of human thioredoxin in transgenic mice controls oxidative stress and life span. Antioxid Redox Signal *4*, 693-696.

Mohr, S., Hallak, H., de Boitte, A., Lapetina, E. G., and Brune, B. (1999). Nitric oxide-induced S-glutathionylation and inactivation of glyceraldehyde-3-phosphate dehydrogenase. J Biol Chem *274*, 9427-9430.

Mosmann, T. (1983). Rapid colorimetric assay for cellular growth and survival: application to proliferation and cytotoxicity assays. J Immunol Methods *65*, 55-63.

Muller, E. G. (1996). A glutathione reductase mutant of yeast accumulates high levels of oxidized glutathione and requires thioredoxin for growth. Mol Biol Cell *7*, 1805-1813.

Mustacich, D., and Powis, G. (2000). Thioredoxin reductase. Biochem J *346 Pt 1*, 1-8.

Nadeau, P. J., Charette, S. J., Toledano, M. B., and Landry, J. (2007). Disulfide Bond-mediated multimerization of Ask1 and its reduction by thioredoxin-1 regulate H(2)O(2)-induced c-Jun NH(2)-terminal kinase activation and apoptosis. Mol Biol Cell *18*, 3903-3913.

Nakamura, H. (2004). Thioredoxin as a key molecule in redox signaling. Antioxid Redox Signal *6*, 15-17.

Nakamura, H. (2005). Thioredoxin and its related molecules: update 2005. Antioxid Redox Signal *7*, 823-828.

Nakamura, H., Bai, J., Nishinaka, Y., Ueda, S., Sasada, T., Ohshio, G., Imamura, M., Takabayashi, A., Yamaoka, Y., and Yodoi, J. (2000). Expression of thioredoxin and glutaredoxin, redox-regulating proteins, in pancreatic cancer. Cancer Detect Prev *24*, 53-60.

Nakamura, H., De Rosa, S. C., Yodoi, J., Holmgren, A., Ghezzi, P., Herzenberg, L. A., and Herzenberg, L. A. (2001). Chronic elevation of plasma thioredoxin: inhibition of chemotaxis and curtailment of life expectancy in AIDS. Proc Natl Acad Sci U S A *98*, 2688-2693.

Nakamura, H., Masutani, H., Tagaya, Y., Yamauchi, A., Inamoto, T., Nanbu, Y., Fujii, S., Ozawa, K., and Yodoi, J. (1992). Expression and growth-promoting effect of adult T-cell leukemia-derived factor. A human thioredoxin homologue in hepatocellular carcinoma. Cancer *69*, 2091-2097.

Nakamura, H., Mitsui, A., and Yodoi, J. (2002). Thioredoxin overexpression in transgenic mice. Methods Enzymol *347*, 436-440.

Nalvarte, I., Damdimopoulos, A. E., Nystom, C., Nordman, T., Miranda-Vizuete, A., Olsson, J. M., Eriksson, L., Bjornstedt, M., Arner, E. S., and Spyrou, G. (2004). Overexpression of enzymatically active human cytosolic and mitochondrial thioredoxin reductase in HEK-293 cells. Effect on cell growth and differentiation. J Biol Chem *279*, 54510-54517.

Nathan, C. (2003). Specificity of a third kind: reactive oxygen and nitrogen intermediates in cell signaling. J Clin Invest *111*, 769-778.

Nishimoto, M., Sakaue, M., and Hara, S. (2006). Short-interfering RNA-mediated silencing of thioredoxin reductase 1 alters the sensitivity of HeLa cells toward cadmium. Biol Pharm Bull *29*, 543-546.

Niwa, T. (2007). Protein glutathionylation and oxidative stress. J Chromatogr B Analyt Technol Biomed Life Sci *855*, 59-65.

Nonn, L., Berggren, M., and Powis, G. (2003a). Increased expression of mitochondrial peroxiredoxin-3 (thioredoxin peroxidase-2) protects cancer cells against hypoxia and drug-induced hydrogen peroxide-dependent apoptosis. Mol Cancer Res *1*, 682-689.

Nonn, L., Williams, R. R., Erickson, R. P., and Powis, G. (2003b). The absence of mitochondrial thioredoxin 2 causes massive apoptosis, exencephaly, and early embryonic lethality in homozygous mice. Mol Cell Biol *23*, 916-922.

Nordberg, J., and Arner, E. S. (2001). Reactive oxygen species, antioxidants, and the mammalian thioredoxin system. Free Radic Biol Med *31*, 1287-1312.

Nordberg, J., Zhong, L., Holmgren, A., and Arner, E. S. (1998). Mammalian thioredoxin reductase is irreversibly inhibited by dinitrohalobenzenes by alkylation of both the redox active selenocysteine and its neighboring cysteine residue. J Biol Chem *273*, 10835-10842.

Novogrodsky, A., Nehring, R. E., Jr., and Meister, A. (1979). Inhibition of amino acid transport into lymphoid cells by the glutamine analog L-2-amino-4-oxo-5-chloropentanoate. Proc Natl Acad Sci U S A *76*, 4932-4935.

Ortenberg, R., Gon, S., Porat, A., and Beckwith, J. (2004). Interactions of glutaredoxins, ribonucleotide reductase, and components of the DNA replication system of Escherichia coli. Proc Natl Acad Sci U S A *101*, 7439-7444.

Osborne, S. A., and Tonissen, K. F. (2001). Genomic organisation and alternative splicing of mouse and human thioredoxin reductase 1 genes. BMC Genomics *2*, 10.

Ozben, T. (2007). Oxidative stress and apoptosis: impact on cancer therapy. J Pharm Sci *96*, 2181-2196.

Padovani, D., Mulliez, E., and Fontecave, M. (2001). Activation of class III ribonucleotide reductase by thioredoxin. J Biol Chem *276*, 9587-9589.

Paget, M. S., and Buttner, M. J. (2003). Thiol-based regulatory switches. Annu Rev Genet *37*, 91-121.

Park, S. H., Chung, Y. M., Lee, Y. S., Kim, H. J., Kim, J. S., Chae, H. Z., and Yoo, Y. D. (2000). Antisense of human peroxiredoxin II enhances radiation-induced cell death. Clin Cancer Res *6*, 4915-4920.

Parrinello, S., Samper, E., Krtolica, A., Goldstein, J., Melov, S., and Campisi, J. (2003). Oxygen sensitivity severely limits the replicative lifespan of murine fibroblasts. Nat Cell Biol *5*, 741-747.

Pekkari, K., Avila-Carino, J., Bengtsson, A., Gurunath, R., Scheynius, A., and Holmgren, A. (2001). Truncated thioredoxin (Trx80) induces production of interleukin-12 and enhances CD14 expression in human monocytes. Blood *97*, 3184-3190.

Pekkari, K., Avila-Carino, J., Gurunath, R., Bengtsson, A., Scheynius, A., and Holmgren, A. (2003). Truncated thioredoxin (Trx80) exerts unique mitogenic cytokine effects via a mechanism independent of thiol oxido-reductase activity. FEBS Lett *539*, 143-148.

Pekkari, K., and Holmgren, A. (2004). Truncated thioredoxin: physiological functions and mechanism. Antioxid Redox Signal *6*, 53-61.

Pineda-Molina, E., Klatt, P., Vazquez, J., Marina, A., Garcia de Lacoba, M., Perez-Sala, D., and Lamas, S. (2001). Glutathionylation of the p50 subunit of NF-kappaB: a mechanism for redox-induced inhibition of DNA binding. Biochemistry *40*, 14134-14142.

Powis, G., Wipf, P., Lynch, S. M., Birmingham, A., and Kirkpatrick, D. L. (2006). Molecular pharmacology and antitumor activity of palmarumycin-based inhibitors of thioredoxin reductase. Mol Cancer Ther *5*, 630-636.

Prinz, W. A., Aslund, F., Holmgren, A., and Beckwith, J. (1997). The role of the thioredoxin and glutaredoxin pathways in reducing protein disulfide bonds in the Escherichia coli cytoplasm. J Biol Chem *272*, 15661-15667.

Radisky, D. C., Levy, D. D., Littlepage, L. E., Liu, H., Nelson, C. M., Fata, J. E., Leake, D., Godden, E. L., Albertson, D. G., Nieto, M. A.*, et al.* (2005). Rac1b and reactive oxygen species mediate MMP-3-induced EMT and genomic instability. Nature *436*, 123-127.

Raffel, J., Bhattacharyya, A. K., Gallegos, A., Cui, H., Einspahr, J. G., Alberts, D. S., and Powis, G. (2003). Increased expression of thioredoxin-1 in human colorectal cancer is associated with decreased patient survival. J Lab Clin Med *142*, 46-51.

Reichheld, J. P., Khafif, M., Riondet, C., Droux, M., Bonnard, G., and Meyer, Y. (2007). Inactivation of thioredoxin reductases reveals a complex interplay between thioredoxin and glutathione pathways in Arabidopsis development. Plant Cell *19*, 1851-1865.

Reynaert, N. L., van der Vliet, A., Guala, A. S., McGovern, T., Hristova, M., Pantano, C., Heintz, N. H., Heim, J., Ho, Y. S., Matthews, D. E.*, et al.* (2006). Dynamic redox control of NF-kappaB through glutaredoxin-regulated S-glutathionylation of inhibitory kappaB kinase beta. Proc Natl Acad Sci U S A *103*, 13086-13091.

Rhee, S. G. (2006). Cell signaling. H2O2, a necessary evil for cell signaling. Science *312*, 1882-1883.

Rhee, S. G., Bae, Y. S., Lee, S.-R. a., and Kwon, J. (2000). Hydrogen peroxide: a key messenger that modulates protein phosphorylation through cysteine oxidation. Science'sstke *2000*, p. pe1-6.

Rhee, S. G., Chae, H. Z., and Kim, K. (2005a). Peroxiredoxins: a historical overview and speculative preview of novel mechanisms and emerging concepts in cell signaling. Free Radic Biol Med *38*, 1543-1552.

Rhee, S. G., Kang, S. W., Jeong, W., Chang, T. S., Yang, K. S., and Woo, H. A. (2005b). Intracellular messenger function of hydrogen peroxide and its regulation by peroxiredoxins. Curr Opin Cell Biol *17*, 183-189.

Richards, G. M., and Mehta, M. P. (2007). Motexafin gadolinium in the treatment of brain metastases. Expert Opin Pharmacother *8*, 351-359.

Rocha, E. R., Tzianabos, A. O., and Smith, C. J. (2007). Thioredoxin reductase is essential for thiol/disulfide redox control and oxidative stress survival of the anaerobe Bacteroides fragilis. J Bacteriol *189*, 8015-8023.

Rodrigues, M. S., Reddy, M. M., and Sattler, M. (2008). Cell cycle regulation by oncogenic tyrosine kinases in myeloid neoplasias: from molecular redox mechanisms to health implications. Antioxid Redox Signal *10*, 1813-1848.

Rosato, R. R., and Grant, S. (2003). Histone deacetylase inhibitors in cancer therapy. Cancer Biol Ther *2*, 30-37.

Rozen, S., and Skaletsky, H. (2000). Primer3 on the WWW for general users and for biologist programmers. Methods Mol Biol *132*, 365-386.

Rubartelli, A., Bajetto, A., Allavena, G., Wollman, E., and Sitia, R. (1992). Secretion of thioredoxin by normal and neoplastic cells through a leaderless secretory pathway. J Biol Chem *267*, 24161-24164.

Rundlof, A. K., Carlsten, M., Giacobini, M. M., and Arner, E. S. (2000). Prominent expression of the selenoprotein thioredoxin reductase in the medullary rays of the rat kidney and thioredoxin reductase mRNA variants differing at the 5' untranslated region. Biochem J *347 Pt 3*, 661-668.

Rundlof, A. K., Fernandes, A. P., Selenius, M., Babic, M., Shariatgorji, M., Nilsonne, G., Ilag, L. L., Dobra, K., and Bjornstedt, M. (2007). Quantification of alternative mRNA species and identification of thioredoxin reductase 1 isoforms in human tumor cells. Differentiation *75*, 123-132.

Rundlof, A. K., Janard, M., Miranda-Vizuete, A., and Arner, E. S. (2004). Evidence for intriguingly complex transcription of human thioredoxin reductase 1. Free Radic Biol Med *36*, 641-656.

Sagara, J., Miura, K., and Bannai, S. (1993). Cystine uptake and glutathione level in fetal brain cells in primary culture and in suspension. J Neurochem *61*, 1667-1671.

Saitoh, M., Nishitoh, H., Fujii, M., Takeda, K., Tobiume, K., Sawada, Y., Kawabata, M., Miyazono, K., and Ichijo, H. (1998). Mammalian thioredoxin is a direct inhibitor of apoptosis signal-regulating kinase (ASK) 1. Embo J *17*, 2596-2606.

Sasada, T., Iwata, S., Sato, N., Kitaoka, Y., Hirota, K., Nakamura, K., Nishiyama, A., Taniguchi, Y., Takabayashi, A., and Yodoi, J. (1996). Redox control of resistance to cis-diamminedichloroplatinum (II) (CDDP): protective effect of human thioredoxin against CDDP-induced cytotoxicity. J Clin Invest *97*, 2268-2276.

Sasada, T., Nakamura, H., Ueda, S., Iwata, S., Ueno, M., Takabayashi, A., and Yodoi, J. (2000). Secretion of thioredoxin enhances cellular resistance to cis-diamminedichloroplatinum (II). Antioxid Redox Signal *2*, 695-705.

Sasada, T., Nakamura, H., Ueda, S., Sato, N., Kitaoka, Y., Gon, Y., Takabayashi, A., Spyrou, G., Holmgren, A., and Yodoi, J. (1999). Possible involvement of thioredoxin reductase as well as thioredoxin in cellular sensitivity to cis-diamminedichloroplatinum (II). Free Radic Biol Med *27*, 504-514.

Sato, H., Shiiya, A., Kimata, M., Maebara, K., Tamba, M., Sakakura, Y., Makino, N., Sugiyama, F., Yagami, K., Moriguchi, T.*, et al.* (2005). Redox imbalance in cystine/glutamate transporter-deficient mice. J Biol Chem *280*, 37423-37429.

Sato, H., Tamba, M., Ishii, T., and Bannai, S. (1999). Cloning and expression of a plasma membrane cystine/glutamate exchange transporter composed of two distinct proteins. J Biol Chem *274*, 11455-11458.

Sattler, M., Winkler, T., Verma, S., Byrne, C. H., Shrikhande, G., Salgia, R., and Griffin, J. D. (1999). Hematopoietic growth factors signal through the formation of reactive oxygen species. Blood *93*, 2928-2935.

Schenk, H., Vogt, M., Droge, W., and Schulze-Osthoff, K. (1996). Thioredoxin as a potent costimulus of cytokine expression. J Immunol *156*, 765-771.

Schuhmacher, M., Kohlhuber, F., Holzel, M., Kaiser, C., Burtscher, H., Jarsch, M., Bornkamm, G. W., Laux, G., Polack, A., Weidle, U. H., and Eick, D. (2001). The transcriptional program of a human B cell line in response to Myc. Nucleic Acids Res *29*, 397-406.

Schumacker, P. T. (2006). Reactive oxygen species in cancer cells: live by the sword, die by the sword. cancer cell *10*, 175-176.

Schwertassek, U., Balmer, Y., Gutscher, M., Weingarten, L., Preuss, M., Engelhard, J., Winkler, M., and Dick, T. P. (2007). Selective redox regulation of cytokine receptor signaling by extracellular thioredoxin-1. Embo J *26*, 3086-3097.

Seiler, A. (2008). Dissecting the molecular mechanism of glutathione-dependent regulation of cell proliferation and cell death.

Seiler, A., Schneider, M., Forster, H., Roth, S., Wirth, E. K., Culmsee, C., Plesnila, N., Kremmer, E., Radmark, O., Wurst, W.*, et al.* (2008). Glutathione peroxidase 4 senses and translates oxidative stress into 12/15-lipoxygenase dependent- and AIF-mediated cell death. Cell Metab *8*, 237-248.

Shi, Q., and Gibson, G. E. (2007). Oxidative stress and transcriptional regulation in Alzheimer disease. Alzheimer Dis Assoc Disord *21*, 276-291.

Shi, Z. Z., Osei-Frimpong, J., Kala, G., Kala, S. V., Barrios, R. J., Habib, G. M., Lukin, D. J., Danney, C. M., Matzuk, M. M., and Lieberman, M. W. (2000). Glutathione synthesis is essential for mouse development but not for cell growth in culture. Proc Natl Acad Sci U S A *97*, 5101-5106.

Smart, D. K., Ortiz, K. L., Mattson, D., Bradbury, C. M., Bisht, K. S., Sieck, L. K., Brechbiel, M. W., and Gius, D. (2004). Thioredoxin reductase as a potential molecular target for anticancer agents that induce oxidative stress. Cancer Res *64*, 6716-6724.

Soerensen, J., Jakupoglu, C., Beck, H., Forster, H., Schmidt, J., Schmahl, W., Schweizer, U., Conrad, M., and Brielmeier, M. (2008). The role of thioredoxin reductases in brain development. PLoS ONE *3*, e1813.

Soini, Y., Kahlos, K., Napankangas, U., Kaarteenaho-Wiik, R., Saily, M., Koistinen, P., Paaakko, P., Holmgren, A., and Kinnula, V. L. (2001). Widespread expression of thioredoxin and thioredoxin reductase in non-small cell lung carcinoma. Clin Cancer Res *7*, 1750-1757.

Spector, A., Yan, G. Z., Huang, R. R., McDermott, M. J., Gascoyne, P. R., and Pigiet, V. (1988). The effect of H2O2 upon thioredoxin-enriched lens epithelial cells. J Biol Chem *263*, 4984-4990.

Spyrou, G., Bjornstedt, M., Skog, S., and Holmgren, A. (1996). Selenite and selenate inhibit human lymphocyte growth via different mechanisms. Cancer Res *56*, 4407-4412.

Spyrou, G., and Holmgren, A. (1996). Deoxyribonucleoside triphosphate pools and growth of glutathione-depleted 3T6 mouse fibroblasts. Biochem Biophys Res Commun *220*, 42-46.

Sumida, Y., Nakashima, T., Yoh, T., Kakisaka, Y., Nakajima, Y., Ishikawa, H., Mitsuyoshi, H., Okanoue, T., Nakamura, H., and Yodoi, J. (2001). Serum thioredoxin elucidates the significance of serum ferritin as a marker of oxidative stress in chronic liver diseases. Liver *21*, 295-299.

Sun, Q. A., Kirnarsky, L., Sherman, S., and Gladyshev, V. N. (2001a). Selenoprotein oxidoreductase with specificity for thioredoxin and glutathione systems. Proc Natl Acad Sci U S A *98*, 3673-3678.

Sun, Q. A., Zappacosta, F., Factor, V. M., Wirth, P. J., Hatfield, D. L., and Gladyshev, V. N. (2001b). Heterogeneity within animal thioredoxin reductases. Evidence for alternative first exon splicing. J Biol Chem *276*, 3106-3114.

Sundaresan, M., Yu, Z. X., Ferrans, V. J., Irani, K., and Finkel, T. (1995). Requirement for generation of H2O2 for platelet-derived growth factor signal transduction. Science *270*, 296-299.

Sykes, M. C., Mowbray, A. L., and Jo, H. (2007). Reversible glutathiolation of caspase-3 by glutaredoxin as a novel redox signaling mechanism in tumor necrosis factor-alpha-induced cell death. Circ Res *100*, 152-154.

Symons, M. C. R., and Gutteridge, J. M. C. (1998). Free radicals and Iron: Chemistry, Biology, and Medicine: Oxford University Press Inc. New York).

Szatrowski, T. P., and Nathan, C. F. (1991). Production of large amounts of hydrogen peroxide by human tumor cells. Cancer Res *51*, 794-798.

Tagaya, Y., Maeda, Y., Mitsui, A., Kondo, N., Matsui, H., Hamuro, J., Brown, N., Arai, K., Yokota, T., Wakasugi, H., and et al. (1989). ATL-derived factor (ADF), an IL-2 receptor/Tac inducer homologous to thioredoxin; possible involvement of dithiol-reduction in the IL-2 receptor induction. Embo J *8*, 757-764.

Takahashi, A., Ohtani, N., Yamakoshi, K., Iida, S., Tahara, H., Nakayama, K., Nakayama, K. I., Ide, T., Saya, H., and Hara, E. (2006). Mitogenic signalling and the p16INK4a-Rb pathway cooperate to enforce irreversible cellular senescence. Nat Cell Biol *8*, 1291-1297.

Tamura, T., Gladyshev, V., Liu, S. Y., and Stadtman, T. C. (1995). The mutual sparing effects of selenium and vitamin E in animal nutrition may be further explained by the discovery that mammalian thioredoxin reductase is a selenoenzyme. Biofactors *5*, 99-102.

Tamura, T., and Stadtman, T. C. (1996). A new selenoprotein from human lung adenocarcinoma cells: purification, properties, and thioredoxin reductase activity. Proc Natl Acad Sci U S A *93*, 1006-1011.

Tanito, M., Masutani, H., Nakamura, H., Ohira, A., and Yodoi, J. (2002). Cytoprotective effect of thioredoxin against retinal photic injury in mice. Invest Ophthalmol Vis Sci *43*, 1162-1167.

Tanito, M., Nakamura, H., Kwon, Y. W., Teratani, A., Masutani, H., Shioji, K., Kishimoto, C., Ohira, A., Horie, R., and Yodoi, J. (2004). Enhanced oxidative stress and impaired thioredoxin expression in spontaneously hypertensive rats. Antioxid Redox Signal *6*, 89-97.

Tatla, S., Woodhead, V., Foreman, J. C., and Chain, B. M. (1999). The role of reactive oxygen species in triggering proliferation and IL-2 secretion in T cells. Free Radic Biol Med *26*, 14-24.

Thomlinson, R. H., and Gray, L. H. (1955). The histological structure of some human lung cancers and the possible implications for radiotherapy. Br J Cancer *9*, 539-549.

Trachootham, D., Zhou, Y., Zhang, H., Demizu, Y., Chen, Z., Pelicano, H., Chiao, P. J., Achanta, G., Arlinghaus, R. B., Liu, J., and Huang, P. (2006). Selective killing of oncogenically transformed cells through a ROS-mediated mechanism by beta-phenylethyl isothiocyanate. Cancer Cell *10*, 241-252.

Trotter, E. W., and Grant, C. M. (2003). Non-reciprocal regulation of the redox state of the glutathione-glutaredoxin and thioredoxin systems. EMBO Rep *4*, 184-188.

Trotter, E. W., and Grant, C. M. (2005). Overlapping roles of the cytoplasmic and mitochondrial redox regulatory systems in the yeast Saccharomyces cerevisiae. Eukaryot Cell *4*, 392-400.

Truscott, R. J. (2000). Age-related nuclear cataract: a lens transport problem. Ophthalmic Res *32*, 185-194.

Turanov, A. A., Su, D., and Gladyshev, V. N. (2006). Characterization of alternative cytosolic forms and cellular targets of mouse mitochondrial thioredoxin reductase. J Biol Chem *281*, 22953-22963.

Ueno, M., Matsutani, Y., Nakamura, H., Masutani, H., Yagi, M., Yamashiro, H., Kato, H., Inamoto, T., Yamauchi, A., Takahashi, R.*, et al.* (2000). Possible association of thioredoxin and p53 in breast cancer. Immunol Lett *75*, 15-20.

Ungerstedt, J. S., Sowa, Y., Xu, W. S., Shao, Y., Dokmanovic, M., Perez, G., Ngo, L., Holmgren, A., Jiang, X., and Marks, P. A. (2005). Role of thioredoxin in the response of normal and transformed cells to histone deacetylase inhibitors. Proc Natl Acad Sci U S A *102*, 673-678.

Ushio-Fukai, M., Alexander, R. W., Akers, M., Yin, Q., Fujio, Y., Walsh, K., and Griendling, K. K. (1999). Reactive oxygen species mediate the activation of Akt/protein kinase B by angiotensin II in vascular smooth muscle cells. J Biol Chem *274*, 22699-22704.

Valko, M., Leibfritz, D., Moncol, J., Cronin, M. T., Mazur, M., and Telser, J. (2007). Free radicals and antioxidants in normal physiological functions and human disease. Int J Biochem Cell Biol *39*, 44-84.

Valko, M., Rhodes, C. J., Moncol, J., Izakovic, M., and Mazur, M. (2006). Free radicals, metals and antioxidants in oxidative stress-induced cancer. Chem Biol Interact *160*, 1-40.

Veal, E. A., Day, A. M., and Morgan, B. A. (2007). Hydrogen peroxide sensing and signaling. Mol Cell *26*, 1-14.

Victor, V. M., Rocha, M., and De la Fuente, M. (2004). Immune cells: free radicals and antioxidants in sepsis. Int Immunopharmacol *4*, 327-347.

Wakasugi, N., Tagaya, Y., Wakasugi, H., Mitsui, A., Maeda, M., Yodoi, J., and Tursz, T. (1990). Adult T-cell leukemia-derived factor/thioredoxin, produced by both human T-lymphotropic virus type I- and Epstein-Barr virus-transformed lymphocytes, acts as an autocrine growth factor and synergizes with interleukin 1 and interleukin 2. Proc Natl Acad Sci U S A *87*, 8282-8286.

Wang, J., Boja, E. S., Tan, W., Tekle, E., Fales, H. M., English, S., Mieyal, J. J., and Chock, P. B. (2001). Reversible glutathionylation regulates actin polymerization in A431 cells. J Biol Chem *276*, 47763-47766.

Wang, X., Zhang, J., and Xu, T. (2008). Thioredoxin reductase inactivation as a pivotal mechanism of ifosfamide in cancer therapy. Eur J Pharmacol *579*, 66-73.

Warburg, O. (1956). On respiratory impairment in cancer cells. Science *124*, 269-270.

Watson, W. H., Chen, Y., and Jones, D. P. (2003). Redox state of glutathione and thioredoxin in differentiation and apoptosis. Biofactors *17*, 307-314.

Watson, W. H., Heilman, J. M., Hughes, L. L., and Spielberger, J. C. (2008). Thioredoxin reductase-1 knock down does not result in thioredoxin-1 oxidation. Biochem Biophys Res Commun *368*, 832-836.

Welsh, S. J., Bellamy, W. T., Briehl, M. M., and Powis, G. (2002). The redox protein thioredoxin-1 (Trx-1) increases hypoxia-inducible factor 1alpha protein expression: Trx-1 overexpression results in increased vascular endothelial growth factor production and enhanced tumor angiogenesis. Cancer Res *62*, 5089-5095.

William, W. N., Jr., Zinner, R. G., Karp, D. D., Oh, Y. W., Glisson, B. S., Phan, S. C., and Stewart, D. J. (2007). Phase I trial of motexafin gadolinium in combination with docetaxel and cisplatin for the treatment of non-small cell lung cancer. J Thorac Oncol *2*, 745-750.

Winkler, B. S., Boulton, M. E., Gottsch, J. D., and Sternberg, P. (1999). Oxidative damage and age-related macular degeneration. Mol Vis *5*, 32.

Winterbourn, C. C., and Hampton, M. B. (2008). Thiol chemistry and specificity in redox signaling. Free Radic Biol Med *45*, 549-561.

Witte, A. B., Anestal, K., Jerremalm, E., Ehrsson, H., and Arner, E. S. (2005). Inhibition of thioredoxin reductase but not of glutathione reductase by the major classes of alkylating and platinum-containing anticancer compounds. Free Radic Biol Med *39*, 696-703.

Wollman, E. E., d'Auriol, L., Rimsky, L., Shaw, A., Jacquot, J. P., Wingfield, P., Graber, P., Dessarps, F., Robin, P., Galibert, F., and et al. (1988). Cloning and expression of a cDNA for human thioredoxin. J Biol Chem *263*, 15506-15512.

Wood, Z. A., Poole, L. B., and Karplus, P. A. (2003a). Peroxiredoxin evolution and the regulation of hydrogen peroxide signaling. Science *300*, 650-653.

Wood, Z. A., Schroder, E., Robin Harris, J., and Poole, L. B. (2003b). Structure, mechanism and regulation of peroxiredoxins. Trends Biochem Sci *28*, 32-40.

Xu, W. S., Perez, G., Ngo, L., Gui, C. Y., and Marks, P. A. (2005). Induction of polyploidy by histone deacetylase inhibitor: a pathway for antitumor effects. Cancer Res *65*, 7832-7839.

Yang, D., Elner, S. G., Bian, Z. M., Till, G. O., Petty, H. R., and Elner, V. M. (2007). Pro-inflammatory cytokines increase reactive oxygen species through mitochondria and NADPH oxidase in cultured RPE cells. Exp Eye Res *85*, 462-472.

Yant, L. J., Ran, Q., Rao, L., Van Remmen, H., Shibatani, T., Belter, J. G., Motta, L., Richardson, A., and Prolla, T. A. (2003). The selenoprotein GPX4 is essential for mouse development and protects from radiation and oxidative damage insults. Free Radic Biol Med *34*, 496-502.

Yokomizo, A., Ono, M., Nanri, H., Makino, Y., Ohga, T., Wada, M., Okamoto, T., Yodoi, J., Kuwano, M., and Kohno, K. (1995). Cellular levels of thioredoxin associated with drug sensitivity to cisplatin, mitomycin C, doxorubicin, and etoposide. Cancer Res *55*, 4293-4296.

Yoo, M. H., Xu, X. M., Carlson, B. A., Gladyshev, V. N., and Hatfield, D. L. (2006). Thioredoxin reductase 1 deficiency reverses tumor phenotype and tumorigenicity of lung carcinoma cells. J Biol Chem *281*, 13005-13008.

Yoo, M. H., Xu, X. M., Carlson, B. A., Patterson, A. D., Gladyshev, V. N., and Hatfield, D. L. (2007). Targeting thioredoxin reductase 1 reduction in cancer cells inhibits self-sufficient growth and DNA replication. PLoS ONE *2*, e1112.

Zafari, A. M., Ushio-Fukai, M., Akers, M., Yin, Q., Shah, A., Harrison, D. G., Taylor, W. R., and Griendling, K. K. (1998). Role of NADH/NADPH oxidase-derived H2O2 in angiotensin II-induced vascular hypertrophy. Hypertension *32*, 488-495.

Zhong, L., Arner, E. S., and Holmgren, A. (2000). Structure and mechanism of mammalian thioredoxin reductase: the active site is a redox-active selenolthiol/selenenylsulfide formed from the conserved cysteine-selenocysteine sequence. Proc Natl Acad Sci U S A *97*, 5854-5859.

Zhong, L., and Holmgren, A. (2000). Essential role of selenium in the catalytic activities of mammalian thioredoxin reductase revealed by characterization of recombinant enzymes with selenocysteine mutations. J Biol Chem *275*, 18121-18128.

9. Appendix

9.1 Acknowledgements

"Life can only be understood backward but it must be lived forward"

Standing at a crucial juncture of my academic journey and before I step across the finish line, its time to take a pause and to express my sincere gratitude in retrospect to all those people who supported me throughout this learning process.

It is customary to start with the supervisor and mentor and I am not the exception to this rule. I would like to thank my supervisor Dr. Marcus Conrad for his support and guidance. I really appreciate the kind of freedom given by him throughout this work. He was always accommodative to the suggestions or criticisms, which stimulated the independent thinking. Nothing can explain the feeling towards him except a simple word: THANKS!

I am indebted to Prof. Georg W. Bornkamm for giving me the opportunity to do my PhD in Germany. It was a great experience working under him. His ideas and suggestions were very valuable which finally culminated in the form of the present manuscript. I was always welcomed in spite of his busy time-schedule, which was a rare experience.

I express my best regards to my Dr. father Prof. Dr. Eckhard Wolf for his extremely supportive attitude towards me. Without his help it would have not been possible to submit the thesis in such a smooth manner.

I thank my present and former lab members Tamara Perisic, Alexander Mannes, Heidi Förster, Katja Möllmann, Ana Banjac and Alexander Seiler for supporting me during day-to-day work, sharing their valuable experiences and making the stay in the lab memorable. I wish all of them a great success in life.

Help and support provided by Juliane Hardina, Manuela Schneider, Matthias Semisch and Dr. Heike Beck deserve a special note of appreciation. They were the integral part of numerous sessions of discussion on ongoing projects.

I would like to thank our collaborator Hideo Sato (Yamagata University, Japan) for valuable suggestions on xCT. In depth discussions on this topic were crucial for fruitful outcome of the ongoing projects. Also I would like to thank Dr. Peter Kuhlencordt and Pirkko Kölle from Medizinische Poliklinik Innenstadt des Klinikum der LMU for doing HPLC measurements which added substantial information to the thesis.

I want to thank Dr. Elisabeth Kremmer for raising monoclonal antibody against mouse thioredoxin reductase 1 for us.

I express my sincere regards to Prof. Dr. Dirk Eick for lending me support and valuable suggestions at numerous times. I thank people in his lab specially Thomas Harasim and Martin Heidemann for sparing reagents and providing support at the hour of need.

I am very obliged to Dr. Ursula Strobl and her group members for helping me with the analysis of B-cells, although these data were not included in the manuscript.

Although I am expressing my gratitude to Dr. Josef Mautner, the extended help provided by him is beyond description. Whether it was related with experimental and scientific discussion or with meticulous correction of the manuscript, he was always there for help. It would not be incorrect to say that he was the only light of hope during “darkest hours”. I really appreciate his endurance specially for correcting 1000 “FORM” to from. It was a lifelong memorable experience with him.

I would like to thank people of KMOLB for help and encouragement.

The effort done by people in the animal facility is really appreciated and I thank all of them.

Additionally, I would like to thank all of my friends (Anirudha & Angha, Avinash, Madhu, Naidu & Sandhya, Purvi, and Vijay) for their support and sharing nice times during my stay in Munich.

To my special friends: Anurag, Bijender, Chandan, Gagan, Shekhar & Vineeta and Vijender back home for decade-long friendship. I am thankful to Almighty for bestowing them on me.

At last I want to dedicate this paragraph to acknowledge my family. I want to thank Pratibha & Partho and Jyoti for providing me the most needed emotional support during my PhD. They were just terrific and instrumental in this regards. Thank you for being with me. I want to dedicate this dissertation to my dear father and uncle. They are the two great mentors in my life. The support provided by my brothers, bhabhi, sister and jija ji is beyond description. I am greatful to Shanti-Vikash, Rupam-Ravi, chotu and kids Ashu and Manshi for their love and affections.

(Pankaj Kumar Mandal)